THE UNIVERSITY
of EDINBURGH

Entanglement Entropy of Locally Perturbed Thermal Systems

Andrius Štikonas

Doctor of Philosophy
University of Edinburgh
2017

Declaration

I declare that this thesis was composed by myself. The work contained therein is my own, except where explicitly stated otherwise in the text. Work in chapter 4 and chapter 5 was produced in a collaboration with Paweł Caputa, Joan Simón, Tadashi Takayanagi and Kento Watanabe and published in [1, 2].

(*Andrius Štikonas*)

Acknowledgement

I would like to thank Joan Simón for his continuous help during my PhD and in particular, for his advice during writing of this thesis.

Lay summary

Theoretical physics in the XX century has seen two groundbreaking developments. One was Einstein's general relativity, a theory explaining gravity as a consequence of curved space and time. The other breakthrough was the Standard Model, a theory describing the world at very small scales. The Standard Model describes what we think of as particles governed by quantum mechanics and subject to uncertainties, so we can only compute probabilities of something happening. On the other hand General Relativity is a classical theory with no uncertainties. However, it suffers from other problems mainly related to black holes where matter is compressed to infinitely small volume. One would expect that in this regime quantum effects are important. However, the Standard Model and General Relativity are mutually incompatible in certain regimes.

So far the most successful candidate for the theory of quantum gravity was String Theory, where a very different picture of gravity emerges. In some cases gravity can be understood as a hologram. The phenomena in gravitational theory can be explained in terms of completely different quantum field theory (although, not the Standard Model) in a lower dimension of space with no gravity at all.

In this thesis we will be exploring some aspects of this duality between gravity and quantum field theory in systems that are close to being in a thermal equilibrium. We will explore how quickly they return to thermal equilibrium. This will be done in both gravitational description and quantum field theory.

Abstract

In this thesis we study the time evolution of Rényi and entanglement entropies of thermal states in Conformal Field Theory (CFT). These quantities are usually hard to compute but Ryu-Takayanagi (RT) and Hubeny-Rangamani-Takayanagi (HRT) proposals allow us to find the same quantities using calculations in general relativity.

We will introduce main concepts of holography, quantum information and conformal field theory that will be used to derive the results of this thesis. In the first part of the thesis, we explicitly compute entanglement entropy of the rotating BTZ black hole by directly applying HRT proposal and finding lengths of spacelike geodesics.

Rényi entropy of thermal state perturbed by a local quantum quench is computed by mapping correlators on two glued cylinders to the plane for field theory containing a single free boson and for 2d CFTs in the large c limit.

We consider Thermofield Double State (TFD) which is an entangled state in direct product of two 2D CFTs. It is conjectured to be holographically equivalent to the eternal BTZ black hole. TFD state is perturbed by a local quench in one CFT and mutual information between two intervals in two CFTs is computed. We find when mutual information vanishes and interpret this as scrambling time, i.e. time scale required for the system to thermalize. This field theory result is modelled with a massive free falling particle in the BTZ black hole. We have computed the back-reaction of the particle on the metric of BTZ and used RT proposal to find holographic entanglement entropy.

Finally, we generalize this calculation to the case of rotating BTZ with inner and outer horizons. It is dual to the CFT with different temperatures for left and right moving modes. We calculate mutual information and scrambling time and find exact agreement between results in the gravity and those in the CFT.

Contents

Chapter 1

Introduction

In modern physics we often encounter problems that cannot be solved exactly using analytic methods. Asymptotic expansions in terms of some small parameter proved to be very useful in tackling such problems. For example, in Quantum Electrodynamics we can perform expansion in terms of fine-structure constant $\alpha \approx \frac{1}{137}$. However, this fails if the parameter in which we want to expand is large, as is the case in Quantum Chromodynamics. Then we have to develop some non-perturbative methods or to try to find some alternative perturbative expansion. When theory admits such different descriptions we say it has duality. Dualities between apparently different quantum theories are examples of this last situation. One of the simplest examples of duality is contained in the theory of classical electromagnetism in vacuum where we can interchange electric and magnetic fields

$$\begin{aligned} \mathbf{E} &\mapsto \mathbf{B}, \\ \mathbf{B} &\mapsto -\frac{1}{c^2}\mathbf{E}. \end{aligned} \tag{1.1}$$

A similar duality exists in quantum theory [3, 4]. It relates strongly interacting Yang-Mills theory to weakly interacting theory. Such dualities are called strong-weak or S-dualities. Another interesting example of S-duality is discussed in [5] where a theory describing scalar field obeying Sine-Gordon equations is dual to a Thirring model describing fermions.

Besides the lack of tools to compute at strong coupling, some physical theories simply break down in certain regimes. For example, the core of most heavy stars undergoes gravitational collapse at the end of nucleosynthesis. If its mass is beyond certain limit [6, 7] then neutron degeneracy pressure is not able to stop the collapse. Once the remnant of the star shrinks below its Schwarzschild radius $r_s = \frac{2GM}{c^2}$ [8], it has no other option but to collapse to a point of zero size and infinite density. Another example of singularity in General Relativity is the Big Bang singularity [9]. Singular and/or undefined behaviour is not acceptable for a complete physical theory, but it is possible that by properly describing gravity together with the rest of fundamental forces may cure these problems. Unfortunately, conventional methods of quantizing gravity failed to produce a consistent theory [10]. String theory is one of the most promising candidates of quantum gravity [11, 12] but our understanding of string theory is still limited, especially in the non-perturbative regime. We will argue in section 1.1 that gravity can be thought of as another example of strong-weak duality if we think of gravity as a hologram.

Even if we would have a microscopic description of gravity together with other fundamental forces, there are important open problems in physics regarding the emergence of macroscopic behaviour from microscopic degrees of freedom. One such problem is how a macroscopic system settles into thermal equilibrium, i.e. *thermalizes*. Even though statistical mechanics and the use of typicality arguments provide a good understanding for certain kinematic questions [13–15], a proper understanding of the different time scales involved in this process and the conditions under which such equilibrium exists or not, remain active areas of research. Only in some cases we have quantitative arguments [16].

In this thesis we study the time evolution of correlation functions in thermal states in two dimensional conformal field theories (CFTs) perturbed by some local perturbation. We will

quantify the amount of correlation between different subsystems in the 2d CFT borrowing concepts from quantum information theory. One of them is the von Neumann entanglement entropy [17], a quantum analogue of Shannon's entropy [18], the magnitude used to define and quantify classical information. The methods required to compute these magnitudes use either uniformization maps or twist operators and results about correlation functions of strongly coupled two dimensional CFTs on the plane. We will discuss these concepts in chapter 2.

The use of holography in this context maps calculations of thermal correlators in a strongly coupled CFT to geometric problems in a black hole geometry solving Einstein's equations, a description that is valid in a weakly coupled regime. In the remaining of this chapter, we will introduce the main ideas and concepts behind this holographic duality. First, we will discuss motivation and justification behind holography in gravity. Various concepts from quantum information will be introduced. We will show how entanglement entropy can be computed in conformal field theories and holography. Finally, we will discuss how thermalization can be described in the language of quantum information and look at how quickly quantum system can reach thermal equilibrium.

1.1 Holographic principle

One of the first questions that we must ask when we consider a physical theory is what are its observables. In Newtonian dynamics we have positions, velocities. But the world is fundamentally quantum and quantum mechanics puts severe restrictions on what the right questions to ask are. For example, we cannot simultaneously know the position and velocity of a particle due to uncertainty principle. In order to measure something exactly with no uncertainty we must be able to do measurement infinitely many times.

Definition of observables is even more subtle in a theory of gravity. It is known that in general relativity there are no local observables [19], so we have to consider non-local observables. Since general relativity is diffeomorphism invariant, it is natural to consider integrals (such as proper time or length of spacelike geodesics) as our observables [20]. Often these integrals are defined as integrals on the boundary at infinity. For example, we can define energy associated with an asymptotic time translations ξ^a as a surface integral [21]

$$E = -\lim_{S_\alpha \to \mathscr{S}} \frac{1}{8\pi} \int_{S_\alpha} \epsilon_{abcd} \nabla^c \xi^d \, dx^a \wedge dx^b, \tag{1.2}$$

where $\{S_\alpha\}$ is a family of spheres approaching cross-section $\mathscr{S}$ of the boundary at infinity.

But if observables in the theory have to be connected to the boundary at infinity then it is natural to ask if we need the interior. It is plausible that there might be some different theory that describes the same phenomena but using a different language just on the boundary of spacetime, something like holography in optics where information about three dimensional object is encoded on two dimensional surface. The study of black hole thermodynamics [22–24] gave rise to holographic principle in gravity. Later, string theory provided further evidence. In this thesis we will be calculating entanglement entropy. In vacuum it generally scales with the area of the local region, we will review this in subsection 1.5.1. This plays a crucial role in condensed matter physics [25] and has emerged strongly in AdS/CFT (section 1.2) which is a particular realization of holography in gravity.

In this chapter of the thesis we will motivate and give examples of holography in gravity. Later, we will introduce key concepts of quantum information that are useful in explaining many aspects of how holography works. Finally, we will introduce various conventions and notations used throughout this thesis.

1.1.1 Black hole thermodynamics

Soon after the laws of general relativity were written down [26], a very exotic solution [8] eventually called [27] a black hole was found. Later, more similar solutions were found. These solutions to Einstein's equations describe regions of spacetime where gravity is so strong that nothing, not even light, can escape. This was very puzzling for a while because it seemingly

allowed to violate the Second Law of Thermodynamics by throwing stuff into the black hole. Consequently, the entropy of the remaining environment would decrease. In 1972 Jacob Bekenstein conjectured [28] that black holes must also carry entropy which is proportional to the area A of the black hole event horizon, the surface of no return. So instead of entropy disappearing when matter crosses the event horizon, it goes into increasing the black hole entropy while the total entropy still increases, thus satisfying the 2nd law of thermodynamics.

At that time Yakov Zel'dovich and Alexei Starobinsky realized that due to quantum mechanics, black holes should emit particles [29]. Stephen Hawking computed radiation emitted by black holes [30] and discovered that its spectrum is that of black body with temperature

$$T_H = \frac{\hbar\kappa}{2\pi} \tag{1.3}$$

in units $c = k_B = 1$. Here, κ is the surface gravity of black hole. Note that for non-rotating Schwarzschild black hole Hawking temperature is inversely proportional to the mass of black hole

$$T_H = \frac{\hbar}{8\pi GM}. \tag{1.4}$$

This temperature can be compared to the First Law of Thermodynamics to fix constant of proportionality for Bekenstein entropy

$$S = \frac{A}{4G}. \tag{1.5}$$

Black hole entropy bounds the maximum possible entropy that can be contained in a given volume.

So in analogy to gas thermodynamics four laws about classical black holes in general relativity were proven in [31]:

Zeroth law. An event horizon of a stationary black hole has a constant surface gravity.

First law. Small perturbations of stationary black holes of mass M with angular velocity Ω, angular momentum J, electrostatic potential Φ and charge Q satisfy

$$dM = \frac{\kappa}{8M} dA + \Omega dJ + \Phi dQ. \tag{1.6}$$

Parameters of black holes such as mass M or angular momentum J may seem obvious from this point of view but are in fact defined in a non-trivial way via integrals using equations like (1.2).

Second law. In any process in general relativity the area of black hole horizon does not decrease

$$\frac{dA}{dt} \geq 0. \tag{1.7}$$

The second law is a consequence of Einstein equations and so is valid for classical general relativity. However, we already discussed above that black holes emit Hawking radiation and they can lose mass quantum mechanically, so instead we should consider total entropy of the system

Generalized second law. In any process the total entropy of the system increases

$$\frac{dS_{\text{BH}}}{dt} + \frac{dS_{\text{outside}}}{dt} \geq 0. \tag{1.8}$$

Third law. Black holes with no surface gravity cannot be created by any physical process.

The laws of gas thermodynamics emerge from statistical mechanics as most likely outcome of dynamics of microscopic degrees of freedom (positions and momenta of gas atoms or molecules). However, many microscopic states give rise to the same macroscopic state. So by ignoring microscopic description we lose information which generates entropy

$$S = \log \Omega, \tag{1.9}$$

where Ω is the number of microstates.

The laws of black hole thermodynamics are proven directly in classical general relativity. We saw that surface gravity and area of black holes were analogous to temperature and entropy of thermodynamic systems. However, Hawking's calculation showed that κ and A represent the actual temperature and entropy of black hole. This suggests that analogy is not just accidental. If we assume that any kind of thermodynamic system must have a microscopic origin then the same story should be true for general relativity. There must be some underlying quantum theory describing gravity whose thermodynamic limit is general relativity and hence it is natural to try to identify this microscopic description. Notably, the number of microscopic degrees of freedom is proportional to the area unlike in all non-gravitating systems where entropy is an extensive quantity, i.e. proportional to the volume of the system. This area law is another motivation of holographic principle.

Superstring theory is the leading candidate for theory of quantum gravity. Firstly, at low energies it reduces to supergravity, i.e. supersymmetric version of general relativity. Secondly, there are calculations in string theory that reproduce Bekenstein-Hawking area law. For example Andrew Strominger and Cumrum Vafa have derived [32] the area law for a certain class of extremal black holes in five dimensions by counting degenerate microstates. They do the calculation in a weak string coupling regime of D1-D5 brane system where strings are open and do not back-react on geometry, so black holes do not exist. However, the number of microstates is one of the quantities protected by supersymmetry, i.e. does not change as we vary coupling constant and make it large where strings become closed, they back-react on geometry and create black hole with a horizon.

Strominger and Vafa counting argument has explained a lot about microscopic nature of gravity but it did not explain dynamic aspects of gravity, e.g. evaporation of black holes and what happens to information that has fallen into the black hole. It also did not answer questions about locality in gravity. However, it motivated to study dynamics of such systems which lead to an even more important breakthrough. In 1997 Juan Maldacena conjectured [33] AdS/CFT correspondence.

1.2 AdS/CFT Correspondence

Let us now describe AdS/CFT correspondence [34]. This is an explicit realization of the holographic principle that we discussed above. While Maldacena's example [33] is specific to CFT, holography defines a general philosophy in modern theoretical physics and is used in a variety of different situations.

Definition 1.1. Maximally symmetric negatively curved spacetime in five dimensions is called anti-de Sitter space (AdS_5). It can be embedded in $\mathbb{R}^{2,4}$ space as

$$-X_0^2 - X_1^2 + X_2^2 + X_3^2 + X_4^2 + X_5^2 = -R^2. \tag{1.10}$$

Correspondence. String theory in a negatively curved spacetime is equivalent to quantum field theory living on its boundary. Hence, gravity holographically emerges from a quantum field theory of one lower dimension. The correspondence is an example of strong-weak duality, i.e. when the theory in the bulk is weakly interacting, it corresponds to a strongly coupled field theory on the boundary.

In the next subsection we will review a particular example that Maldacena considered: the full type IIB superstring theory on $\mathrm{AdS}_5 \times S^5$ background is equivalent to super Yang-Mills conformal field theory (CFT) with $\mathcal{N} = 4$ copies of supersymmetry. The CFT has a gauge symmetry group $SU(N)$ and coupling constant g_{YM}. The gravity is described by the ratio of the radius R of AdS space[1] to the string length ℓ_s and the (closed) string coupling constant g_s.

1.2.1 D3-brane system

In order to further motivate AdS/CFT correspondence we can look at D3-brane system [34–36].

[1] In the context of $\mathrm{AdS}_5 \times S^5$, the five dimensional sphere S^5 has the same radius R.

Superstring theory contains solitonic objects called D-branes [37]. Their gravitational description involves a generalisation of black holes in General Relativity. They break the Poincaré symmetry and their defining property is that open strings can end on their tangential spacelike directions.

After quantization, open strings on the brane produce $U(1)$ Yang-Mills field living in world volume of the brane. When we have more than one D-brane, open string endpoints can stretch between different branes and can have nontrivial interactions. For example, two endpoints of different open strings belonging to the same brane might join and we end up with a single open string. Similarly, if N D-branes are separated, then gauge symmetry group is $U(1)^N$. But if D-branes are stacked together, then there is enhancement of Yang-Mills gauge symmetry group to $U(N)$. Furthermore, interactions of gauge fields are such that $U(1)$ subgroup of $U(N)$ decouples from the remaining fields that transform under $SU(N)$ gauge symmetry group [38].

In addition to open strings, string theory also contains closed strings with no endpoints. They are not constrained to lie on the brane and after quantization do not interact with Yang-Mills fields on the brane. For example, graviton which is one of the massless modes is fully decoupled from $U(N)$ gauge fields.

Let us now look at N stacked D3-branes (so that there are 3 tangential spatial directions) in low energy supergravity limit where massive string states are not accessible. In this limit string coupling g_s is small, gravitational effects are also small, so D3-branes live in ten dimensional Minkowski space. The effective action of D-brane system can be written as

$$S = S_{\text{sugra}} + S_{\text{YM}} + S_{\text{int}}. \tag{1.11}$$

We can interpret these two terms in the action as two decoupled systems. One is supergravity in the bulk. The other is given by brane action which in this limit is maximally supersymmetric $\mathcal{N} = 4$ Super Yang-Mills with $U(N)$ gauge symmetry group. Note that $U(N)$ interaction terms $S_{\text{int}} \to 0$ as $g_s \to 0$, so we are dealing with weakly coupled fields.

Let us consider a case when string coupling g_s is large, i.e. $g_s N \gg 1$. In this case gravitational effects are important. In fact geometry looks similar to that of extremal black hole. The geometry has an infinite throat and a horizon. Near horizon limit of extremal D3-brane is

$$ds^2 \sim R^2 \frac{dx \cdot dx + dz^2}{z^2} + R^2 d\Omega_5^2. \tag{1.12}$$

Here the first term is the metric of AdS_5 space with radius R in Poincaré coordinates and the second is that of a five dimensional sphere S^5 with the same radius R. In this limit we still have two different types of excitations in our system. As before, we have closed strings far away from the horizon in flat space. But now we also have type IIB superstrings living in near horizon geometry (1.12).

Two decoupled systems of strings occur for all values of g_s, not just very small or very large. So we can look at what happens to those systems as we dial g_s. The first system, closed strings in flat space, is always there and nothing changes as we change g_s. The other system changes from $SU(N)$ super Yang-Mills to type IIB superstring theory. If we assume that nothing drastic happens when we dial coupling g_s, then Yang-Mills theory still remains the same theory just with different coupling constant. Similarly, type IIB string theory remains string theory when we reduce g_s. But that means that we have two different descriptions of the same system, one way to talk about it is to use super Yang-Mills and the other is to describe it using type IIB superstring theory. In fact, strongly coupled Yang-Mills theory must be equivalent to weakly coupled string theory and vice versa.

1.2.2 Matching the theories

The parameters of the CFT are the number of colours N and 't Hooft coupling constant λ (or alternatively Yang-Mills coupling constant $g_{YM} = \lambda N^{-1}$). Bulk and boundary parameters are in fact related and can be found for example in [39]

$$\left(\frac{R}{\ell_s}\right)^4 = 4\pi g_s N = 4\pi\lambda. \tag{1.13}$$

Equation (1.13) shows that whenever we are in the supergravity limit of string theory $R \gg \ell_s$ and $g_s \to 0$, we must have a strongly coupled field theory. On the other hand, when we have a weakly interacting field theory, AdS/CFT allows us to study non perturbative aspects of string theory for which we do not have an independent formulation. This is one of the reasons why AdS/CFT remains a conjecture that is heuristically motivated and not a rigorous theorem.

Formally, AdS/CFT dictionary says that (Euclidean) path integral describing partition function of the theory in the bulk M with boundary ∂M is equivalent to the path integral describing CFT on ∂M [40]

$$Z_{\text{gravity}} = Z_{\text{CFT}}. \tag{1.14}$$

To understand relation between theories in the bulk and boundary more intuitively let us recall the picture of scattering used to motivate holographic principle. The simplest possibility is that CFT_4 coordinates directly correspond to non-radial coordinates $x = (t, \theta, \phi, \psi)$ in AdS_5. We can determine what happens to the radial coordinate in the bulk by considering dilations in CFT. If we rescale coordinates of CFT, energy in CFT must be rescaled in the opposite way because mass dimension of coordinates is -1. So CFT is invariant under

$$x \mapsto \alpha x, \qquad E \mapsto \frac{E}{\alpha}. \tag{1.15}$$

Since non-radial AdS coordinates correspond to coordinates in CFT, we must also rescale them in exactly the same way. On the other hand, anti-de Sitter metric is invariant under simultaneous rescaling

$$x \mapsto \alpha x, \qquad z \mapsto \alpha z. \tag{1.16}$$

So we can identify radial coordinate in anti-de Sitter space with energy scale in CFT

$$E \sim \frac{1}{z} = \frac{r}{R}. \tag{1.17}$$

However, physics of bulk is encoded on the boundary in a non-trivial way, bulk information is delocalized in the CFT. To see this, let us consider a massive particle in AdS. Massive particles can never reach boundary of AdS due to its attractive nature. Hence, it will correspond to finite size blob of energy in CFT, i.e. not a localized particle. Another interesting example is Schwarzschild-AdS black hole that corresponds to a thermal state in CFT [41] as is expected from black hole thermodynamics.

Since this is a strongly-weakly coupled duality, it is often difficult to perform calculations on one side of the correspondence. AdS/CFT is still very useful in this case as it allows us to learn non-trivial facts about physics of strongly coupled systems as long as we know the dictionary between the two theories. But suppose we want to compare both sides and test AdS/CFT. One way around is supersymmetry. Some quantities are protected by supersymmetry and do not change as we dial the coupling constant. So we can compare computations in a weekly coupled field theory with those in gravity. Another thing we can look at, are setups where analytic computations are easier. In two dimensions conformal symmetry is a much stronger statement than in higher dimensions because in 2D the symmetry group is infinite dimensional [42, 43]. Similarly, gravity in 3D has no propagating degrees of freedom, and has to be locally anti-de Sitter space. In $\text{AdS}_3/\text{CFT}_2$ case, we do not know precise details of the boundary CFT. And vice versa, given some specific 2D CFT we do not know whether bulk is described by Einstein gravity or some other more complicated gravitational theory. However, some quantities are universal in CFTs with large central charge c and do not depend on precise details.

1.3 Entanglement Entropy in Quantum Mechanics

There have been important conceptual advances in understanding the emergence of spacetime from the dual CFT in recent years. The study of bulk reconstruction originally followed different routes, including holographic renormalisation [44] and the reconstruction of local bulk operators [45]. More recently, the connection between quantum entanglement and the connectivity of

space has led to new insights [46, 47] including the notable bijection between the linearised[2] Einstein's equations and the first law of entanglement entropy [49, 50]. These results provide an AdS/CFT perspective on earlier ideas relating Einstein's equations with thermodynamics, equivalence principle, local Rindler physics and entanglement entropy properties of the vacuum [51, 52]. In this section we will introduce quantum entanglement and related concepts.

1.3.1 Density operators

In quantum mechanics we often use the language of quantum states described by vectors in a Hilbert space. There is another more general formulation of quantum mechanics that uses operators on Hilbert space instead of vectors. It is very suitable for describing quantum systems whose state we do not know with certainty [53].

Definition 1.2. Suppose quantum system is in state ψ_i with probability p_i. Then we define *density matrix* (or density operator)

$$\rho = \sum_i p_i \left|\psi_i\right\rangle \left\langle\psi_i\right| . \tag{1.18}$$

Density operators are usually normalized, so that $\operatorname{tr}\rho = 1$ which corresponds to total probability $\sum_i p_i = 1$.

We can rewrite all quantities used in state vector formalism in this language. To measure observable corresponding to the Hermitian operator $\mathcal{O}$ we can calculate

$$\langle O\rangle = \operatorname{tr}\rho\mathcal{O}, \tag{1.19}$$

instead of usual $\langle\psi|\mathcal{O}|\psi\rangle$.

Definition 1.3. Quantum system with density matrix $\operatorname{tr}\rho^2 = 1$ is said to be in *pure state*.

Definition 1.4. Quantum system that is not pure is said to be in *mixed state*.

Mixed states satisfy $0 < \operatorname{tr}\rho^2 < 1$. They are also said to be *entangled*.

Let us consider the canonical ensemble at temperature $T = \beta^{-1}$ as an example. Probability of each state is given by Boltzmann distribution $p_i = \frac{1}{Z}\exp(-\beta E_i)$. In the language of density matrices the canonical ensemble is just a choice of density operator

$$\rho = \frac{1}{Z}\sum_i e^{-\beta E_i}\left|\Psi_i\right\rangle\left\langle\Psi_i\right| = \frac{1}{Z}e^{-\beta H}, \tag{1.20}$$

where H is the Hamiltonian of the system whose eigenstates corresponding to energy level E_i are $|\Psi_i\rangle$. We will often call this operator thermal density matrix.

1.3.2 Composite systems

In classical physics, we are used to the fact that we can study non interacting parts of the more complicated system separately and learn everything there is about the whole system. That is no longer the case in quantum mechanics. In quantum mechanical system there might be non trivial correlations between different parts of the system. This is the phenomenon of entanglement and is best explained using the formalism of density operators.

When studying any physical system we often prefer to consider them isolated from external factors. Such systems are called closed. However, it is almost never possible to completely isolate physical system from the environment. It is often useful to take interactions with the environment into account and consider open systems. Observers only have access to the system itself and cannot act on the environment.

In quantum mechanical systems we can describe open systems using product Hilbert spaces. Total Hilbert space $\mathcal{H}$ is partitioned into two subspaces $\mathcal{H} \simeq \mathcal{H}_A \otimes \mathcal{H}_B$ and Hilbert space $\mathcal{H}_B$ is not accessible to the observer who can only measure states in $\mathcal{H}_A$. In some cases $\mathcal{H}_B$ can

[2]There is a recent generalization to second order approximation to Einstein's equations in [48]

be thought to be the environment but it does not have to be, density matrix formalism is very general. E.g. $\mathcal{H}_B$ can describe two spatially separated particles. In all such systems observer can use observables of the following form

$$\mathcal{O} = \mathcal{O}_A \otimes \mathbb{I}_B. \tag{1.21}$$

It turns out that density matrix formalism is again more convenient when we describe composite systems.

Definition 1.5. Suppose we have a composite system consisting of subsystems A and B that is described using density operator ρ. Then *reduced* density operator is obtained by tracing over Hilbert space $\mathcal{H}_B$

$$\rho_A = \mathrm{tr}_B\, \rho. \tag{1.22}$$

Let us consider 2 qubit system described by a direct product of two 2D Hilbert spaces. Suppose our system is in the state

$$|\psi\rangle = \frac{1}{\sqrt{2}}\big(|0\rangle_A \otimes |0\rangle_B + |1\rangle_A \otimes |1\rangle_B \big). \tag{1.23}$$

We will sometimes use more compact notation $|ij\rangle := |i\rangle_A \otimes |j\rangle_B$ and similarly for dual vectors. Density matrix is given by

$$\rho = |\psi\rangle\langle\psi| = \frac{1}{2}\left(|00\rangle\langle 00| + |00\rangle\langle 11| + |11\rangle\langle 00| + |11\rangle\langle 11|\right). \tag{1.24}$$

In this case $\rho^2 = \rho$ and so $\mathrm{tr}\,\rho = \mathrm{tr}\,\rho^2 = 1$ as expected since the state (1.23) was not a probabilistic ensemble of states but is known exactly. Nevertheless, if we look at reduced density matrix describing just one qubit

$$\rho_A = \mathrm{tr}_B\, \rho = \frac{1}{2}\big(|0\rangle_A \langle 0|_A + |1\rangle_A \langle 1|_A \big) \equiv \frac{1}{2}\mathbb{I}_A. \tag{1.25}$$

But this time

$$\mathrm{tr}\,\rho_A^2 = \mathrm{tr}\,\frac{\mathbb{I}_A}{4} = \frac{1}{2} < 1. \tag{1.26}$$

When we have no access to qubit B, qubit A can be $|0\rangle$ or $|1\rangle$ with equal probabilities and so the subsystem is in a mixed state even though the whole system was in a pure state. So two qubits in this state are entangled.

We saw two ways of using density operators, one was probabilistic ensembles and the other is composite systems. In the previous subsection we have considered the canonical ensemble. It is natural to ask if thermal states can arise as composite systems. In fact, this is possible for any mixed state [53].

Purification Theorem. Given any density operator $\rho_A \in \mathcal{H}_A$, there is another Hilbert space $\mathcal{H}_B \cong \mathcal{H}_A$ and state $|\psi\rangle \in \mathcal{H}_A \otimes \mathcal{H}_B$ such that

$$\rho_A = \mathrm{tr}_B(|\psi\rangle\langle\psi|). \tag{1.27}$$

Proof. Let us choose eigenbasis $\{|i\rangle\}$ for $\mathcal{H}_A$ with corresponding eigenvalues λ_i and orthonormal basis $\{|i'\rangle\}$ for $\mathcal{H}_B$.

$$|\psi\rangle = \sum_i \sqrt{\lambda_i}\, |i\rangle \otimes |i'\rangle\,. \tag{1.28}$$

Then

$$\mathrm{tr}_B(|\psi\rangle\langle\psi|) = \sum_{i,j} \sqrt{\lambda_i\lambda_j}\, |i\rangle\langle j|\, \mathrm{tr}\,(|i'\rangle\langle j'|) = \sum_{i,j} \sqrt{\lambda_i\lambda_j}\, |i\rangle\langle j|\, \delta_{ij} = \rho_A. \tag{1.29}$$

□

Thermofield double construction does precisely that for thermal states. Let us consider a

particular entangled state in direct product of two (left and right) Hilbert spaces $\mathcal{H}_L \otimes \mathcal{H}_R$

$$|\text{TFD}\rangle = \frac{1}{\sqrt{Z}} \sum_n e^{-\frac{\beta E_n}{2}} |n\rangle_L \otimes |n\rangle_R . \tag{1.30}$$

Density matrix of thermofield double state is

$$\rho_{\text{TFD}} = \frac{1}{Z} \sum_{m,n} e^{-\beta(E_n+E_m)/2} |n\rangle_L \otimes |n\rangle_R \langle m|_L \otimes \langle m|_R . \tag{1.31}$$

Let us do a partial trace over $\mathcal{H}_R$.

$$\rho_L = \text{tr}_R \rho = \frac{1}{Z} \sum_k \sum_{m,n} e^{-\beta(E_n+E_m)/2} |n\rangle_L \langle k|n\rangle_R \langle m|_L \langle m|k\rangle_R = \frac{1}{Z} \sum_n e^{-\beta E_n} |n\rangle_L \langle n|_L . \tag{1.32}$$

So reduced density matrix of thermofield double state is thermal as expected

$$\rho_L = \frac{1}{Z} e^{-\beta H_L}, \tag{1.33}$$

where H_L is the Hamiltonian acting on the left Hilbert space.

Even though $\mathcal{H}_L$ and $\mathcal{H}_R$ are independent, there are non-trivial correlators. This happens because we were in an entangled state. For example, we can consider the correlator with Hamiltonians

$$\langle \text{TFD}|H_L H_R|\text{TFD}\rangle = \frac{1}{Z} \sum_n e^{-\beta E_n} E_n^2 > 0. \tag{1.34}$$

1.3.3 Von Neumann Entropy

It is natural to ask whether we can quantify how entangled the system is. We already encountered one way to do this, checking $\text{tr}\,\rho^2$. It is easy to compute but is not easy to interpret. One of the natural ways to interpret entanglement is to measure amount of information lost when tracing out the second subsystem.

In order to get some intuition how to describe information, let us look at classical systems. In information theory the quantity that measures uncertainty in information (we can also think about it as average information) is Shannon entropy [18].

Definition 1.6. Given a discrete random variable X taking values x_i with probabilities p_i we define Shannon entropy to be

$$H(X) = -\sum_{i=1}^{n} p_i \log p_i. \tag{1.35}$$

For example, a fair coin with $p = \frac{1}{2}$ chance of head or tails has larger entropy than unfair coin where one outcome is more likely than the other. Also, maximally biased coin with certain outcome has zero entropy.

In general we want entropy to satisfy the following properties [54, 55]

- $H(p, 1-p)$ is continuous for $0 \leq p \leq 1$ and positive in at least one point.
- $H(p_1, \ldots, p_n)$ is symmetric in its arguments.
- For $n \geq 1$, $H(p_1, \ldots, p_n, q_1, q_2) = H(p_1, \ldots, p_n, q_1 + q_2) + (q_1 + q_2) H\left(\frac{q_1}{q_1+q_2}, \frac{q_2}{q_1+q_2}\right)$.

  The last condition is necessary for information to be additive.

These conditions fix entropy given by (1.35) up to multiplicative constant (base of logarithm).

In fact Shannon entropy was already used in statistical physics as Gibbs entropy. In statistical physics we do not care about individual positions and momenta of gas particles and only care about macroscopic parameters such as pressure or temperature. Doing this incurs

information loss. Similarly, we lose information about the state when we do partial trace of density operators. We can generalize classical Shannon/Gibbs entropy to quantum systems to measure entanglement. Note that in quantum systems there are many other useful measures of entanglement such as entanglement negativity [56]. But in this thesis we will focus on Von Neumann entropy.

Definition 1.7. Von Neumann entropy (often called entanglement entropy) of density operator is [17]

$$S_A \equiv S(\rho_A) = -\operatorname{tr}_A (\rho_A \log \rho_A) . \tag{1.36}$$

In the equation (1.36) we have to evaluate logarithm of an operator which we define to be the inverse of exponential operator $e^X \equiv \sum_{n=0}^{\infty} \frac{X^n}{n!}$. This is fairly hard to compute even in finite dimensional case when we can use spectral decomposition theorem and express equation (1.36) in terms of eigenvalues λ_i of density matrix:

$$S_A = -\sum_i \lambda_i \log \lambda_i. \tag{1.37}$$

To illustrate the definition of entanglement entropy let us compute it for two simple examples. First example will be quantum system of two particles with n energy levels. Then we will consider the second example which is the canonical ensemble from statistical physics.

n energy level composite system. Quantum states in each of the two subsystems have orthonormal basis $|1\rangle, \ldots, |n\rangle$. Consider the state

$$|\psi\rangle = \frac{1}{\sqrt{n}} \big(|1\rangle \otimes |1\rangle + |2\rangle \otimes |2\rangle + \ldots |n\rangle \otimes |n\rangle \big). \tag{1.38}$$

The corresponding density matrix is

$$\rho = \frac{1}{n} \left(|11\rangle \langle 11| + |11\rangle \langle 22| + \ldots |11\rangle \langle nn| + |22\rangle \langle 11| + \ldots |22\rangle \langle nn| + \ldots |nn\rangle \langle nn| \right). \tag{1.39}$$

Let us now trace over the second subsystem. This loses information as in any kind of averaging process. We obtain the following reduced density matrix

$$\rho_A = \frac{1}{n} \mathbb{I}_n, \tag{1.40}$$

$$\log \rho_A = -\log n \, \mathbb{I}_n. \tag{1.41}$$

Finally, entanglement entropy is

$$S_A = \sum_{i=1}^{n} \frac{1}{n} \log n = \log n. \tag{1.42}$$

In fact this state maximises von Neumann entropy. This is analogous to the classical case of uniform distribution maximising Shannon entropy. To prove this consider the general expression of entanglement entropy in terms of eigenvalues (1.37) with an extra Lagrange multiplier

$$S(\lambda_i; \mu) = -\sum_i \lambda_i \log \lambda_i + \mu \left(\sum_i \lambda_i - 1 \right). \tag{1.43}$$

Then

$$\frac{\partial S}{\partial \lambda_i} = -\log \lambda_i - 1 + \mu = 0 \qquad \forall i. \tag{1.44}$$

This implies that all λ_i must be equal.

The Canonical Ensemble. Von Neumann entropy S_{VN} of thermal states described by (1.20) is equal to Gibbs entropy S_{G}.

$$S_{\mathrm{VN}} = -\operatorname{tr}\left[\frac{1}{Z}e^{-\beta H}\log\left(\frac{1}{Z}e^{-\beta H}\right)\right] = -\frac{1}{Z}\sum_i e^{-\beta E_i}\log\left(\frac{1}{Z}e^{-\beta E_i}\right)$$
$$= \log Z + \frac{1}{Z}\sum_i e^{-\beta E_i}\beta E_i = \log Z + \beta\langle E\rangle = S_G. \tag{1.45}$$

To calculate entanglement entropy we usually use *replica trick* and avoid evaluating equation (1.36) directly.

Lemma (Replica Trick). Let X be a Banach space and $\rho : X \to X$ be an operator. Then

$$\lim_{n\to 0}\frac{\rho^n - 1}{n} = \log\rho. \tag{1.46}$$

Proof. It follows directly from L'Hôpital's rule. □

Using replica trick, equation (1.36) can be rewritten as

$$S_A = -\lim_{n\to 0}\frac{\operatorname{tr}_A(\rho_A^{n+1} - \rho_A)}{n} = -\lim_{\alpha\to 1}\frac{\operatorname{tr}\rho_A^\alpha - \operatorname{tr}\rho_A}{\alpha - 1} = -\frac{d}{d\alpha}\left(\operatorname{tr}_A\rho_A^\alpha\right)\big|_{\alpha=1}$$
$$= -\frac{d}{d\alpha}\left(\log\operatorname{tr}_A\rho_A^\alpha\right)\big|_{\alpha=1}\left(\operatorname{tr}_A\rho_A\right)^{-1}. \tag{1.47}$$

Definition 1.8. Given $\alpha \geq 0$ and $\alpha \neq 1$ we define Rényi entropy as

$$S_A^\alpha = \frac{1}{1-\alpha}\log\operatorname{tr}_A(\rho_A^\alpha). \tag{1.48}$$

Consider limit of Rényi entropy as $\alpha \to 1$

$$\lim_{\alpha\to 1} S_A^\alpha = \lim_{\alpha\to 1}\frac{1}{1-\alpha}\log\operatorname{tr}_A(\rho_A^\alpha) = -\frac{d}{d\alpha}\left(\log\operatorname{tr}_A\rho_A^\alpha\right)\big|_{\alpha=1}. \tag{1.49}$$

In the last equality we have used L'Hôpital's rule. Hence, Rényi entropy converges to entanglement entropy if reduced density matrix is properly normalized

$$S_A = \lim_{\alpha\to 1} S_A^\alpha. \tag{1.50}$$

1.3.4 Mutual information

Suppose we have two random variables X and Y and would like to know how much they have in common. In other words, how much information we can learn about X given that we know Y or vice versa. First, we have to consider a joint random variable (X, Y) with a joint probability distribution $p(x, y)$. We will denote the Shannon entropy of the joint variable $H(X, Y)$, i.e.

$$H(X,Y) = -\sum_{x,y} p(x,y)\log p(x,y). \tag{1.51}$$

Definition 1.9. *(Shannon) Mutual information* of two random variables is defined [53] to be

$$H(X:Y) = H(X) + H(Y) - H(X,Y). \tag{1.52}$$

Note that it vanishes for independent random variables when $p(x, y) = p(x)p(y)$ and is equal to $H(X)$ when Y is a function of X as expected for a measure of correlation between two random variables. Mutual information is not the only possible measure of correlation, for example often correlation coefficient is used $\frac{\operatorname{cov}(X,Y)}{\sigma_X\sigma_Y}$ which is very good at detecting linear dependence. On the other hand, mutual information is more suitable when relation between variables is more complicated.

We can similarly define mutual information for quantum systems [53]. Suppose we have systems A and B. There is a density matrix ρ_{AB} acting on a joint system $\mathcal{H}_A \otimes \mathcal{H}_B$ with the corresponding von Neumann entropy $S(A \cup B)$. Then (von Neumann) mutual information is defined to be

$$I(A:B) = S(A) + S(B) - S(A \cup B). \tag{1.53}$$

1.4 Entanglement Entropy in Quantum Field Theories

To define entanglement entropy in quantum field theories we consider a lattice with spacing a. For simplicity we will not consider gauge quantum field theories. To recover continuum limit we send $a \to 0$. Then powers of density matrix can be written as functional integral over n-sheeted Riemann surface (see [57–59] for detailed description). However, in this limit entanglement entropy diverges and has to be regularized with UV cutoff $\varepsilon_{\mathrm{UV}}$.

1.4.1 Path integrals

In quantum mechanics we usually describe single particle using states that satisfy the Schrödinger equation $i\partial_t |\psi\rangle = H|\psi\rangle$. Instead of using differential equation language we can rewrite Schrödinger equation as an integral equation for wavefunction $\psi(x,t) = \langle x|e^{-iHt}|\psi(0)\rangle$.

$$\psi(x,t) = \int K(x,x_0;t)\psi(x_0,0)\,dx_0, \tag{1.54}$$

where kernel of the integral is defined to be

$$K(x,x_0;t) = \langle x|e^{-iHt}|x_0\rangle\,. \tag{1.55}$$

In order to compute it we can discretize interval $[0,t]$ by splitting it in to n parts and compute $n \to \infty$ limit which is formally given by path integral [60]

$$K(x,x_0,t) = \int [\mathcal{D}x] e^{iS[x]}, \tag{1.56}$$

where $S[x] = \int_0^t L\,dt'$ is the action of the system. Since this integral is not always convergent, we usually consider analytic continuation to Euclidean time $t_E = it$ and calculate

$$\int [\mathcal{D}x] e^{S_E[x]}, \tag{1.57}$$

Path integral formulation is used to generalize quantum mechanics of particles to Quantum Field Theory. Instead of integrating over all possible paths that particle can take we need to integrate over all possible field configurations.

1.4.2 Matrix elements of density operators

Density operator ρ_A acts on fields ϕ in $\mathcal{H}_A$ and can be fully described by specifying its matrix elements. To calculate them we will use the ideas from subsection 1.4.1. Recall that thermal density matrix is given by (1.20), so its matrix elements are

$$\frac{1}{Z}\langle \phi_-|e^{\beta H}|\phi_+\rangle \tag{1.58}$$

which is entirely analogous to equation (1.55). In fact we see that thermal states must have periodic Euclidean time $t_E \sim t_E + \beta$.

Even when the state is not thermal in principle we can define modular Hamiltonian

$$K_A = -\log \rho_A \tag{1.59}$$

and then use path integral techniques with modular Hamiltonian. However, in practice it is usually impossible to find K_A since it is hard to compute log of an operator (similarly how we use replica trick for entanglement entropy and do not calculate it directly). Hence, we usually consider thermal states.

Matrix elements of density operator ρ_A acting on field ϕ in $\mathcal{H}_A$ is given by

$$\rho_A(\phi_-, \phi_+) = \frac{1}{Z} \int [\mathcal{D}\phi] e^{-S_E} \prod_{x \in A} \delta\left(\phi(t = 0^-) - \phi_-\right) \delta\left(\phi(t = 0^+) - \phi_+\right), \tag{1.60}$$

where S_E is the (Euclidean) action of the system and Z is the partition function required to impose condition $\operatorname{tr} \rho_A = 1$, i.e. given by the same path integral as in (1.60) with $\phi_- = \phi_+$.

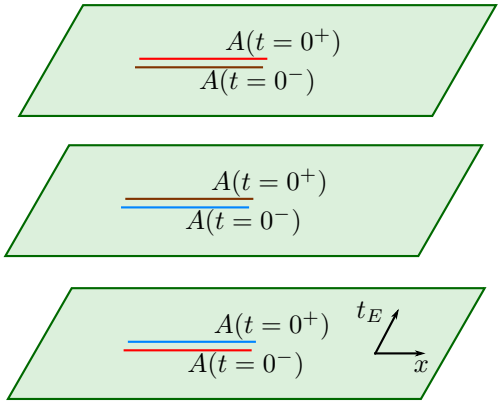

Figure 1.1: Three copies of Euclidean plane for computing $\operatorname{tr} \rho_A^3$. Intervals of the same colour are identified. The region on the first plane at time 0^+ is identified with its copy on the second plane at time 0^- and so on. Finally, the region in the last plane is identified with the region in the first plane to compute trace.

Powers of density operator can be computed by replicating manifold in which we are doing calculation. We will label different copies of fields $\phi_\pm$ as $\phi_\pm^{(i)}$. To compute ρ^n we glue n copies of our manifold by identifying $\phi_+^{(i)} = \phi_-^{(i+1)}$. Finally, to compute $\operatorname{tr} \rho^n$ we identify $\phi_-^{(1)} = \phi_+^{(n)}$ and calculate path integral over the whole n-sheeted Riemann surface.

$$\operatorname{tr} \rho_A^n = \frac{1}{Z^n} \int [\mathcal{D}\phi] e^{-S_E}. \tag{1.61}$$

The pictorial representation of the geometry on which we are integrating equation (1.61) is in Figure 1.1.

This is enough to compute Rényi entropy for integer values of $n > 1$. If Rényi entropies do not grow too fast at ∞ then we can analytically continue it away from integer values using Carlson's theorem[3] [61, 62] and then find limit $n \to 1$.

1.5 Holographic Entanglement Entropy

Entanglement entropy is often hard to compute even in conformal field theories. AdS/CFT duality can be used to calculate entanglement entropy in CFTs with holographic duals. The Ryu-Takayanagi (RT) proposal [58, 63] states that

$$S_A = \frac{\operatorname{Area}(\gamma_A)}{4G_N}, \tag{1.62}$$

[3] According to Carlson's theorem two distinct analytic functions that do not grow too fast cannot coincide at all integer points.

where γ_A is codimension 2, static minimal surface attached to the boundary of A. So to find this surface we first pick a constant time slice $t = t_0$. In this codimension 1 subspace pick surfaces anchored to ∂A and find the minimal surface that is homologous to the boundary. In order to deal with divergences in entanglement entropy we introduce UV cutoff $r = r_\infty$ and attach minimal surface there.

Ryu-Takayanagi proposal was generalized to non static spacetimes by Hubeny, Rangamani and Takayanagi (HRT) [64]. Instead of looking for minimal surfaces on a constant time slice, one has to look for extremal codimension 2 spacelike surfaces in the whole spacetime that are attached to the boundary at the points with the same time coordinate. Away from the boundary the surface is not restricted to constant time slice unlike in the Ryu-Takayanagi proposal.

Arguments for correctness of RT formula for spherical surfaces in vacuum were given in [65]. Later, RT formula was proven for $U(1)$ invariant geometries in [66]. The calculation was generalized by using Schwinger-Keldysh formalism[4] for time dependent quantum states in [68], hence deriving HRT proposal.

Some of the properties of entanglement entropy become trivial or fairly easy to prove in the holographic setup. For example, for zero-temperature states entanglement entropy of an area and its complement $\bar{A}$ are equal but this fails for thermal states. In empty AdS space A and $\bar{A}$ share their boundary and have the same minimal surface. But thermal states correspond to a black hole in the bulk. As can be seen in Figure 1.2, there are two minimal surfaces anchored to the same points but only one of them can be continuously deformed into either A or $\bar{A}$.

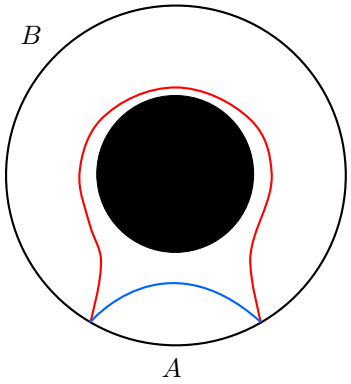

Figure 1.2: Minimal surface anchored to regions A (blue) and B (red) in the presence of black hole.

Another interesting property is *strong subadditivity*

$$S(A) + S(B) \geq S(A \cup B) + S(A \cap B). \tag{1.63}$$

Direct proof of this inequality using properties of density operators can be found in [69]. But a much simpler holographic proof is presented in [70].

Note that it follows that mutual information cannot be negative

$$I(A : B) = S(A) + S(B) - S(A \cup B) \geq 0. \tag{1.64}$$

1.5.1 Entanglement Entropy in anti-de Sitter space

One of the simplest applications of Ryu-Takayanagi proposal is the entanglement entropy in $d + 2$ dimensional AdS spacetime [58]. The metric of this space in Poincaré coordinates is

$$ds^2 = \frac{1}{z^2}\left(dz^2 - dt^2 + \sum_{i=1}^{d-1} dx_i^2\right), \tag{1.65}$$

[4]The Schwinger-Keldysh formalism generalizes unitary time evolution operators to non-equilibrium states by removing the assumption that the ground state remains unchanged (up to a phase) during time evolution [67].

where we use the units in which the radius of AdS is $R = 1$.

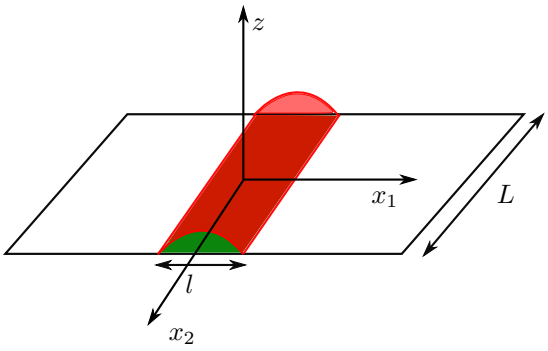

Figure 1.3: Minimal surface (red) anchored to the straight belt (green) in AdS_4.

Suppose we pick region A to be a straight belt, so $-l/2 < x_1 < l/2$ and x_i are unbounded for $i > 1$ but we can regularize these dimensions with some large length scale L. We choose a spatial slice $t = \text{const}$. Then the area of a surface anchored to this boundary is

$$A = L^{d-1} \int_{-l/2}^{l/2} \frac{\sqrt{1 + (\frac{dz}{dx_1})^2}}{z^d}\, dx_1. \tag{1.66}$$

The functional does not depend on x_1, so there is a conserved charge that simplifies the resulting ODE to

$$\frac{dz}{dx_1} = \frac{\sqrt{z_\star^{2d} - z^{2d}}}{z^d} \tag{1.67}$$

where $z_\star$ is the unique turning point. Equation (1.67) can be integrated to find $z_\star$

$$z_\star = \frac{l}{2} \frac{\Gamma(\frac{1}{2d})}{\Gamma(\frac{d+1}{2d})\sqrt{\pi}}. \tag{1.68}$$

Now we can evaluate (1.66). To calculate it we have to change integration variable to z and introduce a cut-off at $z = \varepsilon_{\text{UV}}$.

$$A = 2L^{d-1} \int_{\varepsilon_{\text{UV}}}^{z_\star} \frac{z_\star^d}{z^d \sqrt{z_\star^{2d} - z^{2d}}}\, dz. \tag{1.69}$$

$$A = 2R^d \left(\frac{L}{z_\star}\right)^{d-1} \int_0^1 \frac{1}{y^d} \left(\frac{1}{\sqrt{1 - y^{2d}}} - 1\right) dy + 2R^d \left(\frac{L}{z_\star}\right)^{d-1} \int_{\varepsilon_{\text{UV}}/z_\star}^1 \frac{1}{y^d}\, dy. \tag{1.70}$$

Then for $d > 1$ the entanglement entropy $S = A/4$ is given by

$$S = \frac{1}{2(d-1)} \left(\frac{L}{\varepsilon_{\text{UV}}}\right)^{d-1} - \frac{2^{d-2}\pi^{d/2}}{d-1} \left(\frac{\Gamma(\frac{d+1}{2d})}{\Gamma(\frac{1}{2d})}\right)^d \left(\frac{L}{l}\right)^{d-1}. \tag{1.71}$$

Here, the divergent term is proportional to the area of the boundary ∂A which is typical for many examples. AdS_3 is the notable exception. The second term in (1.70) gives rise to logarithmic divergence and entropy is equal to

$$S = \frac{R}{2} \log \frac{l}{\varepsilon_{\text{UV}}}. \tag{1.72}$$

Note that the answer depends on the geometry of the entanglement region, for example entanglement entropy for spherical regions was discussed in [58] where behaviour of divergent terms depends on dimension being even or odd.

1.5.2 BTZ black hole

It was long believed that three dimensional gravity does not contain any black hole solutions. Surprisingly a very simple black hole solution was found in Einstein gravity with a negative cosmological constant [71, 72]. The metric of rotating BTZ is given by

$$ds^2 = -\frac{(r^2-r_+^2)(r^2-r_-^2)}{R^2r^2}dt^2 + \frac{R^2r^2}{(r^2-r_+^2)(r^2-r_-^2)}dr^2 + r^2\left(d\phi - \frac{r_+r_-}{Rr^2}dt\right)^2, \qquad (1.73)$$

where $\phi \sim \phi + 2\pi$ is periodic and R is the radius of AdS.

BTZ black hole has many of the features of its 4 dimensional analogue, Kerr-AdS black hole [73]. In particular, it has both inner and outer horizons, has no hair[5] [74, 75] and its entropy is proportional to the outer circumference.

In three dimensions it follows from Einstein equations that in vacuum where $T^{\mu\nu} = 0$ the spacetime curvature is constant. Therefore, BTZ black hole is locally AdS_3. In fact it can be obtained by a discrete identification of AdS_3 space [72]. Hence, many calculations that are hard in four dimensional black holes are much easier in BTZ.

1.5.3 Gravity dual description of TFD state

TFD state is especially interesting for two dimensional CFTs. It was proposed to be dual to the eternal BTZ black hole [77]. Each of the CFTs corresponds to the boundary of eternal BTZ black hole.

Euclidean path integral that prepares TFD state is defined [78] on the cylinder of length $\beta/2$. The path integral has two cuts (two circles at each end of the cylinder) that define states in two CFTs. According to AdS/CFT we must match CFT partition function to Euclidean partition function in the bulk as in equation (1.14). This is satisfied by half of the Euclidean black hole (black hole where Euclidean time is restricted to $[0, \frac{\beta}{2}]$). This state is then interpreted [77] as Hartle-Hawking-Israel [79, 80] state of eternal BTZ where spacetime with time reflection symmetry at $t = 0$ is sliced into two halves, the metric of one part is glued to Euclidean metric of the other part. In this construction Euclidean part is interpreted as construction of the initial wavefunction which later evolves in Lorentzian time.

Hamiltonian of the total TFD state can be chosen but there are two natural choices that are discussed by J. Maldacena and L. Susskind in [81]. Let t_- be the time in the left CFT and t_+ in the right CFT (see Figure 1.4). Then we have

- $H = H_L \otimes \mathbb{I}_L - \mathbb{I}_R \otimes H_R$. $t_- = t_+ = t$,
- $H = H_L \otimes \mathbb{I}_L + \mathbb{I}_R \otimes H_R$. $t_- = -t_+ = t$,

where H_L is the Hamiltonian for CFT_L and H_R for CFT_R. The first choice $H = H_L - H_R$ corresponds to a single eternal black hole in a bulk. The second Hamiltonian $H = H_L + H_R$ describes two AdS-Schwarzschild black holes.

1.6 Scrambling

Consider a system in thermal equilibrium. If we perturb it, it is natural to ask whether the system will get back to thermal equilibrium, i.e. thermalizes, and if so, how quickly. We can ask this question locally, in the sense that correlations between two local subsystems behave as if they were in thermal equilibrium. If these subsystems behave in this way, we say they are scrambled, in the sense that the details of the perturbation were scrambled. If this situation

[5] I.e. BTZ black hole is uniquely specified by two numbers such as mass M and angular momentum J or radii of inner and outer horizons.

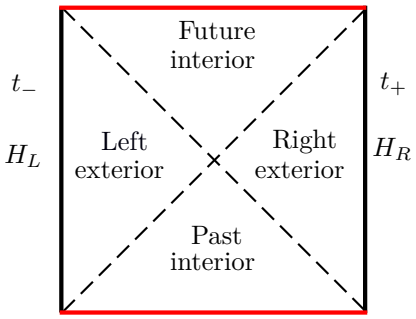

Figure 1.4: Bulk interpretation of TFD state.

occurs, we can introduce the scrambling time $t_\star$ as the time scale it takes to achieve this from the occurrence of the perturbation. For many systems with N degrees of freedom in d dimensions, scrambling time takes form of power law in N, e.g. if interaction happens via diffusion then scrambling time is larger than $c(\beta)N^{2/d}$ [82] where $c(\beta)$ is some constant depending on the temperature.

Susskind et. al. gave some evidence that the scrambling time for the Schwarzschild black hole is $t_\star \sim \frac{\beta}{2\pi}\log S$, where S is the Bekenstein-Hawking entropy of the black hole. They interpreted the logarithmic behaviour as the limit of $d \to \infty$ in the many body scrambling by diffusion mentioned above. They conjectured that this behaviour is true for all black holes and that there are no faster scramblers in nature. They also provided some microscopic intuition as for why this may happen by discussing the D0-brane quantum mechanics and how the interaction between the physical degrees of freedom encoded in the matrix elements of the matrix model may capture this fast scrambling behaviour.

Note that in some cases system can relax to equilibrium much faster. When system is perturbed by linear perturbations, its relaxation to equilibrium is described by quasi normal modes. For BTZ black hole the quasi normal mode frequencies are found in [83]. As we go to the higher modes, the relaxation time that is determined by the imaginary part of the frequency $\Im(\omega) = -2\sqrt{M}n, n \in \mathbb{N}$. So relaxation time is of order β/n and is much smaller than $t_\star$.

An interesting property of thermal systems is that they seem to be chaotic [84]. In quantum mechanics this is known as the Eigenstate Thermalization Hypothesis [85] and was verified for many different systems but there is no general proof [13]. If we start with two similar initial states, then under a time evolution they evolve into very different states. At the same time, density matrix of some small subsystem approaches thermal density matrix.

There are a few ways to estimate scrambling time. One way is to look at the entanglement between two subsystems and how it evolves in time. If entanglement pattern was specific to the initial state and not typical then scrambling would destroy it [84, 86] and two subsystems A and B would decouple, so that $S(A\cup B) = S(A)+S(B)$ (recall that entanglement entropy is additive for independent systems). Looking at when two subsystems decouple allows us to have a local notion of scrambling. Subsystems A and B return to equilibrium but globally the whole system is not in equilibrium. As we will see later, in two dimensions local perturbations tend to create two (non-decaying) energy lumps that are forever traveling in opposite directions. Such system would never relax to equilibrium but locally finite subsystem would look thermal after some time. This motivates the following definition.

Definition 1.10. *Scrambling time* is the minimal time $t_\star$ after perturbation when mutual information vanishes

$$I_{A:B}(t_\star) = 0. \tag{1.74}$$

In this thesis we will be following definition (1.74). However, it is not the only way to quantify scrambling. We can look directly at chaotic behaviour of thermal correlators [87] and

consider

$$C(t) = \langle [W(t), V(0)]^2 \rangle_\beta = \frac{1}{Z} \operatorname{tr} \left(e^{-\beta H} [W(t), V(0)]^2 \right) \tag{1.75}$$

This quantifies the perturbation on W at time t caused by measuring V at time $t = 0$. So in a chaotic system initially we expect it to be small and later start growing.

For technical reasons in conformal field theories it is easier to estimate related quantity (often called out of order correlator)

$$\langle VW(t)VW(t) \rangle_\beta \tag{1.76}$$

which for general operators V and W decays exponentially [88]

$$\frac{\langle VW(t)VW(t) \rangle_\beta}{\langle VV \rangle_\beta \langle W(t)W(t) \rangle_\beta} \approx 1 - \frac{1}{c} e^{\lambda_L t} f(x) + \dots \tag{1.77}$$

where c is the central charge of CFT (see chapter 2 for more details) and represents degrees of freedom in a CFT, $f(x)$ is a function independent of time. In thermal systems Lyapunov exponent λ_L satisfies bound [87]

$$\lambda_L \leq \frac{2\pi}{\beta}. \tag{1.78}$$

and the bound is saturated in Einstein gravity. It follows from equations (1.77) and (1.78) that decay becomes significant at timescale $\frac{\beta}{2\pi} \log c$. The time the decay of out of order correlator becomes significant is another way to define scrambling time.

In Einstein gravity out of order correlators can be interpreted as scattering of a particle in the presence of another energetic particle. This gives rise to shock-wave geometries discussed in [84, 89–91].

1.7 Summary of the thesis

In chapter 2 we will discuss conformal symmetry and conformal field theories. We will look at how conformal symmetry fixes two and three point functions. Then infinite dimensional local conformal transformations will be introduced for two dimensional CFT. Key concepts of 2D CFTs such as stress energy tensor, central charge and operator product expansions will be introduced too. Rényi entropy will be calculated for locally perturbed vacuum state. Finally, we will describe some concepts that are useful in deriving the results of this thesis such as twist operators or four point functions in large c limit.

In chapter 3 we will calculate holographic entanglement entropy of spinning BTZ black hole by directly employing covariant Hubeny-Rangamani-Takayanagi proposal.

In chapter 4 locally perturbed thermal states are considered. We will perturb thermal state and calculate energy momentum tensor for such states. Then we will investigate second Rényi entropy and mutual information for two models. First is a two dimensional CFT with a single boson. Second is any two dimensional CFT in a large c limit.

In chapter 5 we will calculate von Neumann entropy and mutual information for large c CFTs using twist operators and approximation for four point functions with two heavy and two light operators. Then we will compute scrambling and discuss validity of our results. We will also do the same calculation in the bulk gravitational theory. A free falling particle model will be described. We will calculate a back-reaction of a massive free falling particle on the geometry of BTZ black hole. Then we will find the length of spacelike geodesics in the back-reacted geometry.

In chapter 6 we will generalize results from chapter 5 to the case of rotating BTZ.

In chapter 7 we will summarize the results of this thesis and discuss possible future work.

Chapter 2

Conformal Field Theory

Conformal field theories arise in a variety of situations in physics [92]. For example, condensed matter systems that are close to phase transition exhibit scale invariant behaviour. In particle physics, if typical energy scale of processes is much higher than mass of interacting particles then we can approximate it with scale invariant theory of massless particles. Moreover, two dimensional CFT is a fundamental building block of string theory. We saw in chapter 1 that quantum field theories that appear in standard setups of AdS/CFT correspondence are conformal.

Since the conformal symmetry is larger than the Poincaré symmetry for a fixed dimension, observables are further constrained by kinematic considerations. This is even more so in two dimensions, where the local symmetry algebra is infinite dimensional, as first pointed out in [42]. This feature makes 2d CFTs, especially in their large c limit, as theoretical laboratories where some further analytic control can be achieved.

In this chapter, we will review some basic features of 2d CFTs that will be useful later in the thesis. In particular, besides introducing the main classical and quantum properties of basic operators, we will quote relevant results for 4-pt functions in the large c limit, calculations of entanglement entropy in 2d CFTs in a ground state and some analytic properties of the thermofield double state.

2.1 The Conformal Group

The conformal group is the set of d-dimensional spacetime transformations that preserve the metric up to some factor

$$g'_{\mu\nu}(x') = \Lambda(x) g_{\mu\nu}(x). \tag{2.1}$$

In particular, conformal group contains rotations, translations, dilations and special conformal transformations (2.10) (these can be thought as inversion followed by translation and another inversion [93] but inversion by itself is a discrete symmetry). In $d \geq 3$ dimensions the conformal group is isomorphic to $SO(d+1,1)$ and contains Poincaré group as a subgroup. Let us consider a scale transformation which is not part of Poincaré group. it is given by

$$x' = \lambda x. \tag{2.2}$$

For the sake of simplicity let us consider spinless fields. Under the scale transformation they transform as

$$\phi'(x') = \lambda^{-\Delta} \phi(x), \tag{2.3}$$

where Δ is the conformal dimension of the field and depends on which theory we are looking at. Under the general conformal transformation the field will then transform as

$$\phi'(x') = \left| \frac{\partial x'}{\partial x} \right|^{-\frac{\Delta}{d}} \phi(x) = \Lambda(x)^{-\frac{d}{2}} \phi(x), \tag{2.4}$$

where $\left| \frac{\partial x'}{\partial x} \right|$ is the Jacobian. Fields that transform under (2.4) are called *quasi-primary*.

Let us consider a free scalar field as an example. The action describing this field is

$$S = \int d^d x \; \partial_\mu \phi \, \partial^\mu \phi. \tag{2.5}$$

Action (2.5) will remain invariant under (2.2) and (2.3) if

$$d - 2 - 2\Delta = 0. \tag{2.6}$$

2.2 Conformal invariance of quantum fields

In Quantum Field Theories we usually work with observables called correlators or n-point functions

$$\langle \phi(x_1)\phi(x_2)\dots\phi(x_n)\rangle := \frac{1}{Z}\int \mathcal{D}\phi \; e^{-S[\phi]}\phi(x_1)\dots\phi(x_n). \tag{2.7}$$

Conformal invariance places a strong constraint on the form that (2.7) can take. Let us assume that action S and measure $\mathcal{D}\phi$ are conformally invariant[1]. Then two point function must transform as

$$\langle \phi(x_1)\phi(x_2)\rangle = \left|\frac{\partial x'}{\partial x}\right|^{\frac{\Delta_1}{d}}_{x=x_1} \left|\frac{\partial x'}{\partial x}\right|^{\frac{\Delta_2}{d}}_{x=x_2} \langle \phi(x_1')\phi(x_2')\rangle \,. \tag{2.8}$$

Poincaré invariance implies that $\langle \phi(x_1)\phi(x_2)\rangle$ can only depend on distance $x_{12} := |x_1 - x_2|$. This, together with (2.8) applied for dilations fixes two point function to be

$$\langle \phi(x_1)\phi(x_2)\rangle = \frac{C_{12}}{x_{12}^{\Delta_1+\Delta_2}}. \tag{2.9}$$

Conformal invariance under special conformal transformation

$$x'^\mu = \frac{x^\mu - b^\mu x^2}{1 - 2b\cdot x + b^2 x^2} \tag{2.10}$$

imposes additional requirement that C_{12} vanishes if $\Delta_1 \neq \Delta_2$. In this case, by redefining our fields we can always normalize $C_{12} = 1$. Hence [95],

$$\langle \phi(x_1)\phi(x_2)\rangle = \begin{cases} \dfrac{1}{x_{12}^{2\Delta_1}} & \text{if } \Delta_1 = \Delta_2, \\ 0 & \text{otherwise.} \end{cases} \tag{2.11}$$

The same arguments applied to three point function result [95] in

$$\langle \phi(x_1)\phi(x_2)\phi(x_3)\rangle = \frac{C_{123}}{x_{12}^{\Delta_1+\Delta_2-\Delta_3}\; x_{23}^{\Delta_2+\Delta_3-\Delta_1}\; x_{31}^{\Delta_3+\Delta_1-\Delta_2}}. \tag{2.12}$$

Unlike in the case of two point functions, we can no longer do field redefinition, so constants C_{123} depend on which particular conformal field theory we are looking at.

We saw that conformal invariance imposes very strong constraints on two and three point functions. However, this does not generalize to 4-point functions. The reason is that given four points we can construct cross-ratios that are invariant under conformal transformations, e.g.

$$\frac{x_{12}x_{34}}{x_{13}x_{24}}, \quad \frac{x_{12}x_{34}}{x_{23}x_{14}}. \tag{2.13}$$

so conformal invariance does not fix higher point functions.

[1] This does not always happen and failure to do so is called conformal anomaly [12, 94].

2.3 Two dimensional conformal field theory

In two dimensions we can use the tools available to us from complex analysis to understand conformal mappings. In order to do that let us complexify coordinates on the plane as

$$z = x + iy, \qquad \bar{z} = x - iy. \tag{2.14}$$

We can treat these z and $\bar{z}$ as two independent complex variables. So we went from $\mathbb{R}^2$ to $\mathbb{C}^2$ but in the end we will have to identify $\bar{z}$ with the complex conjugate z^* to get physical results.

Theorem 2.1 (Conformal mapping theorem [96])**.** If $f : D \to \mathbb{C}$ is analytic then f preserves angles at each point $z_0 \in D$ where $f'(z_0) \neq 0$.

A natural question is what is the group of conformal transformations f on $\mathbb{C}$. Liouville's theorem tells that f must be either constant or unbounded. So to have interesting conformal transformations we need to break analyticity at a point and consider functions on $\mathbb{C} \cup \{\infty\}$. The set of such transformations form the Möbius group

$$f(z) = \frac{az + b}{cz + d}, \tag{2.15}$$

where $a, b, c, d \in \mathbb{C}$ and $ad - bc = 1$ and hence isomorphic to $SL(2, \mathbb{C})/\mathbb{Z}_2$. In particular we can obtain arbitrary dilations, rotations and translations by $z \mapsto az + b$ and it contains inversion z^{-1}, so we can obtain special conformal transformations as well. As before, fields that transform via (2.4) are called quasi-primary. In two dimensions this definition also applies to fields with spin [95]. Let us define holomorphic and antiholomorphic conformal dimensions

$$h = \frac{\Delta + s}{2}, \qquad \bar{h} = \frac{\Delta - s}{2}. \tag{2.16}$$

Then quasi-primary fields transform under the Möbius transformations $z \mapsto f(z)$ and $\bar{z} \mapsto \bar{f}(\bar{z})$ as

$$\phi'(f(z), \bar{f}(\bar{z}) = f'(z)^{-h} \bar{f}'(\bar{z})^{-\bar{h}} \phi(z, \bar{z}). \tag{2.17}$$

We can go further and break analyticity at two points. Without the loss of generality they can be taken to be $z = 0$ and $z = \infty$. Then infinitesimal version of conformal transformation is given by Laurent series in some open neighbourhood around 0

$$z' = z + \epsilon(z) = z + \sum_{n \in \mathbb{Z}} \epsilon_n z^{n+1}. \tag{2.18}$$

and similarly for $\bar{z}$.

Definition 2.1. The fields that transform like (2.17) under local conformal transformations (2.18) are called *primary fields*.

Infinitesimal transformation of primary field is given by [93, 95].

$$\delta\phi = -\epsilon(z)\frac{\partial \phi}{\partial z} - \bar{\epsilon}(\bar{z})\frac{\partial \phi}{\partial \bar{z}}. \tag{2.19}$$

From these two equations we can read off generators corresponding to infinitesimal conformal transformation

$$l_n = -z^{n+1}\frac{\partial}{\partial z}, \tag{2.20}$$

$$\bar{l}_n = -\bar{z}^{n+1}\frac{\partial}{\partial \bar{z}}. \tag{2.21}$$

These form two copies of an infinite dimensional Witt algebra $[l_n, l_m] = (n - m)l_{n+m}$ [97]. When we consider quantum fields we get Virasoro algebra

$$[L_n, L_m] = (n - m)L_{n+m} + \frac{c}{12}(n^3 - n)\delta_{n+m,0}, \tag{2.22}$$

where constant c is the central charge that will be discussed later. So, Virasoro algebra is the central extension of Witt algebra.

Note that l_{-1}, l_0, l_1 generate translations, rotations and special conformal transformations that give rise to Möbius transformations, so every primary operator is also a quasi-primary operator.

2.3.1 Correlation functions in 2D CFT

The expressions for correlation functions in equations (2.11) and (2.12) in two dimensional CFT can be written in complex coordinates. Suppose we have primary fields ϕ_1 and ϕ_2 with *equal* conformal dimensions $h_1 = h_2 = h$ and $\bar{h}_1 = \bar{h}_2 = \bar{h}$. Then two point function is given by

$$\langle \phi_1(z_1, \bar{z}_1), \phi_2(z_2, \bar{z}_2) \rangle = \frac{1}{z_{12}^{2h} \bar{z}_{12}^{2\bar{h}}}. \tag{2.23}$$

Three point functions can be written in complex coordinates analogously. However, four point functions in 2D CFT are a bit simpler. Given 4 points there is just one independent cross ratio

$$z = \frac{z_{12} z_{34}}{z_{13} z_{24}}, \tag{2.24}$$

and with the help of Möbius transformation we can always map four arbitrary points to $\infty, z, 1, 0$.

Definition 2.2. Canonical four point function $G(z, \bar{z})$ is defined to be

$$G(z, \bar{z}) = \lim_{z_4, \bar{z}_4 \to \infty} z_4^{2h} \bar{z}_4^{2\bar{h}} \left\langle \phi_1(z_4, \bar{z}_4) \phi_2(z, \bar{z}) \phi_3(1, 1) \phi_4(0, 0) \right\rangle. \tag{2.25}$$

One of the interesting features of CFTs was discovered by Wilson and Zimmermann [98]. Suppose we have CFT with all of its operators $\mathcal{O}_k$. Then we can replace any pair of operators in any n-point function with absolutely convergent sum

$$\mathcal{O}_i(z, \bar{z}) \mathcal{O}_j(w, \bar{w}) = \sum_k C_{ij}^k (z - w, \bar{z} - \bar{w}) \mathcal{O}_k(w, \bar{w}). \tag{2.26}$$

In general this expansion is singular in the $w \to z$ limit. For quasi primary operators we can write it as [95]

$$\mathcal{O}_1(z) \mathcal{O}_2(w) = \sum_{n \in \mathbb{Z}} \frac{\mathcal{C}_n(w)}{(z - w)^n}. \tag{2.27}$$

Expressions like (2.26), (2.27) are called Operator Product Expansion (OPE) and are particularly interesting when one of the operators is energy-momentum tensor.

2.3.2 Energy-momentum tensor

Two dimensional conformal field theory must have a symmetric energy momentum tensor just like other QFTs

$$T^{\mu\nu} = -\frac{2}{\sqrt{-g}} \frac{\delta S}{\delta g_{\mu\nu}}. \tag{2.28}$$

This is a quasi-primary operator, so it only transforms as a tensor under Möbius transformations.

Let us consider a scale transformation $g_{\mu\nu} \mapsto (1 + \epsilon) g_{\mu\nu}$. Then

$$\delta S = -\frac{1}{2} \int d^2x \sqrt{-g} T^{\mu\nu} \delta g_{\mu\nu} = -\frac{1}{2} \int d^2x \sqrt{-g} \epsilon T_\mu^\mu. \tag{2.29}$$

So in order to have invariance of the action $\delta S = 0$ we must require tracelessness of stress-energy tensor

$$T_\mu^\mu = 0. \tag{2.30}$$

Hence, in two dimensions $T_{\mu\nu}$ has two independent components. In addition, conservation equation $\partial_\mu T^{\mu\nu} = 0$ states that $\partial_{\bar{z}} T_{zz} = 0$. So in complex coordinates we can define holomorphic and antiholomorphic components of energy momentum tensor

$$T := -T_{zz}(z), \qquad \bar{T} := -T_{\bar{z}\bar{z}}(\bar{z}). \tag{2.31}$$

Let us look at OPEs of primary field $\mathcal{O}$ whose conformal dimensions are h and $\bar{h}$ with T and $\bar{T}$. It can be shown that OPE terminates at $(z-w)^{-2}$ term [95]

$$T(z)\mathcal{O}(w,\bar{w}) = h\frac{O(w,\bar{w})}{(z-w)^2} + \frac{\partial_w O(w,\bar{w})}{z-w} + \text{finite terms}, \tag{2.32}$$

$$\bar{T}(\bar{z})\mathcal{O}(w,\bar{w}) = \bar{h}\frac{O(w,\bar{w})}{(\bar{z}-\bar{w})^2} + \frac{\partial_{\bar{w}} O(w,\bar{w})}{\bar{z}-\bar{w}} + \text{finite terms}. \tag{2.33}$$

So primary fields have a fairly simple OPE. Another interesting example is energy momentum tensor with itself. It follows from conformal symmetry [95] that two point function must terminate at $(z-w)^{-4}$ term. However, this quartic term is dependent on the theory

$$T(z)T(w) = \frac{c/2}{(z-w)^4} + \frac{2T(w)}{(z-w)^2} + \frac{\partial_z T(w)}{z-w} + \text{finite terms}, \tag{2.34}$$

where constant c is called *central charge*. We can similarly define $\bar{c}$ via OPE of $\bar{T}\bar{T}$. Equation (2.34) shows that T is only quasi-primary operator with conformal dimension $h = 2$. Hence, T does not transform as tensor under local conformal transformations [95]

$$T'(w) = \left(\frac{dw}{dz}\right)^{-2}\left(T(z) - \frac{c}{12}\{w;z\}\right), \tag{2.35}$$

where *Schwarzian derivative* is defined as

$$\{w;z\} = \frac{w'''}{w'} - \frac{3}{2}\left(\frac{w''}{w'}\right)^2. \tag{2.36}$$

2.3.3 Free boson field

Let us consider a free scalar field whose action is

$$S = \frac{g}{2}\int d^2x\, \partial_\mu\phi\, \partial^\mu\phi \equiv \frac{g}{2}\int dz d\bar{z}\, \partial_z\phi\, \partial_{\bar{z}}\phi, \tag{2.37}$$

where g is a normalization constant and can be fixed later.

The equation of motion is

$$\partial_z\partial_{\bar{z}}\phi = 0. \tag{2.38}$$

Thus the solution splits into holomorphic and antiholomorphic parts

$$\phi(z,\bar{z}) = \phi_L(z) + \phi_R(\bar{z}). \tag{2.39}$$

Similarly, two point function for free boson also splits into modes and is equal to [93]

$$\langle\phi(z,\bar{z})\phi(w,\bar{w})\rangle = -\frac{1}{4\pi g}\left(\log(z-w) + \log(\bar{z}-\bar{w})\right). \tag{2.40}$$

This also shows that free boson is not a primary operator. But, for example, $\partial_z\phi$ or $\partial_{\bar{z}}\phi$ are primary operators and with correlator is given by

$$\langle\partial_z\phi(z,\bar{z})\partial_w\phi(w,\bar{w})\rangle = -\frac{1}{4\pi g}\frac{1}{(z-w)^2}. \tag{2.41}$$

Energy momentum tensor for free boson is

$$T_{\mu\nu} = \lambda \left(\partial_\mu \phi \, \partial_\nu \phi - \frac{1}{2} \eta_{\mu\nu} \partial_\lambda \phi \, \partial^\lambda \phi \right). \tag{2.42}$$

This can be rewritten in complex coordinates. Note that quantized energy momentum tensor also needs normal ordering, so that vacuum expectation value vanishes [95]

$$T(z) = -g{:}\partial\phi\partial\phi{:}, \tag{2.43}$$

where normal ordering is defined to be

$$:\partial\phi\partial\phi: = \lim_{w \to z} \left(\partial\phi(z)\partial\phi(w) - \langle \partial\phi(z)\partial\phi(w) \rangle \right). \tag{2.44}$$

So OPE of T with itself is

$$T(z)T(w) = -g^2 {:}\partial\phi(z)\partial(z)\phi{::}\partial\phi(w)\partial\phi(w){:} \tag{2.45}$$

$$= \frac{1}{2} \frac{1}{(z-w)^4} + \frac{2T(w)}{(z-w)^2} + \frac{\partial T(w)}{z-w} + \text{finite terms}. \tag{2.46}$$

Hence, this theory has central charge $c = 1$. Had we considered a theory with two boson fields ϕ and ψ, T would have terms corresponding to both fields and we would have obtained $c = 2$. So central charge c scales with the number of fields although not every field contributes 1, e.g. fermions contribute $\frac{1}{2}$.

2.4 Entanglement entropy in 2D CFT

Let us consider some examples of states in 2D CFT and calculate Rényi entropy of an interval of length L on a plane. One of the special features of conformal field theories is that each local operator in the CFT corresponds to the state and vice versa, so in order to uniquely specify the state it is enough to give operator and the point where operator is inserted [100]. Suppose we want to insert operator $\mathcal{O}$ at point $-l$. Then we can construct a state

$$|\Psi\rangle = \mathcal{N} \mathcal{O}(-l, t) \, |0\rangle \,, \tag{2.47}$$

where $\mathcal{N}$ is the normalization factor to ensure $\mathrm{tr}(\rho) = 1$. This state has a corresponding density matrix [101, 102]

$$\rho(t) = e^{-iHt} e^{\epsilon H} \mathcal{O}^\dagger(-l, t) \, |0\rangle \, \langle 0| \, \mathcal{O}(-l, t) e^{-\epsilon H} e^{iHt}, \tag{2.48}$$

where smearing parameter ϵ is required to regularize density matrix [103]. As we saw earlier, when points in the OPE of local operator approach one another, there is a pole. It is even more apparent how ϵ separates operator insertion points in complex coordinates $(w, \bar{w}) = (x + i\tau, x - i\tau)$ where τ is Euclidean time. Then operator is inserted at points

$$w_1 = \quad i(\epsilon - it) - l, \qquad w_2 = -i(\epsilon + it) - l, \tag{2.49}$$

$$\bar{w}_1 = -i(\epsilon - it) - l, \qquad \bar{w}_2 = \quad i(\epsilon + it) - l. \tag{2.50}$$

Then density matrix takes form

$$\rho = \mathcal{N} \mathcal{O}(w_2, \bar{w}_2) \, |0\rangle \, \langle 0| \, \mathcal{O}^\dagger(w_1, \bar{w}_1). \tag{2.51}$$

According to replica trick we need to trace out region $A = [0, L]$ in n copies of the plane that we will denote $\mathcal{R}_n$. Then the difference of Rényi entropy between excited and ground state is [101]

$$\Delta S_A^{(n)} = \frac{1}{1-n} \log \frac{\mathrm{tr}(\rho_A^n)}{\mathrm{tr}(\rho_A^{(0)})^n} = \frac{1}{1-n} \log \left[\frac{\langle \mathcal{O}(w_1, \bar{w}_1) \mathcal{O}^\dagger(w_2, \bar{w}_2) ... \mathcal{O}^\dagger(w_{2n}, \bar{w}_{2n}) \rangle_{\mathcal{R}_n}}{\left(\langle \mathcal{O}(w_1, \bar{w}_1) \mathcal{O}^\dagger(w_2, \bar{w}_2) \rangle_{\mathcal{R}1} \right)^n} \right]. \tag{2.52}$$

Let us focus on the case $n = 2$ when we have two planes glued along the branch cut A. We

can map this manifold to a single plane using a conformal transformation [102]

$$\frac{w}{w-L} = z^2, \tag{2.53}$$

Map (2.53) maps insertion points w_1 and w_2 to

$$z_1 = -z_3 = \sqrt{\frac{l-t-i\epsilon}{l+L-t-i\epsilon}} \tag{2.54}$$

$$z_2 = -z_4 = \sqrt{\frac{l-t+i\epsilon}{l+L-t+i\epsilon}}. \tag{2.55}$$

We can use Möbius transformation to map these points to $0, 1, \infty$ and cross ratio z_A

$$z_A \equiv \frac{z_{12}z_{34}}{z_{13}z_{24}} = \frac{1}{2}\left(1 - \frac{z_1^2+z_2^2}{2z_1z_2}\right), \tag{2.56}$$

where in the last equality we used that $z_3 = -z_1$ and $z_4 = -z_2$. Note that all dependence on time and geometry of the problem (i.e. length of the entanglement interval L) is encoded in cross ratios z_A and $\bar{z}_A$. In the limit $\epsilon \to 0$ when perturbation is small cross ratios

$$\lim_{\epsilon\to 0}(z_A, \bar{z}_A) = \begin{cases} (1,0) & \text{when} \quad l < t < L + l, \\ (0,0) & \text{otherwise.} \end{cases} \tag{2.57}$$

In other words cross ratio z_A does not vanish when perturbation is traveling in the region of entanglement A.

Four point function in (2.52) transforms under conformal map (2.53) as [102]

$$\langle \mathcal{O}(w_1,\bar{w}_1)\mathcal{O}^\dagger(w_2,\bar{w}_2)\mathcal{O}(w_3,\bar{w}_3)\mathcal{O}^\dagger(w_4,\bar{w}_4)\rangle_{\mathcal{R}_2} = (4L)^{-8h}\left|\frac{(z_1^2-1)(z_2^2-1)}{z_1z_2}\right|^{8h} G(z_A,\bar{z}_A). \tag{2.58}$$

Thus for *any* two dimensional CFT we can write

$$\Delta S_A^{(2)} = -\log\left(|z_A(1-z_A)|^{4h} G(z_A,\bar{z}_A)\right). \tag{2.59}$$

Let us now consider an example with $c = 1$. Given a free boson $\phi(z,\bar{z})$ we can consider a state excited with one of these primary operators

$$\mathcal{O}_1 = e^{i\phi/2}, \qquad \mathcal{O}_2 = \frac{1}{\sqrt{2}}\left(e^{i\phi/2} + e^{-i\phi/2}\right). \tag{2.60}$$

Such systems were considered in [102] and they found that

$$G_1(z,\bar{z}) = \frac{1}{\sqrt{|z(1-z)|}}, \tag{2.61}$$

$$G_2(z,\bar{z}) = \frac{1}{\sqrt{|z(1-z)|}}(|z| + 1 + |1-z|). \tag{2.62}$$

So operator $\mathcal{O}_1$ gives rise to vanishing Rényi entropy since $z_A \to 0$ (in fact all Rényi entropies $\Delta S_A^{(n)}$ vanish [101]). But Rényi entropy does not vanish for operator $\mathcal{O}_2$ when perturbation travels in the region A

$$\Delta S_A^{(2)} = \log 2 \quad \text{when} \quad l < t < L + l. \tag{2.63}$$

So Rényi entropy matches the one of the maximally entangled state in two level system in quantum mechanics. Later, in chapter 4 we will look at energy momentum tensor for locally excited states and confirm interpretation of this state as entangled Einstein-Podolsky-Rosen (EPR) pair [104].

2.5 Some useful results in 2D CFTs

2.5.1 Twist operators

We saw an example how Rényi entropy can be computed on n-sheeted Riemann surface. Suppose our branch cut is an interval $A = [L_1, L_2]$. Then, following (2.53) we can map L_1 and L_2 to 0 and ∞ by using the following Möbius map

$$f(w) = \frac{w - L_1}{w - L_2}. \tag{2.64}$$

Now, we can map it to $\mathbb{C}$ plane simply by taking n^{th} root [57]

$$z = f(w)^{\frac{1}{n}}. \tag{2.65}$$

An alternative way to calculate Rényi entropy is to start with a field that lives on a complex plane and promote it to live on each of n-copies of the plane, i.e. consider CFT on cyclic orbifold $\mathbb{C}^n/\mathbb{Z}_n$ (c.f. equation (1.61) where we compute $\operatorname{tr}\rho^n = \frac{Z_n}{Z^n}$). Then gluing along the boundary can be implemented by inserting primary twist operators at the ends of branch cut. Their role is to create conical defects that are equivalent to computing (2.65). Then partition function of orbifolded theory can be computed as correlator of twist operators [57, 105, 106].

We can read off conformal dimension of twist operators from transformation properties (2.35) of energy momentum operator. Let us assume that $\langle T(z)\rangle_{\mathbb{C}} = 0$. Then [57]

$$\langle T(w)\rangle_{\mathcal{R}_n} = \frac{c}{12}\{z, w\} = \frac{c}{24}\left(1 - \frac{1}{n^2}\right)\frac{(L_1 - L_2)^2}{(w - L_1)^2(w - L_2)^2}. \tag{2.66}$$

Finally, compare it to $\langle T(w)\sigma(L_1)\tilde{\sigma}(L_2)\rangle_{\mathbb{C}}$ which is fixed by conformal invariance to read off conformal dimensions of twist operators

$$H_\sigma = \frac{cn}{24}\left(1 - \frac{1}{n^2}\right). \tag{2.67}$$

Therefore,

$$\operatorname{tr}\rho_A^n \sim \left(\frac{L_2 - L_1}{\epsilon_{\text{UV}}}\right)^{-4H_\sigma}. \tag{2.68}$$

Therefore, in a two dimensional CFT with entanglement interval A the entanglement entropy is

$$S_A = 2 \cdot 4 \cdot \frac{c}{24}\log\frac{L_2 - L_1}{\epsilon_{\text{UV}}} = \frac{c}{3}\log\frac{L_2 - L_1}{\epsilon_{\text{UV}}}, \tag{2.69}$$

which matches the result in AdS_3 given in (1.72).

2.5.2 Four point functions for twist operators

In order to compute entanglement entropy of excited states we will have to compute correlators like $G(z, \bar{z}) = \langle\psi\sigma\tilde{\sigma}\psi\rangle$ in the $n \to 1$ limit. In this limit conformal dimension of twist operators (2.67) goes to 0, so we will call those operators light.

Such correlators were considered in [107, 108]. Four point functions can be expanded using OPE in terms of CFT data (this is known as conformal block expansion).

When we have two light and to heavy operators the terms in the OPE expansion become exponentials [109, 110]. The argument of exponentials is proportional to c, so in the $c \to \infty$ limit sum is dominated by one term. This allows to derive [110]

$$\log G(z, \bar{z}) \simeq -\frac{c(n-1)}{6}\log\left(\frac{z^{\frac{1}{2}(1-\alpha_\psi)}\bar{z}^{\frac{1}{2}(1-\bar{\alpha}_\psi)}(1 - z^{\alpha_\psi})(1 - \bar{z}^{\bar{\alpha}_\psi})}{\alpha_\psi\bar{\alpha}_\psi}\right) + \mathcal{O}((n-1)^2), \tag{2.70}$$

where

$$\alpha_\psi = \sqrt{1 - \frac{24h_\psi}{c}}. \tag{2.71}$$

Note that all information about perturbation is in α_ψ and z does not depend on h_ψ.

2.5.3 Thermofield double state

Let us now return to thermofield double state that we already considered in quantum mechanical systems. We can consider it for two non-interacting 2D CFTs as well. We will show that one sided and two sided correlators are related [111]. Recall that thermofield double state was constructed as purification of some thermal CFT. Given operator $\mathcal{O}$ in the CFT we will have two operators $\mathcal{O}_L$ and $\mathcal{O}_R$ in the purified theory acting in the left and right CFTs respectively.

Single sided correlation functions in thermofield double state are given by thermal correlators

$$\langle \Psi_\beta | \, \mathcal{O}_L(x_1, t_1) \dots \mathcal{O}_L(x_n, t_n) \, | \Psi_\beta \rangle = \mathrm{tr}_L \left(\rho_L(\beta) \mathcal{O}_L(x_1, t_1) \dots \mathcal{O}_L(x_n, t_n) \right) . \tag{2.72}$$

In particular two point correlator is

$$\langle \Psi_\beta | \mathcal{O}_L(x,0) \mathcal{O}_L^\dagger(y,t) | \Psi_\beta \rangle = \sum_{n,m} e^{-\beta E_n + it(E_n - E_m)} \langle n |_L \mathcal{O}_L(x,0) | m \rangle_L \langle m |_L \mathcal{O}_L^\dagger(y,0) | n \rangle_L \tag{2.73}$$

On the other hand, two-sided correlator can be written as

$$\begin{aligned} \langle \Psi_\beta | \mathcal{O}_L(x,0) \mathcal{O}_R(y,t) | \Psi_\beta \rangle &= \sum_{n,m} e^{-\frac{\beta}{2}(E_n + E_m) + it(E_n - E_m)} \langle n |_L \mathcal{O}_L(x,0) | m \rangle_L \langle n |_R \mathcal{O}_R(y,0) | m \rangle_R \\ &= \sum_{n,m} e^{-\beta E_n + i\left(t - i\frac{\beta}{2}\right)(E_n - E_m)} \langle n |_L \mathcal{O}_L(x,0) | m \rangle_L \langle m |_R \mathcal{O}_R^\dagger(y,0) | n \rangle_R \end{aligned} \tag{2.74}$$

Operators $\mathcal{O}_{L,R}$ are copies of the same operator $\mathcal{O}$, so $\langle m |_L \mathcal{O}_L^\dagger(y,0) | n \rangle_L = \langle m |_R \mathcal{O}_R^\dagger(y,0) | n \rangle_R$. Observe that (2.73) and (2.74) evaluated at $t + i\beta/2$ are the same. Therefore one-sided and two-sided correlators in thermofield double state are related via

$$\langle \Psi_\beta | \mathcal{O}_L(x,0) \mathcal{O}_L(y,t) | \Psi_\beta \rangle = \langle \Psi_\beta | \mathcal{O}_L(x,0) \mathcal{O}_R^\dagger \left(y, t + i\frac{\beta}{2} \right) | \Psi_\beta \rangle \tag{2.75}$$

or in other words by shifting Euclidean time halfway through imaginary thermal circle

$$t \mapsto t + i\frac{\beta}{2}. \tag{2.76}$$

So quantum entanglement of initial state is responsible for non-trivial correlators between two CFTs even though they do not interact.

The TFD state is also related to the Schwinger-Keldysh formalism that allows us to compute time evolution in non-equilibrium systems. In this formalism we are doubling the degrees of freedom Φ of some system into conjugate pairs (Φ_L, Φ_R) [67] and then we find S-matrix by integrating in the complex time plane from $t = -\infty$ to $t = +\infty$ then backwards in time but under the real axis with $\Im(t) = -i\sigma$ [112]. We can compare this with definition of TFD state where left and right fields are separated by imaginary time $i\beta/2$. Thus by considering contour with $\sigma = \beta/2$ we can compute out of equilibrium correlation functions in TFD state.

Chapter 3

Holographic Entanglement Entropy of Rotating BTZ Black Hole

In this chapter we will compute the holographic entanglement entropy for rotating BTZ black holes (see subsection 1.5.2) to gain some intuition how entanglement entropy calculations work. This example is interesting because it is possible to introduce rotation while still keeping problems relatively simple unlike in four dimensional analogue, Kerr-AdS black hole [73].

The BTZ black hole metric (1.73) is stationary but not static except for the non-rotating case $r_- = 0$. As stressed in section 1.5, to compute holographic entanglement entropy in non-static spacetimes, we need to use covariant proposal of Hubeny-Rangamani-Takayanagi (HRT). In fact entanglement entropy of rotating BTZ black hole was one of the examples considered in [64] to illustrate the general proposal. This was computed by mapping the BTZ metric to AdS_3 in Poincaré coordinates using the map [113]

$$w_\pm = \sqrt{\frac{r^2 - r_+^2}{r^2 - r_-^2}} e^{2\pi T_\pm u_\pm}, \tag{3.1}$$

$$y = \sqrt{\frac{r^2 - r_+^2}{r^2 - r_-^2}} e^{\pi T_+ u_+ + \pi T_- u_-}, \tag{3.2}$$

where we define[1]

$$T_\pm \equiv \frac{1}{\beta_\pm} = \frac{r_+ \mp r_-}{2\pi R}, \qquad u_\pm = \phi \pm \frac{t}{R}. \tag{3.3}$$

The AdS_3 Poincaré metric is

$$ds^2 = R^2 \frac{dw_+ dw_- + dz^2}{z^2}, \tag{3.4}$$

where geodesics can be computed easier as was discussed in subsection 1.5.1. Similarly to hyperbolic plane, spacelike geodesics correspond to semi-circles [58]. Using the holographic entanglement entropy in Poincaré coordinates of AdS and expressing it in rotating BTZ coordinates [64], derived the entanglement entropy of an interval of length $2L$ in the rotating BTZ

$$S = \frac{A}{4G_3} = \frac{c}{6} \log \left[\frac{\beta_+ \beta_-}{\pi^2 \epsilon_{\text{UV}}^2} \sinh\left(\frac{2\pi L}{\beta_+}\right) \sinh\left(\frac{2\pi L}{\beta_-}\right) \right], \tag{3.5}$$

where central charge c is related to three dimensional Newton constant via $c = 3R/(2G_3)$ [114]. This matches their independent 2d CFT derivation. In chapter 6 we will discuss similar maps when calculating entanglement entropy of locally perturbed rotating BTZ.

In three spacetime dimensions, codimension-2 extremal spacelike surfaces become space-like geodesics. In this chapter we will rederive equation (3.5) by analytically computing the spacelike

[1] We can interpret $T_\pm$ as the temperatures of the left and right moving modes in the dual CFT.

geodesics in rotating BTZ black holes satisfying the covariant HRT boundary conditions.

3.1 Spacelike geodesics in rotating BTZ

3.1.1 Variational problem

The length of geodesics in rotating BTZ is given by[2]

$$A = \int_{s_i}^{s_f} \sqrt{g_{\mu\nu}\dot{x}^\mu \dot{x}^\nu}\, ds = \int_{s_i}^{s_f} \sqrt{-\frac{f(r)}{r^2}\dot{t}^2 + \frac{r^2}{f(r)}\dot{r}^2 + r^2\left(\dot{\phi} + \frac{r_+ r_-}{r^2}\dot{t}\right)^2}\, ds, \tag{3.6}$$

where

$$f(r) = (r^2 - r_+^2)(r^2 - r_-^2). \tag{3.7}$$

The length of extremal geodesics corresponds to holographic entanglement entropy when we impose two additional boundary conditions. Equal boundary time condition is

$$t_f - t_i \equiv \int_{s_i}^{s_f} \dot{t}\, ds = 0. \tag{3.8}$$

The holographic entanglement entropy is expected to match the CFT answer at time $t = t_i = t_f$.

We would like to consider the entanglement entropy of the region with length $2L$. This corresponds to the boundary condition

$$2L \equiv \int_{-L}^{L} d\phi = \int_{s_i}^{s_f} \dot{\phi}\, ds. \tag{3.9}$$

These boundary conditions automatically impose requirement for geodesics to be spacelike. Points at the end of the region of interest on the boundary are spacelike separated, so there are no causal geodesics connecting them.

3.1.2 Equations of motion

Minimizing equation (3.6) is standard problem in variational calculus. Let us denote the integrand of (3.6) by $\mathcal{L}$. The Lagrangian $\mathcal{L}$ is independent of both ϕ and t, so Noether's theorem gives us two conserved charges H and K

$$\frac{\partial \mathcal{L}}{\partial \dot{\phi}} = H \Rightarrow r^2\left(\dot{\phi} + \frac{r_+ r_-}{r^2}\dot{t}\right) = H\sqrt{g_{\mu\nu}\dot{x}^\mu\dot{x}^\nu}, \tag{3.10}$$

$$\frac{\partial \mathcal{L}}{\partial \dot{t}} = K \Rightarrow r_+ r_-\left(\dot{\phi} + \frac{r_+ r_-}{r^2}\dot{t}\right) - \frac{f(r)}{r^2}\dot{t} = K\sqrt{g_{\mu\nu}\dot{x}^\mu\dot{x}^\nu}. \tag{3.11}$$

We can solve equation (3.10) for $\dot{r}$ and obtain

$$\frac{r^2\dot{r}^2}{f(r)} = \frac{f(r)}{r^2}\dot{t}^2 + r^2\left(\frac{r^2}{H^2} - 1\right)\left(\dot{\phi} + \frac{r_+ r_-}{r^2}\dot{t}\right)^2. \tag{3.12}$$

On the other hand, we can eliminate $\sqrt{g_{\mu\nu}\dot{x}^\mu\dot{x}^\nu}$ from equations (3.10) and (3.11)

$$r_+ r_-\left(\dot{\phi} + \frac{r_+ r_-}{r^2}\dot{t}\right) - \frac{f(r)}{r^2}\dot{t} = \frac{Kr^2}{H}\left(\dot{\phi} + \frac{r_+ r_-}{r^2}\dot{t}\right), \tag{3.13}$$

$$\dot{t}\left(\frac{(r_+ r_-)^2}{r^2} - \frac{f(r)}{r^2} - \frac{K r_+ r_-}{H}\right) = \frac{Kr^2}{H}\dot{\phi} - r_+ r_-\dot{\phi}. \tag{3.14}$$

[2]In this chapter we will use units such that radius of AdS is $R = 1$.

We obtain just one solution

$$\dot{t} = \frac{-Kr^2 + Hr_+r_-}{Kr_+r_- + H(r^2 - r_+^2 - r_-^2)}\dot{\phi}. \tag{3.15}$$

Now we plug this back into (3.12)

$$\frac{\dot{r}^2}{f(r)} = \frac{f(r)\left(K^2r^2 - 2HKr_+r_- + f(r) - H^2(r^2 - r_+^2 - r_-^2)\right)}{r^2\left[Kr_+r_- + H(r^2 - r_+^2 - r_-^2)\right]^2}\dot{\phi}^2. \tag{3.16}$$

Let us now impose equal time boundary condition (3.8). We change integration variable to r and consider only half of the curve by integrating from the turning point $r_\star$ to ∞.

$$2\int_{r_\star}^{\infty} \frac{\dot{t}}{\dot{r}}\, dr = 0. \tag{3.17}$$

Let us consider the indefinite integral

$$\begin{aligned} I &= 2\int \frac{\dot{t}}{\dot{r}}\, dr \\ &= 2\int \frac{r\left[Kr_+r_- + H(r^2 - r_+^2 - r_-^2)\right]}{f(r)\sqrt{K^2r^2 - 2HKr_+r_- + f(r) - H^2(r^2 - r_+^2 - r_-^2)}} \frac{-Kr^2 + Hr_+r_-}{Kr_+r_- + H(r^2 - r_+^2 - r_-^2)}\, dr \\ &= 2\int \frac{r(-Kr^2 + Hr_+r_-)}{f(r)\sqrt{K^2r^2 - 2HKr_+r_- + f(r) - H^2(r^2 - r_+^2 - r_-^2)}}\, dr. \end{aligned} \tag{3.18}$$

We can change variables to $y = r^2$

$$I = \int \frac{(-Ky + Hr_+r_-)}{(y - r_+^2)(y - r_-^2)\sqrt{K^2y - 2HKr_+r_- + (y - r_+^2)(y - r_-^2) - H^2(y - r_+^2 - r_-^2)}}\, dy. \tag{3.19}$$

So we have the integral of the form

$$\int \frac{Ay + B}{(y - C)(y - D)\sqrt{(y - E)^2 - F^2}}\, dy, \tag{3.20}$$

where we introduced 6 constants

$$\begin{aligned} A &= -K, \\ B &= Hr_+r_-, \\ C &= r_+^2, \\ D &= r_-^2, \\ E &= \frac{1}{2}(H^2 - K^2 + r_+^2 + r_-^2), \qquad (3.21) \\ F &= \sqrt{\frac{1}{4}(H^2 - K^2 + r_+^2 + r_-^2)^2 - r_+^2r_-^2 + 2HKr_+r_- - H^2(r_+^2 + r_-^2)}. \qquad (3.22) \end{aligned}$$

We will argue in subsection 3.1.3 why $F^2 > 0$ (so $F \in \mathbb{R}$).

Similarly, we deal with the boundary condition on the length of the boundary region (3.9)

$$L = \int_{r_\star}^{\infty} \frac{\dot{\phi}}{\dot{r}}\, dr \tag{3.23}$$

$$2L = 2\int \frac{r\left[Kr_+r_- + H(r^2 - r_+^2 - r_-^2)\right]}{f(r)\sqrt{K^2r^2 - 2HKr_+r_- + f(r) - H^2(r^2 - r_+^2 - r_-^2)}}\,dr \tag{3.24}$$

So after the change of variables we again get integral (3.20) but with $A = H$ and $B = Kr_+r_- - H(r_+^2 + r_-^2)$.

3.1.3 Turning point

Let us find the points where $\frac{dr}{d\phi} = 0$. From equation (3.16) we can see that possibilities are either r_+, r_- or roots of

$$K^2r^2 - 2HKr_+r_- + f(r) - H^2(r^2 - r_+^2 - r_-^2) = 0. \tag{3.25}$$

$F = 0$ case (single turning point) does not work because the integrals diverge at the turning point. Therefore, we must choose the case when quadratic equation has two roots. This justifies the previous convention that $F^2 > 0$. Turning points are given by

$$r_\star^2 = E \pm F. \tag{3.26}$$

We will assume that spacelike geodesics do not probe deep enough to reach r_+. Actually, geodesics only reach point $E + F$. The integrand of (3.20) is not even defined for $E - F < y < E + F$ which again indicates that we cannot see such geodesics. This phenomena happens more generally in spacetimes away from pure AdS [115] and the regions not probed by spacelike geodesics are called *entanglement shadows*[3].

3.1.4 Evaluating the integral

Having found the turning point we can calculate the definite integral

$$I = \int_{E+F}^{\infty} \frac{Ay + B}{(y - C)(y - D)\sqrt{(y - E)^2 - F^2}}\,dy = \int_{F}^{\infty} \frac{Au + AE + B}{(u + E - C)(u + E - D)\sqrt{u^2 - F^2}}\,du. \tag{3.27}$$

Now we change variables to $v = uF^{-1}$.

$$I = \int_{1}^{\infty} \frac{AFv + AE + B}{(Fv + E - C)(Fv + E - D)\sqrt{v^2 - 1}}\,dv. \tag{3.28}$$

Let $v = \cosh w$. Then

$$I = \int_{0}^{\infty} \frac{AF\cosh w + AE + B}{(F\cosh w + E - C)(F\cosh w + E - D)}\,dw. \tag{3.29}$$

Now we apply the rationalizing substitution

$$z = \tanh\frac{w}{2}, \qquad dw = \frac{2\,dz}{1 - z^2}, \qquad \cosh w = \frac{1 + z^2}{1 - z^2}.$$

$$I = 2\int_{0}^{1} \frac{(AF - AE - B)z^2 + AF + AE + B}{\left[(F - E + C)z^2 + F + E - C\right]\left[(F - E + D)z^2 + F + E - D\right]}\,dz, \tag{3.30}$$

[3] Another interesting class of geometries where entanglement shadows exist are conical defects [115]. We will discuss them in chapter 5.

We write the integrand as

$$\frac{\alpha}{(F-E+C)z^2+F+E-C}+\frac{\beta}{(F-E+D)z^2+F+E-D}.$$

provided that $C \neq D$ (non-extreme case). We will also assume that $F+E-C \neq 0$ as well as $F+E-D \neq 0$. So

$$(F-E+D)\alpha+(F-E+C)\beta=(AF-AE-B), \tag{3.31}$$
$$(F+E-D)\alpha+(F+E-C)\beta=(AF+AE+B). \tag{3.32}$$

This has a solution

$$\alpha=\frac{AC+B}{C-D}, \qquad \beta=-\frac{AD+B}{C-D}. \tag{3.33}$$

So we are left with two integrals of the form

$$\int_0^1 \frac{1}{az^2+b}\,dz. \tag{3.34}$$

Its value depends on whether $az^2+b=0$ has real roots, or not, i.e. whether $ab>0$ or $ab<0$.

$$(F-E+C)(F+E-C)=F^2-(E-C)^2=-(Hr_- - Kr_+)^2<0. \tag{3.35}$$

and similarly for the second integral. In this case

$$\int_0^1 \frac{1}{az^2+b}\,dz=-\frac{\tanh^{-1}\sqrt{-\frac{a}{b}}}{\sqrt{-ab}}. \tag{3.36}$$

Finally,

$$\begin{aligned} I=&\frac{2(Ar_-^2+B)}{(r_+^2-r_-^2)|Hr_+-Kr_-|}\tanh^{-1}\sqrt{\frac{E-D-F}{E-D+F}}\\ &-\frac{2(Ar_+^2+B)}{(r_+^2-r_-^2)|Hr_--Kr_+|}\tanh^{-1}\sqrt{\frac{E-C-F}{E-C+F}}. \end{aligned} \tag{3.37}$$

If we impose equal time boundary condition ($I=0, A=-K, B=Hr_+r_-$) we get the following relation

$$\begin{aligned} &\operatorname{sgn}(Hr_+-Kr_-)\,r_-\tanh^{-1}\sqrt{\frac{E-D-F}{E-D+F}}\\ =&\operatorname{sgn}(Hr_--Kr_+)\,r_+\tanh^{-1}\sqrt{\frac{E-C-F}{E-C+F}}. \end{aligned} \tag{3.38}$$

Let us impose the second boundary condition

$$\begin{aligned} L=&-\frac{Hr_-^2+Kr_+r_--H(r_+^2+r_-^2)}{(r_+^2+r_-^2)|Hr_+-Kr_-|}\tanh^{-1}\sqrt{\frac{E-D-F}{E-D+F}}\\ &+\frac{Hr_+^2+Kr_+r_--H(r_+^2+r_-^2)}{(r_+^2+r_-^2)|Hr_--Kr_+|}\tanh^{-1}\sqrt{\frac{E-C-F}{E-C+F}}, \end{aligned} \tag{3.39}$$

$$L = \operatorname{sgn}(Hr_+ - Kr_-)\frac{r_+}{(r_+^2 + r_-^2)} \tanh^{-1}\sqrt{\frac{E-D-F}{E-D+F}}$$
$$- \operatorname{sgn}(Hr_- - Kr_+)\frac{r_-}{(r_+^2 + r_-^2)} \tanh^{-1}\sqrt{\frac{E-C-F}{E-C+F}}. \tag{3.40}$$

3.1.5 Solving for boundary conditions

We use equation (3.38) to simplify (3.40) and get rid of one of the $\tanh^{-1}$ functions.

$$L = \frac{1}{r_+} \tanh^{-1}\sqrt{\frac{E-D-F}{E-D+F}}. \tag{3.41}$$

Alternatively, we can eliminate the other $\tanh^{-1}$ provided that $r_- \neq 0$

$$L = \frac{1}{r_-} \tanh^{-1}\sqrt{\frac{E-C-F}{E-C+F}}. \tag{3.42}$$

Equations (3.41) and (3.42) are simpler but are still independent and contain all information from (3.38) and (3.40). We can use them to find F and E.

$$\tanh^2 r_+L = \frac{E-D-F}{E-D+F}, \tag{3.43}$$
$$\tanh^2 r_-L = \frac{E-C-F}{E-C+F}. \tag{3.44}$$

We rewrite these equations using $\cosh 2x = \frac{1+\tanh^2 x}{1-\tanh^2 x}$. So

$$\cosh 2r_+L = \frac{E-D}{F}, \tag{3.45}$$
$$\cosh 2r_-L = \frac{E-C}{F}. \tag{3.46}$$

Now they can be solved for F

$$\cosh(2r_+L) - \cosh(2r_-L) = \frac{r_+^2 - r_-^2}{F}. \tag{3.47}$$

The answer can also be written using hyperbolic sum-to-product formulae as

$$F = \frac{r_+^2 - r_-^2}{2\sinh\big((r_+ + r_-)L\big)\sinh\big((r_+ - r_-)L\big)}. \tag{3.48}$$

We can also find E in terms of the given parameters r_+, r_- and L

$$E = \frac{r_+^2\cosh(2r_+L) - r_-^2\cosh(2r_-L)}{\cosh(2r_+L) - \cosh(2r_-L)} = \frac{r_+^2\cosh(2r_+L) - r_-^2\cosh(2r_-L)}{2\sinh\big((r_+ + r_-)L\big)\sinh\big((r_+ - r_-)L\big)}. \tag{3.49}$$

Let us use equations (3.21) and (3.22) to find H and K

$$H^2 - K^2 = 2E - (r_+^2 + r_-^2), \tag{3.50}$$
$$F^2 = E^2 - r_+^2r_-^2 + 2HKr_+r_- - H^2(r_+^2 + r_-^2). \tag{3.51}$$

We can substitute K from equation (3.51) into (3.50) and obtain a quadratic equation in H^2

$$-(r_+^2 - r_-^2)^2H^4 + H^2\left(r_+^2 + r_-^2 - 2E - \frac{(F^2 - E^2 + r_+^2r_-^2)(r_+^2 + r_-^2)}{2r_+^2r_-^2}\right)(4r_+^2r_-^2) - (F^2 - E^2 + r_+^2r_-^2)^2 = 0. \tag{3.52}$$

$$(r_+^2-r_-^2)^2H^4-2H^2\left((E^2-F^2+r_+^2r_-^2)(r_+^2+r_-^2)-4r_+^2r_-^2E\right)+(F^2-E^2+r_+^2r_-^2)^2=0. \quad (3.53)$$

A straightforward calculation shows that this equation has two positive solutions (by Vieta's formulae). They are given by

$$H=\frac{r_+\sinh(2r_+L)\pm r_-\sinh(2r_-L)}{\cosh(2r_+L)-\cosh(2r_-L)}. \quad (3.54)$$

If we take a minus sign then the result agrees with the non rotating and extreme limits[4] (see section 3.2).

$$H=\frac{r_+\sinh(2r_+L)-r_-\sinh(2r_-L)}{\cosh(2r_+L)-\cosh(2r_-L)}, \quad (3.55)$$

$$K=\frac{r_-\sinh(2r_+L)-r_+\sinh(2r_-L)}{\cosh(2r_+L)-\cosh(2r_-L)}. \quad (3.56)$$

3.2 Special cases

3.2.1 Extremal BTZ

In this case we have $r_+=r_-$. The other constants are

$$\begin{aligned}
A&=-K,\\
B&=Hr_+^2,\\
E&=\frac{1}{2}(H^2-K^2+2r_+^2),\\
F&=\sqrt{\frac{1}{4}(H^2-K^2+2r_+^2)^2-r_+^4+2HKr_+^2-2H^2r_+^2}.
\end{aligned}$$

The second boundary condition (3.24) has $A=H$, $B=(K-2H)r_+^2$.

The solution follows the general case until equation (3.30) which becomes

$$I=2\int_0^1\frac{(AF-AE-B)z^2+AF+AE+B}{\left[(F-E+D)z^2+F+E-D\right]^2}\,dz, \quad (3.57)$$

After a long but straightforward calculation we obtain

$$I=\frac{AD+B}{(F-E+D)(F+E-D)}+\frac{2\big(A(DE+F^2-E^2)+B(D-E)\big)\tanh^{-1}\sqrt{\frac{E-D-F}{E-D+F}}}{\sqrt{-(F-E+D)(F+E-D)}(F-E+D)(F+E-D)}. \quad (3.58)$$

Equal time boundary condition (3.8) is

$$\frac{1}{|H-K|}=\frac{1}{r_+}\tanh^{-1}\sqrt{\frac{E-D-F}{E-D+F}}. \quad (3.59)$$

And the condition for the length (3.9) of entanglement region is

$$L=\frac{1}{H-K}+\frac{1}{r_+}\frac{H-K}{|H-K|}\tanh^{-1}\sqrt{\frac{E-D-F}{E-D+F}}. \quad (3.60)$$

This can be simplified using (3.59)

$$H-K=\frac{1}{L}. \quad (3.61)$$

Hence, equation (3.59) is exactly the same as in non-extreme case (3.41). However, we do not have an analogue of equation (3.42), so we have to solve equations for H. Equation (3.59) now

[4] As we will see later, the answer only depends on E and F, so it does not matter which branch we use.

reads

$$\tanh^2(Lr_+) = \frac{E - r_+^2 - F}{E - r_+^2 + F}. \tag{3.62}$$

$$\cosh(2Lr_+) = \frac{E - D}{F} = \frac{H + K}{2LF}. \tag{3.63}$$

We can substitute the value of F and solve quadratic equation for H

$$H = \frac{1}{2L} \pm r_+ \coth(2Lr_+). \tag{3.64}$$

We can now compute F using (3.63)

$$H + K = 2H - \frac{1}{L} = \pm 2r_+ \coth(2Lr_+). \tag{3.65}$$

Only the positive branch is consistent, so

$$F = \frac{r_+}{L \sinh(2Lr_+)}, \tag{3.66}$$

$$E = r_+^2 + \frac{r_+}{L} \coth(2Lr_+), \tag{3.67}$$

$$\frac{2}{F} = \frac{2L}{r_+} \sinh(2Lr_+). \tag{3.68}$$

Hence, we obtained the value which one would expect by taking a limit $r_- \to r_+$.

3.2.2 Non rotating BTZ

Here we have $r_- = 0$. In this case equal boundary time condition is

$$\frac{K}{|Hr_+ - Kr_-|} \tan^{-1} \sqrt{\frac{E - C - F}{E - C + F}} = 0. \tag{3.69}$$

So either $K = 0$ or $E - C - F = 0$. However, the second condition actually simplifies to $K = 0$.

The other boundary condition is still given by (3.45) (with $D = K = 0$). We can write it in terms of H

$$(H^2 + r_+^2)^2 = (H^2 - r_+^2)^2 \cosh^2(2r_+L). \tag{3.70}$$

$$H^2 = r_+ \frac{\cosh(2r_+L) \pm 1}{\cosh(2r_+L) \mp 1} = r_+ \frac{(\cosh(2r_+L) \pm 1)^2}{\sinh^2(2r_+L)}. \tag{3.71}$$

This corresponds to

$$E = r_+^2 \frac{\cosh(2r_+L)}{\cosh(2r_+L) \mp 1}, \tag{3.72}$$

$$F = \frac{r_+^2}{\cosh(2r_+L) \mp 1}, \tag{3.73}$$

$$\frac{2}{F} = \frac{2(\cosh(2r_+L) \mp 1)}{r_+^2}. \tag{3.74}$$

To pick the correct branch we will use a continuity argument. Values of E, F and H must be continuous. There is only one consistent solution in the extremal case, so we have to pick the

second sign in the general case and the first sign in non-rotating case:

$$H = r_+ \coth(r_+ L), \tag{3.75}$$

$$E = r_+^2 \frac{\cosh(2r_+ L)}{\cosh(2r_+ L) - 1}, \tag{3.76}$$

$$F = \frac{r_+^2}{\cosh(2r_+ L) - 1}, \tag{3.77}$$

$$\frac{2}{F} = \frac{4\sinh^2(r_+ L)}{r_+^2}. \tag{3.78}$$

Note that the other branch has $H = r_+ \tanh(r_+ L)$ and it is not possible to obtain it as a limit of a general case.

3.3 Entanglement entropy

We have to introduce a cut-off $r_\infty = \epsilon_{\mathrm{UV}}^{-1}$ at infinity in order to calculate entanglement entropy

$$A = \int_{s_i}^{s_f} \sqrt{g_{\mu\nu}\dot{x}^\mu \dot{x}^\nu}\, ds. = 2\int_{r_\star}^{r_\infty} \frac{\sqrt{g_{\mu\nu}\dot{x}^\mu \dot{x}^\nu}}{\dot{r}}\, dr. \tag{3.79}$$

Using equation (3.10) we can eliminate the square root

$$A = 2\int_{r_\star}^{r_\infty} \frac{r^2\dot{\phi} + r_+ r_- \dot{t}}{H\dot{r}}\, dr. \tag{3.80}$$

We insert the values of $\dot{t}$ and $\dot{r}$ from (3.15) and (3.16)

$$A = 2\int_{r_\star}^{r_\infty} \frac{r\left(r^2(r^2 - r_+^2 - r_-^2) + (r_+ r_-)^2\right)}{f(r)\sqrt{Kr^2 - 2HKr_+ r_- + f - H(r^2 - r_+^2 - r_-^2)}}\, dr, \tag{3.81}$$

$$A = 2\int_{r_\star}^{r_\infty} \frac{r}{\sqrt{Kr^2 - 2HKr_+ r_- + f - H(r^2 - r_+^2 - r_-^2)}}\, dr. \tag{3.82}$$

Let us change variables to $y = r^2$.

$$A = \int_{E+F}^{r_\infty^2} \frac{1}{\sqrt{(y-E)^2 - F^2}}\, dy. \tag{3.83}$$

$$A = \int_F^{r_\infty^2 - E} \frac{1}{\sqrt{u^2 - F^2}}\, du = \cosh^{-1}\frac{r_\infty^2 - E}{F} - \cosh^{-1} 1 = \log\left(\frac{r_\infty^2 - E}{F} + \sqrt{\left(\frac{r_\infty^2 - E}{F}\right)^2 - 1}\right). \tag{3.84}$$

To leading order we can expand this as

$$A = \log\left(\frac{2r_\infty^2}{F}\right) + \mathcal{O}(r_\infty^{-2}). \tag{3.85}$$

Hence, the the length of the geodesic is

$$A = \log\left[\frac{4}{\epsilon_{\mathrm{UV}}^2(r_+^2 - r_-^2)} \sinh\left(2L(r_+ + r_-)\right)\sinh\left(2L(r_+ - r_-)\right)\right] + \mathcal{O}(\epsilon_{\mathrm{UV}}^2). \tag{3.86}$$

Thus the entanglement entropy of the BTZ black hole is given by

$$S = \frac{A}{4G_3} = \frac{c}{6} \log \left[\frac{\beta_+ \beta_-}{\pi^2 \epsilon_{\text{UV}}^2} \sinh \left(\frac{2\pi L}{\beta_+} \right) \sinh \left(\frac{2\pi L}{\beta_-} \right) \right], \tag{3.87}$$

which precisely matches equation (3.5) as we wanted to show. In later chapters when we consider perturbations of the BTZ black hole we will see this term as the main contribution. Note, that in this calculation it was more convenient to use the length of entanglement region to be $2L$ and not L as in later chapters.

Chapter 4

Rényi entropy of locally excited thermal states

One advantage of the concept of entanglement entropy over thermal entropy is that it holds for out of equilibrium systems where there is no well defined temperature. A particular class of such systems are perturbations of thermal states. These perturbations have two interesting subclasses: global and local quenches. Global quenches are perturbations arising due to a global change of parameters in the Hamiltonian [103, 116–119]. I.e. we start with a system in equilibrium, then some process suddenly changes the Hamiltonian thus putting the system out of equilibrium. Recently, local quenches [120] that can be produced by a change of parameters of the system in some localized region have become increasingly popular.

In chapter 2 we considered the second Rényi entropy for a free boson in two dimensional CFT in a ground state. Our goal in this chapter is to compute the time evolution of Rényi entropy and mutual information for perturbations of thermal states. We will do the calculation for a free boson and also for large c two dimensional CFTs. As discussed in chapter 1, large c CFTs are particularly interesting from the point of view of holography. We expect the dual gravity picture to involve a perturbed black hole. We will postpone the connection to holography till section 5.5.

4.1 Energy momentum of excited state at finite temperature

Before we proceed with Rényi entropy calculations, let us determine the physical interpretation of a thermal state perturbed by a primary operator. The physical interpretation of a vacuum state perturbed by a primary operator was discussed in [121]. It was shown that the energy density after a local quench consists of two lumps of energy traveling at a speed of light to opposite directions and can be interpreted as an entangled EPR pair. Also, the analysis in this section will allow us to quantify the total energy of the perturbation. In order to compute energy density on a cylinder we will first compute in on a complex plane and then use the exponential map to map everything to the cylinder.

The state is created by the primary operator $\mathcal{O}$ having conformal dimensions $(h, \bar{h})$ inserted at $x = -l < 0$ and time $t_\omega = 0$. Then we evolve the state in time with $\exp(-iHt)$. Density matrix of such state is

$$\rho(t) = \mathcal{N} \cdot \mathcal{O}(w_2, \bar{w}_2) \left|0\right\rangle \left\langle 0\right| \mathcal{O}^\dagger(w_1, \bar{w}_1). \tag{4.1}$$

where $\mathcal{N}$ is a normalization constant and

$$w_1 = \quad t - l + i\epsilon, \qquad w_2 = \quad t - l - i\epsilon, \tag{4.2}$$

$$\bar{w}_1 = -t - l - i\epsilon, \qquad \bar{w}_2 = -t - l + i\epsilon. \tag{4.3}$$

The energy density is then given by

$$\langle T_{tt}\rangle = \langle T\rangle + \langle \bar{T}\rangle = \frac{\langle \mathcal{O}^\dagger(w_2,\bar{w}_2)\left(T(x,x)+\bar{T}(x,x)\right)\mathcal{O}(w_1,\bar{w}_1)\rangle}{\langle \mathcal{O}^\dagger(w_2,\bar{w}_2)\mathcal{O}(w_1,\bar{w}_1)\rangle}. \tag{4.4}$$

Two and three point functions can be determined by conformal invariance

$$\langle \mathcal{O}^\dagger(w_2,\bar{w}_2)\mathcal{O}(w_1,\bar{w}_1)\rangle = \frac{1}{(w_2-w_1)^{2h}(\bar{w}_2-\bar{w}_1)^{2\bar{h}}}. \tag{4.5}$$

Conformal dimensions of T and $\bar{T}$ are $(h_T,\bar{h}_T)=(2,0)$ and $(h_{\bar{T}},\bar{h}_{\bar{T}})=(0,2)$ respectively. Unlike generic three point function, that is only determined up to a constant, three-point function which has energy momentum tensor is fully determined by a special structure of OPEs of energy momentum tensor with a primary operator (2.32).

$$\langle \mathcal{O}^\dagger(w_2,\bar{w}_2)T(x,x)\mathcal{O}(w_1,\bar{w}_1)\rangle = \frac{h}{(w_2-x)^2(x-w_1)^2(w_2-w_1)^{2h-2}(\bar{w}_2-\bar{w}_1)^{2\bar{h}},} \tag{4.6}$$

and similarly for antiholomorphic coordinates.

After plugging in values of w we obtain

$$\langle T_{tt}\rangle = 4\epsilon^2\left[\frac{h}{\left((x+l-t)^2+\epsilon^2\right)^2}+\frac{\bar{h}}{\left((x+l+t)^2+\epsilon^2\right)^2}\right]. \tag{4.7}$$

We see two lumps of energy moving into opposite direction as was discussed in [121]. They have widths ϵ and in the limit $\epsilon\to 0$ can be approximated by Dirac's delta function. Thus the total energy of perturbation is

$$E=\int T_{tt}\,dx \approx \frac{2(h+\bar{h})}{\epsilon}. \tag{4.8}$$

4.1.1 Energy density on the cylinder

Instead of considering energy density for CFT on the plane we can consider it on the cylinder.

Let us focus on the holomorphic part for simplicity. Antiholomorphic part is exactly the same but t comes with minus sign and w_1 is interchanged with w_2 (which does not affect anything). Then from equations (4.6) and (4.5) we obtain

$$\langle T_{tt}(x,\bar{x})\rangle_{\text{hol}} = \frac{h(w_2-w_1)^2}{(w_2-x)^2(w_1-x)^2}. \tag{4.9}$$

Let us apply conformal map to map plane to the cylinder

$$x\mapsto e^{\frac{2\pi}{\beta}y}. \tag{4.10}$$

This map sends

$$w_1 = e^{\frac{2\pi}{\beta}(t-l-i\epsilon)}, \tag{4.11}$$

$$w_2 = e^{\frac{2\pi}{\beta}(t-l+i\epsilon)}. \tag{4.12}$$

Stress energy tensor transforms as in equation (2.35)

$$\langle T_{tt}(y,\bar{y})\rangle = \frac{4\pi^2}{\beta^2}e^{\frac{4\pi}{\beta}y}\left[\langle T_{tt}(x,\bar{x})\rangle - \frac{c}{12}\{y;x\}\right]. \tag{4.13}$$

So the energy density on the cylinder is given by

$$\langle T_{tt}(y,\bar{y})\rangle_{\text{hol}} = \frac{h\pi^2}{\beta^2}\sin^2\left(\frac{2\pi\epsilon}{\beta}\right)\frac{1}{\left[\sinh^2\left(\frac{\pi}{\beta}(y+l-t)\right)+\sin^2\left(\frac{\pi\epsilon}{\beta}\right)\right]^2}+\frac{c\pi^2}{6\beta^2}. \tag{4.14}$$

There is a similar term for antiholomorphic component of the stress energy tensor

$$\langle T_{tt}(y,\bar{y})\rangle_{\text{antihol}} = \frac{\bar{h}\pi^2}{\beta^2}\sin^2\left(\frac{2\pi\epsilon}{\beta}\right)\frac{1}{\left[\sinh^2\left(\frac{\pi}{\beta}(y+l+t)\right)+\sin^2\left(\frac{\pi\epsilon}{\beta}\right)\right]^2}+\frac{c\pi^2}{6\beta^2}. \tag{4.15}$$

So the sum of (4.14) and (4.15) has a piece that is well known energy density of unperturbed thermal state of two dimensional CFT on a cylinder

$$\langle T_{\text{thermal}}\rangle = \frac{c\pi^2}{3\beta^2} \tag{4.16}$$

and two identical narrow lumps of energy of width ϵ/β moving in opposite directions. Note that it is also possible to study asymmetric lumps by considering perturbations by derivative operators [122].

4.2 Rényi entropy for 2d CFTs in a perturbed thermal state

4.2.1 Free bosons

Let us return to an example that we considered in section 2.4. We can generalize it to a thermal state perturbed by a primary operator $\mathcal{O}_2$ from equation (2.60) and find corrections to Rényi entropy which was equal to $\log 2$ (see equation (2.63)).

Since the vacuum result did not depend on the length of the interval L, let us consider region of the entanglement to be $A = [0,\infty]$. Density matrix is given by

$$\rho(t) = \mathcal{N}\mathcal{O}(x_2,\bar{x}_2)e^{-\beta H}\mathcal{O}^\dagger(x_1,\bar{x}_1), \tag{4.17}$$

with the insertion points as before in (4.2). The second Rényi entropy is given by

$$\Delta S_A^{(2)} = -\log\left[\frac{\langle\mathcal{O}(x_1,\bar{x}_1)\mathcal{O}^\dagger(x_2,\bar{x}_2)\mathcal{O}(x_3,\bar{x}_3)\mathcal{O}^\dagger(x_4,\bar{x}_4)\rangle_{C_2}}{\left(\langle\mathcal{O}(x_1,\bar{x}_1)\mathcal{O}^\dagger(x_2,\bar{x}_2)\rangle_{C_1}\right)^2}\right], \tag{4.18}$$

where 4-point function is computed on the 2-sheeted cylinder C_2. It can be mapped to a plane with a map

$$z(x) = \sqrt{e^{\frac{2\pi x}{\beta}}-1}. \tag{4.19}$$

This map can be derived as a composition of conformal maps. Firstly, we map each cylinder with a cut $A = [0,\infty]$ to the plane with a cut $[1,\infty]$ using the exponential map $w(x) = \exp(2\pi x/\beta)$. Secondly, we subtract 1 to go back to $[0,\infty]$. Finally, we use the uniformization map $z^2(w) = w$ to map two planes to one.

Again, Rényi entropy will be given by equation (2.59). The only difference is finite temperature β but all dependence on the temperature and time is carried by the cross ratio z_A given

by equation (2.56)

$$z_A = \frac{1}{2}\left(1 + \frac{\cos\left(\frac{2\pi\epsilon}{\beta}\right) e^{\frac{2\pi(t-l)}{\beta}} - 1}{\sqrt{\left(\cos\left(\frac{2\pi\epsilon}{\beta}\right) e^{\frac{2\pi(t-l)}{\beta}} - 1\right)^2 + \sin^2\left(\frac{2\pi\epsilon}{\beta}\right) e^{\frac{4\pi(t-l)}{\beta}}}}\right) \tag{4.20}$$

$$\bar{z}_A = \frac{1}{2}\left(1 + \frac{\cos\left(\frac{2\pi\epsilon}{\beta}\right) e^{-\frac{2\pi(t+l)}{\beta}} - 1}{\sqrt{\left(\cos\left(\frac{2\pi\epsilon}{\beta}\right) e^{-\frac{2\pi(t+l)}{\beta}} - 1\right)^2 + \sin^2\left(\frac{2\pi\epsilon}{\beta}\right) e^{-\frac{4\pi(t+l)}{\beta}}}}\right)$$

At late times when $t > l \gg \epsilon$ we can approximate cross-ratios as

$$z_A = 1 - \frac{\pi^2\epsilon^2}{4\beta^2} \frac{e^{\frac{2\pi}{\beta}(t-l)}}{\sinh^2 \frac{\pi}{\beta}(t-l)} + \mathcal{O}(\epsilon^4), \tag{4.21}$$

$$\bar{z}_A = \frac{\pi^2\epsilon^2}{4\beta^2} \frac{e^{-\frac{2\pi}{\beta}(t+l)}}{\sinh^2 \frac{\pi}{\beta}(t+l)} + \mathcal{O}(\epsilon^4). \tag{4.22}$$

Note that for $t \gg l$ expressions for cross-rations simplify even further as time dependence is exponentially suppressed. However, as we can see in Figure 4.2–Figure 4.5, growth of entanglement entropy is time dependent process. At early times, time dependence is important but later Rényi entropy obtained from equations (2.59) and (2.62) saturates to

$$\Delta S_A^{(2)} = \log\left(\frac{2}{1 + |z_A| + |1 - z_A|}\right) = \log 2 - \frac{\pi\epsilon}{\beta} + \mathcal{O}(\epsilon^2). \tag{4.23}$$

So entanglement between EPR pairs is partially disrupted by the presence of thermal fluctuations.

4.2.2 Large c general 2d CFT

In order to compare results to AdS/CFT gravity dual it would be interesting to consider large c CFT as in [123]. We will consider perturbation by a primary operator with conformal dimension h such that $1 \ll h \ll c$. It was shown in [124] that Rényi entropy of vacuum state perturbed by such primary operator is

$$\Delta S_A^{(2)} = 4h \log\left(\frac{2t}{\epsilon}\right). \tag{4.24}$$

Note that entropy growth is unbounded because we consider semi-infinite entanglement regions rather than finite intervals. Our goal in this section will be to determine what is the effect non-zero temperature on the result above.

In this limit we can use approximation for canonical four point function [125]

$$G(z, \bar{z}) \approx |z|^{-4h}. \tag{4.25}$$

Hence, equation (2.59) becomes

$$\Delta S_A^{(2)} = -4h \log|1 - z_A|. \tag{4.26}$$

The cross ratios in equation (4.20) depend on whether $t < l$ or vice versa. At early times both z_A and $\bar{z}_A \to 0$, so Rényi entropy $\Delta S_A^{(2)}$ vanishes. On the other hand, for $t > l$ we have that $z_A \to 1$ but $\bar{z}_A \to 0$. Thus Rényi entropy is

$$\Delta S_A^{(2)} = 4h \log\left(\frac{\beta}{\pi\epsilon}\right) + \mathcal{O}(\epsilon^2). \tag{4.27}$$

So the difference from the zero temperature case where Rényi entropy diverges logarithmically

in time is that β adds a time cut-off $t_{\max} = \frac{\beta}{2\pi}$. This has a nice interpretation in terms of a gravity dual theory. Empty anti-de Sitter space corresponds to the zero temperature case. On the other hand, gravity dual of a thermal state is a black hole. As mentioned earlier, local quench can be modelled by a massive particle. In the black hole background particle falls into the black hole, so we interpret $t_{\max}$ as the proper time it takes for the particle to reach black hole horizon.

4.3 Rényi mutual information in the thermofield double state

In previous sections we discussed the formalism introduced in [101, 102, 124] to compute Rényi entanglement entropies in 2d CFTs whose thermal states are locally excited by a primary operator. This formalism can be extended to thermofield double state. Mutual information for TFD was computed in [126]. Below we will do analogous calculations for locally perturbed TFD state.

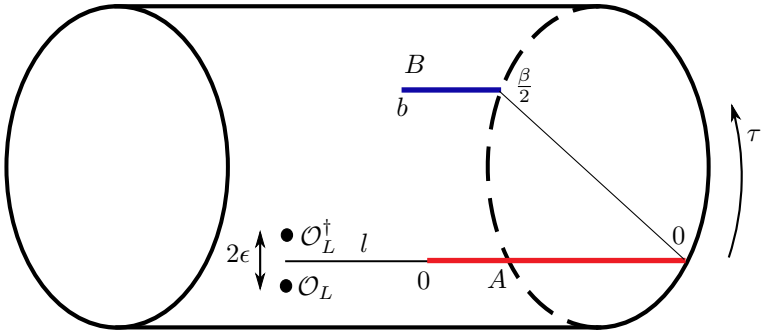

Figure 4.1: Cylinder with two cuts. $\mathrm{CFT_L}$ is at $\tau = 0$ and $\mathrm{CFT_R}$ is at $\tau = \frac{1}{2}\beta$.

Let us consider TFD state with semi-infinite cuts $A = [0, \infty]$ in $\mathrm{CFT_L}$ and $B = [b, \infty]$ in $\mathrm{CFT_R}$ as shown in Figure 4.1. Both branch cuts live on a single manifold but interval B is located at $t = i\beta/2$ as discussed in subsection 2.5.3. We perturb the TFD by the insertion of a local primary operator $\mathcal{O}_L$ acting on $\mathrm{CFT_L}$ at $x = -l,\ t = 0$. In this system we will investigate the behaviour of (Rényi) mutual information

$$\Delta I^{(2)}_{A:B}(t) = \Delta S^{(2)}_A + \Delta S^{(2)}_B - \Delta S^{(2)}_{A\cup B}. \tag{4.28}$$

Time evolution of TFD state depends on the choice of Hamiltonian. It is up to us to choose a particular Hamiltonian but there are two natural choices $H_L\otimes\mathbb{I}_R \pm \mathbb{I}_L\otimes H_R$ (see subsection 1.5.3). Therefore, we will consider two different density operators

$$\begin{aligned}\rho(t) &= \mathcal{N} e^{-i(H_L-H_R)t} e^{-\epsilon H_L} \mathcal{O}_L(-l)\,|\Psi_\beta\rangle\langle\Psi_\beta|\,\mathcal{O}_L^\dagger(-l) e^{-\epsilon H_L} e^{i(H_L-H_R)t} \\ &\equiv \mathcal{N}\mathcal{O}_L(x_2,\bar{x}_2)\,|\Psi_\beta\rangle\langle\Psi_\beta|\,\mathcal{O}_L^\dagger(x_1,\bar{x}_1)\,,\end{aligned} \tag{4.29}$$

where operator insertion points are

$$x_1 = \quad t - l + i\epsilon, \qquad x_2 = \quad t - l - i\epsilon, \tag{4.30}$$

$$\bar{x}_1 = -t - l - i\epsilon, \qquad \bar{x}_2 = -t - l + i\epsilon. \tag{4.31}$$

In this case the positions of the cuts are fixed.

On the other hand, the Hamiltonian $H_L + H_R$ gives rise to the density matrix

$$\begin{aligned}\rho(t) &= \mathcal{N} e^{-i(H_L+H_R)t} e^{-\epsilon H_L} \mathcal{O}_L(-l)\,|\Psi_\beta\rangle\langle\Psi_\beta|\,\mathcal{O}_L^\dagger(-l) e^{-\epsilon H_L} e^{i(H_L+H_R)t} \\ &= \mathcal{N}\mathcal{O}_L(x_2,\bar{x}_2) e^{-i(H_L+H_R)t}\,|\Psi_\beta\rangle\langle\Psi_\beta|\,e^{i(H_L+H_R)t}\mathcal{O}_L^\dagger(x_1,\bar{x}_1).\end{aligned} \tag{4.32}$$

Time evolution under $H_L + H_R$ keeps the branch cut A as before. On the other hand, branch cut B now starts at $(x_B, \bar{x}_B) = (b + i\beta/2 + 2t, b - i\beta/2 - 2t)$.

As before when we computed Rényi entropy, we can consider both CFT with a single free boson and general large c 2d CFT.

4.3.1 Evolution under $H_L - H_R$

Let $X = \{A, B, A \cup B\}$. The calculation of $\Delta S_X^{(2)}$ involves a 4-pt function which we compute by mapping our two glued cylinders to the plane. These maps are given below for the different X:

$$\begin{aligned} z(x) &= \sqrt{e^{\frac{2\pi}{\beta}x} - 1}\,, \qquad \text{for} \quad X = A, \\ z(x) &= \sqrt{e^{\frac{2\pi}{\beta}x} + e^{\frac{2\pi}{\beta}b}}\,, \quad \text{for} \quad X = B, \\ z(x) &= \sqrt{\frac{e^{\frac{2\pi}{\beta}x} - 1}{e^{\frac{2\pi}{\beta}x} + e^{\frac{2\pi b}{\beta}}}}\,, \quad \text{for} \quad X = A \cup B\,. \end{aligned} \tag{4.33}$$

The same maps apply for $\bar{z}(\bar{x})$.

We can evaluate equation (2.56) for maps given in (4.33).

$$\begin{aligned} z_B &= \frac{1}{2}\left(1 - \frac{\cos\left(\frac{2\pi\epsilon}{\beta}\right) e^{\frac{2\pi(t-l)}{\beta}} + e^{\frac{2\pi b}{\beta}}}{\sqrt{e^{\frac{4\pi(t-l)}{\beta}} + 2\cos\left(\frac{2\pi\epsilon}{\beta}\right) e^{\frac{2\pi(t-l+b)}{\beta}} + e^{\frac{4\pi b}{\beta}}}}\right) \\ \bar{z}_B &= \frac{1}{2}\left(1 - \frac{\cos\left(\frac{2\pi\epsilon}{\beta}\right) e^{-\frac{2\pi(l+t)}{\beta}} + e^{\frac{2\pi b}{\beta}}}{\sqrt{e^{-\frac{4\pi(l+t)}{\beta}} + 2\cos\left(\frac{2\pi\epsilon}{\beta}\right) e^{-\frac{2\pi(t+l-b)}{\beta}} + e^{\frac{4\pi b}{\beta}}}}\right) \end{aligned} \tag{4.34}$$

$$\begin{aligned} z_{A\cup B} &= \frac{1}{2}\left(1 + \frac{e^{\frac{4\pi(t-l)}{\beta}} - \left(1 - e^{\frac{2\pi b}{\beta}}\right)\cos\left(\frac{2\pi\epsilon}{\beta}\right) e^{\frac{2\pi(t-l)}{\beta}} - e^{\frac{2\pi b}{\beta}}}{\sqrt{\left(-2\cos\left(\frac{2\pi\epsilon}{\beta}\right) e^{\frac{2\pi(t-l)}{\beta}} + e^{\frac{4\pi(t-l)}{\beta}} + 1\right)\left(e^{\frac{4\pi b}{\beta}} + 2\cos\left(\frac{2\pi\epsilon}{\beta}\right) e^{\frac{2\pi(b-l+t)}{\beta}} + e^{\frac{4\pi(t-l)}{\beta}}\right)}}\right) \\ \bar{z}_{A\cup B} &= \frac{1}{2}\left(1 + \frac{e^{-\frac{4\pi(l+t)}{\beta}} - \left(1 - e^{\frac{2\pi b}{\beta}}\right)\cos\left(\frac{2\pi\epsilon}{\beta}\right) e^{-\frac{2\pi(l+t)}{\beta}} - e^{\frac{2\pi b}{\beta}}}{\sqrt{\left(e^{-\frac{4\pi(l+t)}{\beta}} - 2\cos\left(\frac{2\pi\epsilon}{\beta}\right) e^{-\frac{2\pi(l+t)}{\beta}} + 1\right)\left(e^{\frac{4\pi b}{\beta}} + 2\cos\left(\frac{2\pi\epsilon}{\beta}\right) e^{\frac{2\pi(b-l-t)}{\beta}} + e^{-\frac{4\pi(l+t)}{\beta}}\right)}}\right) \end{aligned} \tag{4.35}$$

Free boson. We can compute Rényi mutual information using (2.62) and (2.59) with two additional cross-ratios. First, consider z_B. For small ϵ we can Taylor expand it as

$$z_B = \frac{1}{2}\left(1 + e^{\frac{2\pi(b+l-t)}{\beta}}\right)^{-2} \epsilon^2 + \mathcal{O}(\epsilon^4). \tag{4.36}$$

Similarly, $\bar{z}_B = \mathcal{O}(\epsilon^2)$. Thus,

$$\Delta S_B^{(2)} = \mathcal{O}(\epsilon^2). \tag{4.37}$$

Since we only perturbed $\mathrm{CFT_L}$ it is natural to expect that at the leading order nothing happens in $\mathrm{CFT_R}$.

Thus the change in mutual information equals

$$\Delta I_{A:B}^{(2)} = \Delta S_A^{(2)} - \Delta S_{A\cup B}^{(2)} = \log\left(\frac{1 + |z_{A\cup B}| + |1 - z_{A\cup B}|}{(1 + |z_A| + |1 - z_A|)}\right). \tag{4.38}$$

Time evolution of (4.38) is shown in Figure 4.2. We see that $\Delta S_{A\cup B}^{(2)} \approx \Delta S_A^{(2)}$ for $t < l + b$.

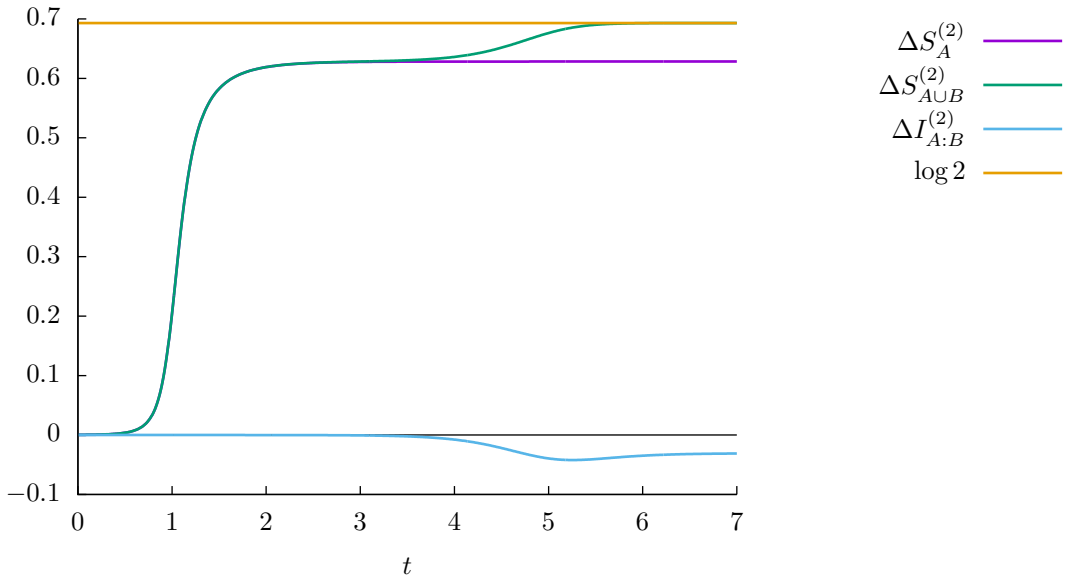

Figure 4.2: Growth of the Rényi entanglement entropies and mutual information for free scalar in TFD state. Parameters are $\epsilon = 0.2$, $\frac{\epsilon}{\beta} = \frac{1}{12}, l = 1$ and $b = 4$. Note that small increase of mutual information seen in the graph is an artifact of $\mathcal{O}(\epsilon)$ terms that we ignored.

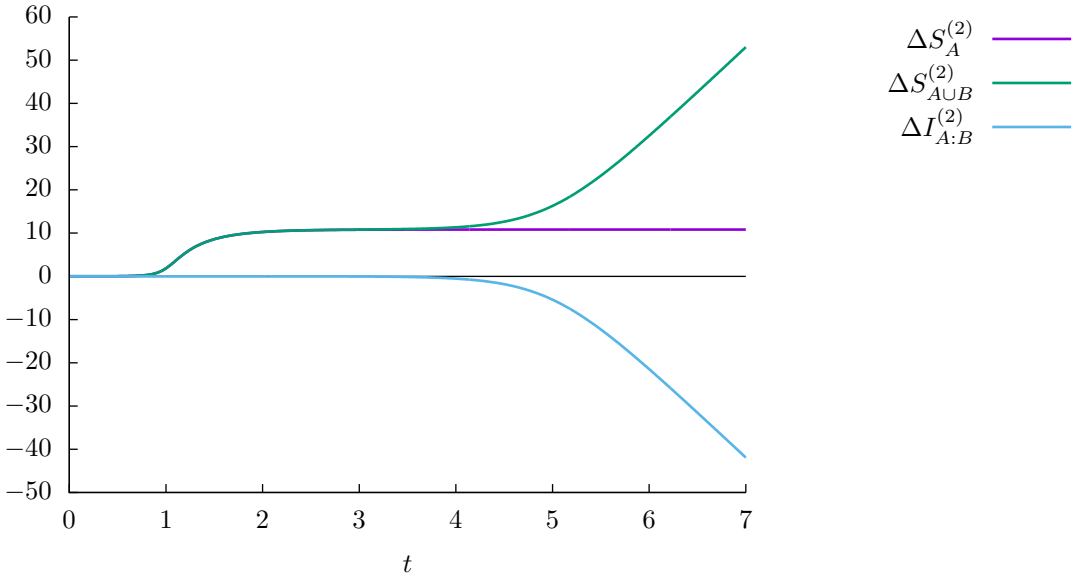

Figure 4.3: Growth of the Rényi entanglement entropies and mutual information for generic two dimensional CFT with large central charge c. Parameters are $\epsilon = 0.2$, $\frac{\epsilon}{\beta} = \frac{1}{12}, l = 1$ and $b = 4$.

But $\Delta S^{(2)}_{A\cup B}$ quickly approaches $\log 2$ for $t > l+b$. So the difference of mutual information from unperturbed thermal state is initially 0, starts decreasing at about $t \approx L+b$ and then saturates at

$$\Delta I^{(2)}_{A:B} = -\frac{\pi\epsilon}{\beta} + \mathcal{O}(\epsilon^2). \tag{4.39}$$

Large c CFT. Similarly, mutual information for large c 2d CFT is given by

$$\Delta I^{(2)}_{A:B} \simeq 4h \log\left(\frac{|1-z_{A\cup B}|}{|1-z_A|}\right). \tag{4.40}$$

In this case time evolution of mutual information is shown in Figure 4.3. As found in equation (4.27), $\Delta S^{(2)}_A$ saturates. On the other hand $\Delta S^{(2)}_{A\cup B}$ grows linearly forever. So mutual information decreases as

$$\Delta I^{(2)}_{A:B} \simeq -\frac{8\pi h}{\beta}(t-l-b). \tag{4.41}$$

4.3.2 Evolution under $H_L + H_R$

Rényi mutual information can be computed as before but we have to take into account the new location of branch cut B. This changes uniformazation maps to

$$\begin{aligned}
&z(x) = \sqrt{e^{\frac{2\pi}{\beta}x} - 1}, && \bar{z}(\bar{x}) = \sqrt{e^{\frac{2\pi}{\beta}\bar{x}} - 1}\,, && \text{for} \quad A \\
&z(x) = \sqrt{e^{\frac{2\pi}{\beta}x} + e^{\frac{2\pi}{\beta}(b+2t)}}, && \bar{z}(\bar{x}) = \sqrt{e^{\frac{2\pi}{\beta}\bar{x}} + e^{\frac{2\pi}{\beta}(b-2t)}}, && \text{for} \quad B \\
&z(x) = \sqrt{\frac{e^{\frac{2\pi}{\beta}x} - 1}{e^{\frac{2\pi}{\beta}x} + e^{\frac{2\pi}{\beta}(b+2t)}}}, && \bar{z}(\bar{x}) = \sqrt{\frac{e^{\frac{2\pi}{\beta}\bar{x}} - 1}{e^{\frac{2\pi}{\beta}\bar{x}} + e^{\frac{2\pi}{\beta}(b-2t)}}}\,, && \text{for} \quad A\cup B
\end{aligned} \tag{4.42}$$

Notice these maps encode the time evolution of the cuts inserted at $\tau = i\frac{\beta}{2}$ through the shifts $b \to b+2t$ for functions of x and $b \to b-2t$ for functions of $\bar{x}$, when compared with the maps (4.33). But they still satisfy $z_3 = -z_1$ and $z_4 = -z_2$, so we can use equation (2.59) to compute Rényi entropy.

The exact cross-ratios under these maps are

$$\begin{aligned}
z_B &= \frac{1}{2}\left(1 - \frac{\cos\left(\frac{2\pi\epsilon}{\beta}\right)e^{\frac{2\pi(t-l)}{\beta}} + e^{\frac{2\pi(b+2t)}{\beta}}}{\sqrt{e^{\frac{4\pi(t-l)}{\beta}} + 2\cos\left(\frac{2\pi\epsilon}{\beta}\right)e^{\frac{2\pi(3t-l+b)}{\beta}} + e^{\frac{4\pi(b+2t)}{\beta}}}}\right) \\
\bar{z}_B &= \frac{1}{2}\left(1 - \frac{\cos\left(\frac{2\pi\epsilon}{\beta}\right)e^{-\frac{2\pi(l+t)}{\beta}} + e^{\frac{2\pi(b-2t)}{\beta}}}{\sqrt{e^{-\frac{4\pi(l+t)}{\beta}} + 2\cos\left(\frac{2\pi\epsilon}{\beta}\right)e^{-\frac{2\pi(3t+l-b)}{\beta}} + e^{\frac{4\pi(b-2t)}{\beta}}}}\right)
\end{aligned} \tag{4.43}$$

$$\begin{aligned}
z_{A\cup B} = \quad & \frac{1}{2}\left(1 + \frac{e^{\frac{4\pi(t-l)}{\beta}} - \left(1 - e^{\frac{2\pi(b+2t)}{\beta}}\right)\cos\left(\frac{2\pi\epsilon}{\beta}\right)e^{\frac{2\pi(t-l)}{\beta}} - e^{\frac{2\pi(b+2t)}{\beta}}}{\sqrt{\left(-2\cos\left(\frac{2\pi\epsilon}{\beta}\right)e^{\frac{2\pi(t-l)}{\beta}} + e^{\frac{4\pi(t-l)}{\beta}} + 1\right)\left(e^{\frac{4\pi(b+2t)}{\beta}} + 2\cos\left(\frac{2\pi\epsilon}{\beta}\right)e^{\frac{2\pi(b-l+3t)}{\beta}} + e^{\frac{4\pi(t-l)}{\beta}}\right)}}\right) \\
\bar{z}_{A\cup B} = \quad & \frac{1}{2}\left(1 + \frac{e^{-\frac{4\pi(l+t)}{\beta}} - \left(1 - e^{\frac{2\pi(b-2t)}{\beta}}\right)\cos\left(\frac{2\pi\epsilon}{\beta}\right)e^{-\frac{2\pi(l+t)}{\beta}} - e^{\frac{2\pi(b-2t)}{\beta}}}{\sqrt{\left(e^{-\frac{4\pi(l+t)}{\beta}} - 2\cos\left(\frac{2\pi\epsilon}{\beta}\right)e^{-\frac{2\pi(l+t)}{\beta}} + 1\right)\left(e^{\frac{4\pi(b-2t)}{\beta}} + 2\cos\left(\frac{2\pi\epsilon}{\beta}\right)e^{\frac{2\pi(b-l-3t)}{\beta}} + e^{-\frac{4\pi(l+t)}{\beta}}\right)}}\right)
\end{aligned} \tag{4.44}$$

The behaviour of mutual information is plotted in Figure 4.4 and Figure 4.5. At early times

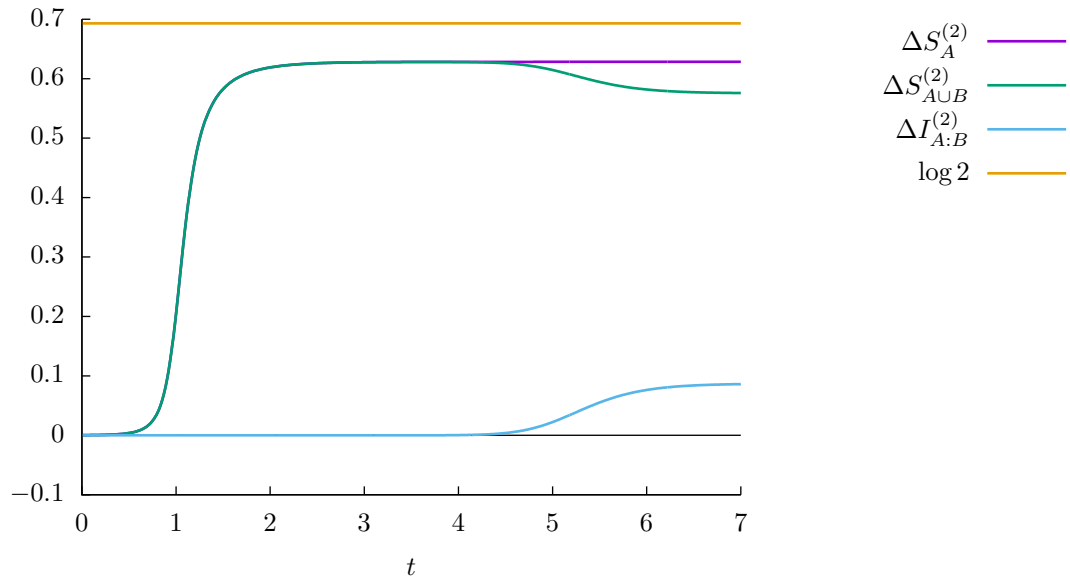

Figure 4.4: Growth of the Rényi entanglement entropies and mutual information for free scalar in TFD state. Parameters are $\epsilon = 0.2$, $\frac{\epsilon}{\beta} = \frac{1}{12}, l = 1$ and $b = 4$.

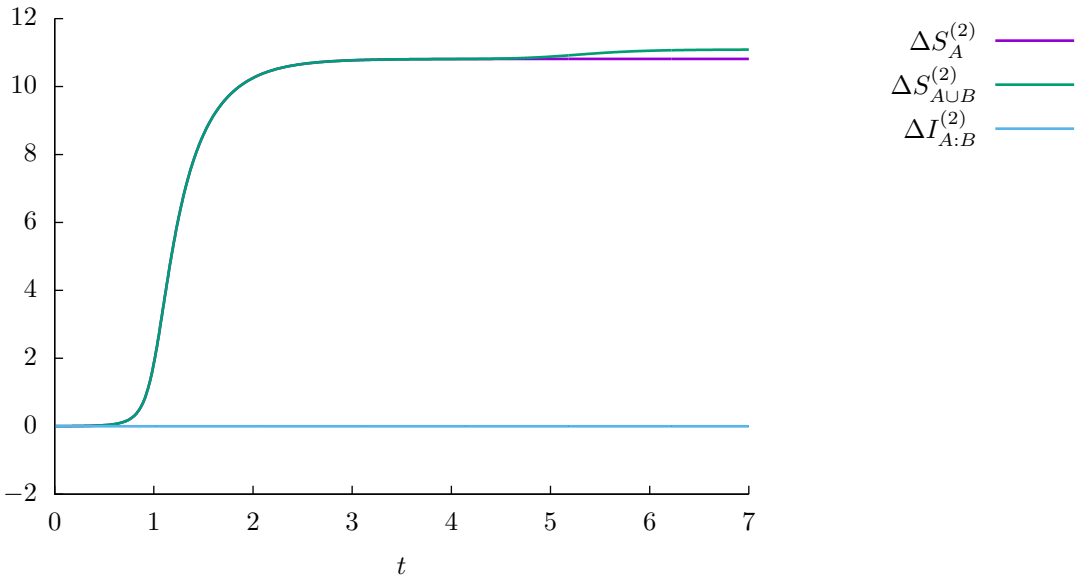

Figure 4.5: Growth of the Rényi entanglement entropies and mutual information for generic two dimensional CFT with large central charge c. Parameters are $\epsilon = 0.2$, $\frac{\epsilon}{\beta} = \frac{1}{12}, l = 1$ and $b = 4$.

$t < l + b$, Rényi entropy and mutual information behave just like in $H_L - H_R$ case for both free boson and generic large c CFT.

At late time for free boson CFT, Rényi entropy $\Delta S^{(2)}_{A\cup B}$ approaches

$$\Delta S^{(2)}_{A\cup B} \simeq \log 2 - \frac{2\pi\epsilon}{\beta} \tag{4.45}$$

Consequently,

$$\Delta I^{(2)}_{A\cup B} \simeq \log 2 - \frac{\pi\epsilon}{\beta} + \mathcal{O}(\epsilon^2). \tag{4.46}$$

In the large c limit we need to be slightly more careful and take into an account contribution from $S^{(2)}_B$ since it turns out that $S^{(2)}_A - S^{(2)}_{A\cup B} = \mathcal{O}(\epsilon^2)$. Then mutual information can be computed using

$$\Delta I^{(2)}_{A:B} \simeq 4h \log\left(\frac{|1 - z_{A\cup B}|}{|1 - z_A||1 - z_B|}\right). \tag{4.47}$$

At $\mathcal{O}(\epsilon^2)$, contribution from $S^{(2)}_B$ exactly cancels $S^{(2)}_A - S^{(2)}_{A\cup B}$ and at all times

$$\Delta I^{(2)}_{A:B}(t) = \mathcal{O}(\epsilon^4). \tag{4.48}$$

However, for $t > l + b$, exact value of mutual information quickly approaches 0

$$\lim_{t\to\infty} \Delta I^{(2)}_{A:B}(t) = 0. \tag{4.49}$$

4.3.3 Physical interpretation

We showed that energy density of local quench consists of two entangled localized energy lumps traveling in opposite directions at the speed of light. Perturbation does not reach the region of entanglement until $t = l$. Therefore, all Rényi entanglement entropies are suppressed for times $0 < t < l$. It is also hard for perturbation in CFT_L to affect entanglement in CFT_R. In all four cases we had S_B approximately thermal.

Let us now consider what happens with $H = H_L - H_R$ for free boson. Then one part of EPR pair enters the entanglement region that is highly entangled with B^c, the complement of entanglement region B in CFT_R as shown in Figure 4.6. However, entanglement entropy has a property that limits simultaneous entanglement with two distinct parties [127]. Therefore, for $l < t < l + b$, both ΔS_A and $\Delta S_{A\cup B}$ are reduced by $\mathcal{O}(\frac{\epsilon}{\beta})$. On the other hand, this mechanism does not apply to $\Delta S_{A\cup B}$ for times $t > l + b$ because there is no original entanglement between degrees of freedom in CFT_L located at $x > b$ and B^c in CFT_R.

In the large c case we deal with strongly interacting CFT, so it is harder to give qualitative interpretation. In this case $\Delta S_{A\cup B}$ grows linearly. Our results suggest that breaking of original entanglement between A and B lasts forever. In case of evolution with $H = H_L + H_R$, the interpretation is similar but we have to take into account that the position of cut B moves with time, so only entanglement between A and B^c is broken but not between A and B, this $\Delta S_A = \Delta S_{A\cup B}$.

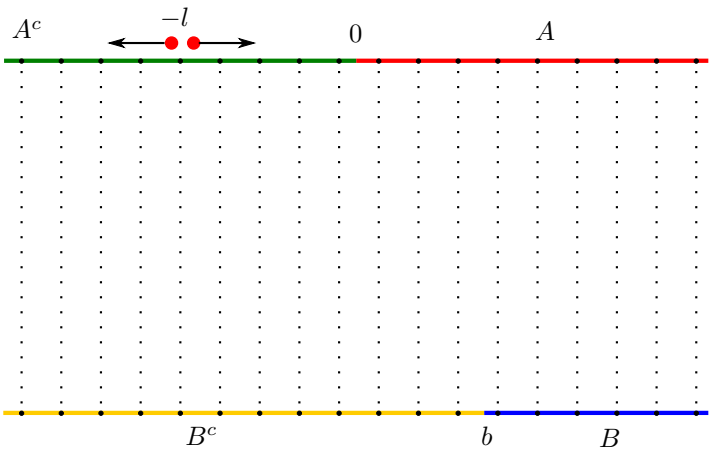

Figure 4.6: The structure of entanglement in thermofield double state at $t = 0$. We insert local perturbation at $-l$ in the left CFT.

Chapter 5

Scrambling time from local perturbations of the eternal BTZ black hole

In this chapter we compute entanglement entropy and mutual information for the thermofield double state perturbed by a local operator using twist operators (see section 2.5). Unlike in the case of uniformization maps used in chapter 4, this calculation will depend on a four point function. We will evaluate this using the results valid at large c reviewed in subsection 2.5.2. This will allow us to compute the von Neumann mutual information and to extract the scrambling time from our definition (1.74).

After the CFT calculation, we describe the same calculation in the bulk gravitational theory. This is done by using the observation that local CFT quenches can be modelled by a free falling particle in AdS [121], whose back-reaction on the metric can be computed analytically in three dimensions. We note that this setup can be approximated by shock wave geometries [84,89–91]. We will not pursue this direction here, though it has the advantage of being generalisable to higher dimensions. To describe TFD in 2d with two Hilbert spaces we will consider BTZ in Kruskal coordinates and two asymptotic regions as in [77]. We will determine how massive particles back-react on the geometry of BTZ black hole. This step provides the holographic description of the local CFT quench. Once the bulk geometry is known, we compute the holographic entanglement entropy using the RT prescription. This is achieved by noticing that geometries are locally AdS_3. CFT and gravity results agree precisely.

5.1 Local perturbation of TFD state

We are interested in what happens when we locally perturb TFD state. This can be done by inserting a primary operator ψ in the CFT_L at time $-t_\omega$ in the past[1]. However, when we calculate density matrix, we will have two copies of ψ inserted at the same point. This can be avoided by spreading out perturbation on a scale ϵ. We choose ϵ to be much larger than ultraviolet cut-off but other limits can be investigated too. Now, we can write down time-evolved reduced density matrix

$$\rho_L(t) = \mathcal{N} e^{-iH_L t} e^{-\epsilon H_L} \psi(0, -t_\omega) e^{2\epsilon H_L + \beta H_L} \psi^\dagger(0, -t_\omega) e^{-\epsilon H_L} e^{iH_L t}. \tag{5.1}$$

5.2 Single sided entropy

Let us choose our region A to be a finite interval with endpoints y and $y + L$.

Instead of working on $n-$sheeted Riemann surface directly we can use twist operators that glue different copies of the cylinder to compute entanglement entropy on non-replicated manifold

[1] t_ω here is entirely optional and is for convenience when comparing our results to other results in the literature that use out of order correlators in the CFT and shock wave geometries in the bulk.

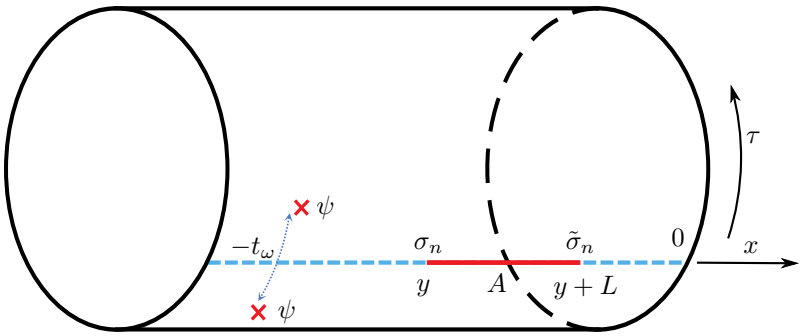

Figure 5.1: Region A depicted on the thermal cylinder.

[57, 105]. Recall that we have to compute Rényi entropy (1.48) which requires us to compute trace of ρ_A^n. It can be expressed via twist operators as

$$\operatorname{tr}\rho_A^n(t) = \frac{\langle \Psi(x_1,\bar{x}_1)\sigma_n(x_2,\bar{x}_2)\tilde{\sigma}_n(x_3,\bar{x}_3)\Psi^\dagger(x_4,\bar{x}_4)\rangle_{C_n}}{\left(\langle \psi(x_1,\bar{x}_1)\psi^\dagger(x_4,\bar{x}_4)\rangle_{C_1}\right)^n}, \tag{5.2}$$

where $\Psi = \psi_1 \cdot \psi_2 \cdots \psi_n$ is the product of local perturbation operators in each copy of the cylinder. Operator insertion points are

$$\begin{aligned} x_1 &= -i\epsilon, \quad x_2 = y - t_\omega - t_-, \quad x_3 = y + L - t_\omega - t_-, \quad x_4 = \quad i\epsilon, \\ \bar{x}_1 &= \quad i\epsilon, \quad \bar{x}_2 = y + t_\omega + t_-, \quad \bar{x}_3 = y + L + t_\omega + t_-, \quad \bar{x}_4 = -i\epsilon, \end{aligned}$$

conformal dimension of twist operators is

$$\Delta_\sigma = 2H_\sigma = \frac{c}{24}\left(n - \frac{1}{n}\right). \tag{5.3}$$

Two point function on the cylinder can be found by using exponential map (the same map is used for antiholomorphic coordinates too)

$$w(x) = e^{\frac{2\pi}{\beta}x} \tag{5.4}$$

to map it to the plane where it is fixed by conformal invariance

$$\langle \psi(x_1,\bar{x}_1)\psi(x_4,\bar{x}_4)\rangle_{C_1} = \left|\frac{\beta}{\pi}\sinh\left(\frac{\pi x_{14}}{\beta}\right)\right|^{-4h_\psi}. \tag{5.5}$$

To calculate 4-point function we should first map it from the cylinder using the same exponential map (5.4). Then we can simplify things further by mapping insertion points to the standard set of points $w_1 \mapsto 0, w_2 \mapsto z, w_3 \mapsto 1, w_4 \mapsto \infty$ with a map

$$z(w) = \frac{(w_1 - w)w_{34}}{w_{13}(w - w_4)}, \tag{5.6}$$

where we define $w_{ij} = w_i - w_j$ and cross ratios are as usual

$$z = \frac{w_{12}w_{34}}{w_{13}w_{24}}, \qquad 1 - z = \frac{w_{14}w_{23}}{w_{13}w_{24}}. \tag{5.7}$$

Primary fields transform as usual via equation (2.17). This allows us to write them in terms

of canonical four point function $G(z,\bar{z})$ on the complex plane.

$$\sigma(x_2,\bar{x}_2)\tilde{\sigma}(x_3,\bar{x}_3) = \left|\left(\frac{2\pi}{\beta}\right)^2 w_2 w_3\right|^{2H_\sigma} \left|\frac{w_{14}}{w_{13}w_{24}}\right|^{4H_\sigma} \sigma(z,\bar{z})\tilde{\sigma}(1,1) \tag{5.8}$$

$$= \left|\frac{\beta}{\pi}\sinh\left(\frac{\pi x_{23}}{\beta}\right)\right|^{-4H_\sigma} |1-z|^{4H_\sigma}\sigma(z,\bar{z})\tilde{\sigma}(1,1). \tag{5.9}$$

Similarly, ψ inserted at x_1 and x_4 is mapped to 0 and ∞.

Putting everything together results in

$$\operatorname{tr}\rho_A^n(t) = \left|\frac{\beta}{\pi\epsilon_{\text{UV}}}\sinh\left(\frac{\pi x_{23}}{\beta}\right)\right|^{-4H_\sigma} |1-z|^{4H_\sigma}\, G(z,\bar{z}). \tag{5.10}$$

The Rényi entropies are computed by inserting (5.10) into (1.48)

$$S_A^{(n)} = \frac{c(n+1)}{6}\log\left(\frac{\beta}{\pi\varepsilon_{UV}}\sinh\frac{\pi L}{\beta}\right) + \frac{1}{n-1}\log(|1-z|^{4H_\sigma}G(z,\bar{z})). \tag{5.11}$$

The first term is the Rényi entropy of 2d CFT in a thermal state. The second term is contribution due to perturbation. Note that the dependence on the conformal dimension of the local operator h_ψ is encoded in $G(z,\bar{z})$. Once we have Rényi entropy we can take $n\to 1$ limit. The first term is the standard thermal entanglement entropy. We will be mostly focusing on the second term, i.e. the difference between entanglement entropy of perturbed state and that of thermal state.

5.2.1 Large c limit

In chapter 2 we discussed properties of 4-point functions involving two light and two heavy operators that were considered in [107, 108, 110]. In this limit

$$\log G(z,\bar{z}) \simeq -\frac{c(n-1)}{6}\log\left(\frac{z^{\frac{1}{2}(1-\alpha_\psi)}\bar{z}^{\frac{1}{2}(1-\bar{\alpha}_\psi)}(1-z^{\alpha_\psi})(1-\bar{z}^{\bar{\alpha}_\psi})}{\alpha_\psi\bar{\alpha}_\psi}\right) + \mathcal{O}((n-1)^2) \tag{5.12}$$

where

$$\alpha_\psi = \sqrt{1-\frac{24h_\psi}{c}}. \tag{5.13}$$

Entanglement entropy corresponding to region A has a thermal contribution because we are on a cylinder and a contribution due to perturbation by a local operator

$$S_A = \frac{c}{3}\log\left(\frac{\beta}{\pi\epsilon_{\text{UV}}}\sinh\frac{\pi L}{\beta}\right) + \Delta S_A. \tag{5.14}$$

where

$$\Delta S_A = \frac{c}{6}\log\left(\frac{z^{\frac{1}{2}(1-\alpha_\psi)}\bar{z}^{\frac{1}{2}(1-\bar{\alpha}_\psi)}(1-z^{\alpha_\psi})(1-\bar{z}^{\bar{\alpha}_\psi})}{\alpha_\psi\bar{\alpha}_\psi(1-z)(1-\bar{z})}\right). \tag{5.15}$$

Equation (5.15) is exact so far and can be evaluated numerically but we can also work with analytic formulas by expanding in the size of perturbation ϵ. Then cross-ratios (5.6) are

$$\begin{aligned} z &\simeq 1 + \frac{2\pi i\epsilon}{\beta}\frac{\sinh\frac{\pi L}{\beta}}{\sinh\frac{\pi(y+L-t_--t_\omega)}{\beta}\sinh\frac{\pi(y-t_--t_\omega)}{\beta}} + \mathcal{O}(\epsilon^2), \\ \bar{z} &\simeq 1 - \frac{2\pi i\epsilon}{\beta}\frac{\sinh\frac{\pi L}{\beta}}{\sinh\frac{\pi(y+L+t_-+t_\omega)}{\beta}\sinh\frac{\pi(y+t_-+t_\omega)}{\beta}} + \mathcal{O}(\epsilon^2). \end{aligned} \tag{5.16}$$

Logarithm has a branch cut on the complex plane, so we must choose appropriate phases

for the cross-ratios. Imaginary part of z flips sign when $t_- + t_\omega \in (y, y+L)$, so $(z, \bar{z}) \to (e^{2\pi i}, 1)$ for $y < t + t_\omega < y + L$ and tends to $(1,1)$ for other regions. Hence,

$$\Delta S_A = \begin{cases} 0\,, & t_- + t_\omega < y \text{ or } t_- + t_\omega > y + L, \\ \dfrac{c}{6} \log \left[\dfrac{\beta}{\pi\epsilon} \dfrac{\sin \pi\alpha_\psi}{\alpha_\psi} \dfrac{\sinh\left(\dfrac{\pi(y+L-t_- - t_\omega)}{\beta}\right) \sinh\left(\dfrac{\pi(t_- + t_\omega - y)}{\beta}\right)}{\sinh\left(\dfrac{\pi L}{\beta}\right)} \right] & \text{otherwise}\,. \end{cases} \tag{5.17}$$

5.3 Two sided entropy

5.3.1 S_B

Calculation for region B on the second boundary is similar. This time twist operators are inserted in CFT_R, so we must add $\frac{i\beta}{2}$ to the insertion points of twist operators.

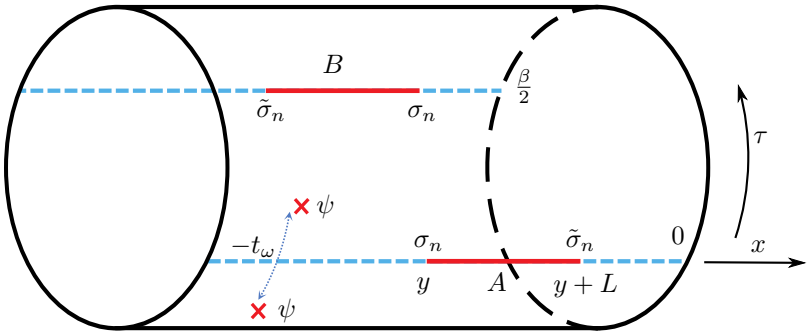

Figure 5.2: Region B depicted on the thermal cylinder.

Cross rations are

$$\begin{aligned} z = z_5 &\simeq 1 - \frac{2\pi i\epsilon}{\beta} \frac{\sinh \frac{\pi L}{\beta}}{\cosh \frac{\pi(y - t_+ - t_\omega)}{\beta} \cosh \frac{\pi(y+L-t_+-t_\omega)}{\beta}} + \mathcal{O}(\epsilon^2)\,, \\ \bar{z} = \bar{z}_5 &\simeq 1 + \frac{2\pi i\epsilon}{\beta} \frac{\sinh \frac{\pi L}{\beta}}{\cosh \frac{\pi(y + t_+ + t_\omega)}{\beta} \cosh \frac{\pi(y+L+t_++t_\omega)}{\beta}} + \mathcal{O}(\epsilon^2)\,. \end{aligned} \tag{5.18}$$

Note that this time imaginary part does not flip sign for any time. Hence $(z, \bar{z}) \to (1,1) \quad \forall t_+$. In this case entanglement entropy of region B stays thermal to leading order in ϵ and

$$S_B \simeq \frac{c}{3} \log \left(\frac{\beta}{\pi\epsilon_{\text{UV}}} \sinh \frac{\pi L}{\beta} \right). \tag{5.19}$$

This reproduces the CFT answer obtained by Cardy and Calabrese in [57].

5.3.2 $S_{A\cup B}$

Entanglement entropy of $A \cup B$ involves calculating the 6-point function

$$\text{tr}\, \rho^n_{A\cup B} = \frac{\langle \psi(x_1, \bar{x}_1) \sigma_n(x_2, \bar{x}_2) \tilde{\sigma}_n(x_3, \bar{x}_3) \sigma_n(x_5, \bar{x}_5) \tilde{\sigma}_n(x_6, \bar{x}_6) \psi^\dagger(x_4, \bar{x}_4) \rangle}{\left(\langle \psi(x_1, \bar{x}_1) \psi^\dagger(x_4, \bar{x}_4) \rangle_{C_1} \right)^n}. \tag{5.20}$$

After mapping to the plane with exponential map (5.4) and another transformation to map insertion points to the four standard points

$$z(w) = \frac{(w_1 - w)(w_3 - w_4)}{(w_1 - w_3)(w - w_4)}, \tag{5.21}$$

we obtain the following 6-point function

$$\langle\psi|\sigma_n(z,\bar{z})\tilde{\sigma}_n(1,1)\sigma_n(z_5,\bar{z}_5)\tilde{\sigma}_n(z_6,\bar{z}_6)|\psi\rangle\,. \tag{5.22}$$

There are two ways in which we can expand 6-point function in terms of 4-point functions. S-channel

$$\begin{aligned}&\langle\psi|\sigma_n(z,\bar{z})\tilde{\sigma}_n(1,1)\sigma_n(z_5,\bar{z}_5)\tilde{\sigma}_n(z_6,\bar{z}_6)|\psi\rangle\\&= \sum_\alpha \langle\psi|\sigma_n(z,\bar{z})\tilde{\sigma}_n(1,1)|\alpha\rangle\,\langle\alpha|\sigma_n(z_5,\bar{z}_5)\tilde{\sigma}_n(z_6,\bar{z}_6)|\psi\rangle\end{aligned} \tag{5.23}$$

and T-channel

$$\begin{aligned}&\langle\psi|\sigma_n(z,\bar{z})\tilde{\sigma}_n(1,1)\sigma_n(z_5,\bar{z}_5)\tilde{\sigma}_n(z_6,\bar{z}_6)|\psi\rangle\\&= \sum_\alpha \langle\psi|\sigma_n(z,\bar{z})\tilde{\sigma}_n(z_6,\bar{z}_6)|\alpha\rangle\,\langle\alpha|\sigma_n(z_5,\bar{z}_5)\tilde{\sigma}_n(1,1)|\psi\rangle\,.\end{aligned} \tag{5.24}$$

These channels in the CFT correspond to the two ways geodesic can wrap around the black hole horizon [110] (also see Figure 1.2). So to compute entanglement entropy we need to minimize over both channels.

For S-channel, we can write an operator product expansion (OPE) of twist operators

$$\sigma_n(z,\bar{z})\tilde{\sigma}_n(1,1) \sim \mathbb{I} + \mathcal{O}\left((z-1)^r\right) \qquad r \in \mathbb{N}. \tag{5.25}$$

The dominant contribution is just an identity operator. We will ignore all higher order terms. Then summation over $|\alpha\rangle$ reduces to state $|\psi\rangle$ due to orthogonality of 2-point functions

$$\sum_\alpha \langle\psi|\sigma_n(z,\bar{z})\tilde{\sigma}_n(1,1)|\alpha\rangle\,\langle\alpha| \simeq \langle\psi|\sigma_n(z,\bar{z})\tilde{\sigma}_n(1,1)|\psi\rangle\,\langle\psi| \tag{5.26}$$

So the first 4-pt function in equation (5.23) is the same as in S_A while the second the same as in S_B. Hence, mutual information vanishes in S-channel.

For T-channel, the state $|\psi\rangle$ is again the dominant contribution. Equation (5.24) again reduces to the product of two 4-point functions

$$\langle\psi|\sigma_n(z_5,\bar{z}_5)\tilde{\sigma}_n(1,1)|\psi\rangle = G(z_5,\bar{z}_5), \tag{5.27}$$

$$\langle\psi|\sigma_n(z,\bar{z})\tilde{\sigma}_n(z_6,\bar{z}_6)|\psi\rangle = |1-\tilde{z}_2|^{4H_\sigma}|z_2-z_6|^{-4H_\sigma}G(\tilde{z}_2,\bar{\tilde{z}}_2), \tag{5.28}$$

but the cross-ratios are not the same as in S-channel:

$$z_5 = 1 - \frac{2\pi i\epsilon}{\beta}\frac{\cosh\frac{\pi(t_- - t_+)}{\beta}}{\sinh\frac{\pi(y+L-t_- -t_\omega)}{\beta}\cosh\frac{\pi(y+L-t_+-t_\omega)}{\beta}} + \mathcal{O}(\epsilon^2), \tag{5.29}$$

$$\bar{z}_5 = 1 + \frac{2\pi i\epsilon}{\beta}\frac{\cosh\frac{\pi(t_- - t_+)}{\beta}}{\sinh\frac{\pi(y+L+t_- +t_\omega)}{\beta}\cosh\frac{\pi(y+L+t_++t_\omega)}{\beta}} + \mathcal{O}(\epsilon^2), \tag{5.30}$$

$$\tilde{z}_2 = 1 + \frac{2\pi i\epsilon}{\beta}\frac{\cosh\frac{\pi(t_- - t_+)}{\beta}}{\sinh\frac{\pi(y-t_- -t_\omega)}{\beta}\cosh\frac{\pi(y-t_+-t_\omega)}{\beta}} + \mathcal{O}(\epsilon^2), \tag{5.31}$$

$$\bar{\tilde{z}}_2 = 1 - \frac{2\pi i\epsilon}{\beta}\frac{\cosh\frac{\pi(t_- - t_+)}{\beta}}{\sinh\frac{\pi(y+t_- +t_\omega)}{\beta}\cosh\frac{\pi(y+t_++t_\omega)}{\beta}} + \mathcal{O}(\epsilon^2). \tag{5.32}$$

As before, we need to check monodromies when we use cross-ratios in equation (5.12). All antiholomorphic cross rations tend to 1. In fact this can be interpreted as antiholomorphic modes moving to the opposite direction and they never reach entanglement region. On the other hand, holomorphic cross ratios are $z_5 \simeq e^{-2\pi i}$ for $t_- + t_\omega > y + L$ and $\tilde{z}_2 \simeq e^{2\pi i}$ for $t_- + t_\omega > y$.

Hence, entanglement entropy is

$$S_{A\cup B} \simeq \frac{2c}{3}\log\left|\frac{\beta}{\pi\epsilon_{\rm UV}}\cosh\left(\frac{\pi\Delta t}{\beta}\right)\right| \quad t_- + t_\omega < y, \tag{5.33}$$

$$\begin{aligned} S_{A\cup B} \simeq{}& \frac{2c}{3}\log\left|\frac{\beta}{\pi\epsilon_{\rm UV}}\cosh\left(\frac{\pi\Delta t}{\beta}\right)\right| \\ &+ \frac{c}{6}\log\left(\frac{\beta}{\pi\epsilon}\frac{\sin\pi\alpha_\psi}{\alpha_\psi}\frac{\sinh\frac{\pi(t_-+t_w-y)}{\beta}\cosh\frac{\pi(t_++t_w-y)}{\beta}}{\cosh\frac{\pi\Delta t}{\beta}}\right) \quad y < t_- + t_\omega < y + L, \end{aligned} \tag{5.34}$$

$$\begin{aligned} S_{A\cup B} \simeq{}& \frac{2c}{3}\log\left|\frac{\beta}{\pi\epsilon_{\rm UV}}\cosh\left(\frac{\pi\Delta t}{\beta}\right)\right| + \frac{c}{3}\log\left(\frac{\beta}{\pi\epsilon}\frac{\sin\pi\alpha_\psi}{\alpha_\psi}\right) \\ &+ \frac{c}{6}\log\left(\frac{\sinh\frac{\pi(t_-+t_\omega-y)}{\beta}\cosh\frac{\pi(t_++t_\omega-y)}{\beta}}{\cosh\frac{\pi\Delta t}{\beta}}\right) \\ &+ \frac{c}{6}\log\left(\frac{\sinh\frac{\pi(t_-+t_\omega-y-L)}{\beta}\cosh\frac{\pi(t_++t_\omega-y-L)}{\beta}}{\cosh\frac{\pi\Delta t}{\beta}}\right) \quad t_- + t_\omega > y + L, \end{aligned} \tag{5.35}$$

where $\Delta t = t_- - t_+$.

5.4 Scrambling time

At early times $t_- + t_\omega < y$, perturbation has not reached the region of entanglement, so the single sided entropies are both thermal and mutual information is

$$I^0_{A:B} \equiv \frac{2c}{3}\log\left(\frac{\sinh\frac{\pi L}{\beta}}{\cosh\frac{\pi\Delta t}{\beta}}\right). \tag{5.36}$$

In the region $(y, y+L)$ mutual information evolves as

$$I_{A:B} \simeq I^0_{A:B} + \frac{c}{6}\log\left[\frac{\sinh\frac{\pi(y+L-t_--t_\omega)}{\beta}\cosh\frac{\pi\Delta t}{\beta}}{\cosh\frac{\pi(t_++t_w-y)}{\beta}\sinh\frac{\pi L}{\beta}}\right]. \tag{5.37}$$

It is notable that equation (5.37) is independent of the conformal dimension h_ψ.

At late times $t_- + t_\omega > y + L > y$ the mutual information equals

$$\begin{aligned} I_{A:B} \simeq{}& I^0_{A:B} - \frac{c}{3}\log\left(\frac{\beta}{\pi\epsilon}\frac{\sin\pi\alpha_\psi}{\alpha_\psi}\right) \\ &- \frac{c}{6}\log\left(\frac{\sinh\frac{\pi(t_-+t_\omega-y)}{\beta}\cosh\frac{\pi(t_++t_\omega-y)}{\beta}}{\cosh\frac{\pi\Delta t}{\beta}}\frac{\sinh\frac{\pi(t_-+t_\omega-y-L)}{\beta}\cosh\frac{\pi(t_++t_\omega-y-L)}{\beta}}{\cosh\frac{\pi\Delta t}{\beta}}\right). \end{aligned} \tag{5.38}$$

This defines late time behaviour of the mutual information and we are interested in the time $t^\star_w$ called the *scrambling time* defined by [84]

$$I_{A:B}(t^\star_w) = 0 \tag{5.39}$$

at $t_- = t_+ = 0$.

In the limit $t^\star_\omega \gg \beta$ we can approximate hyperbolic functions with exponentials. Then

$$t^\star_\omega = y + \frac{L}{2} - \frac{\beta}{2\pi}\log\left(\frac{\beta}{\pi\epsilon}\frac{\sin\pi\alpha_\psi}{\alpha_\psi}\right) + \frac{\beta}{\pi}\log\left(2\sinh\frac{\pi L}{\beta}\right) \tag{5.40}$$

Due to the non-compactness of the 2d CFT, no recurrences were expected to be seen in our calculation. Working in the small h_ψ/c limit, as required by our analysis, then

$$\frac{\beta}{\pi\epsilon}\frac{\sin\pi\alpha_\psi}{\alpha_\psi} \sim \frac{E_\psi}{S_{\text{density}}}, \qquad \text{where} \qquad S_{\text{density}} = \frac{\pi c}{3\beta}, \tag{5.41}$$

and $E_\psi = \frac{\pi h_\psi}{\epsilon}$ is the total energy of our local excitation given by integrating the energy density as in [124]. In this limit, the scrambling time reduces to

$$t^\star_\omega = y + \frac{L}{2} + \frac{\beta}{2\pi}\log\left(\frac{\pi S_{\text{density}}}{4E_\psi}\right) + \frac{\beta}{\pi}\log\left(2\sinh\frac{\pi L}{\beta}\right). \tag{5.42}$$

The $\log S$ dependence is indeed consistent with the original fast scrambling conjecture [82, 84].

5.4.1 Scrambling time when $t_- + t^\star_w > y + L$

In the calculation above we have calculated scrambling time in a certain limit. However, approximations that we did above are not always valid. In particular, mutual information diverges at $y + L$. In this section we will analyze our expressions more carefully and argue that

- Mutual information in the T-channel has at most one root.
- Mutual information is not increasing and is smooth at $y + L$.

It is useful to have expressions without using exponential approximation to investigate uniqueness of the root of mutual information.

In the regime $t_- + t^\star_w > y + L$

$$\begin{aligned} I_{A:B}(t^\star_w) \simeq \frac{c}{6}\log\left(\frac{\sinh^4\frac{\pi L}{\beta}}{\cosh\left(\frac{\pi(t^\star_w-y)}{\beta}\right)\sinh\left(\frac{\pi(t^\star_w-y)}{\beta}\right)\sinh\left(\frac{\pi(t^\star_w-y-L)}{\beta}\right)\cosh\left(\frac{\pi(t^\star_w-y-L)}{\beta}\right)}\right) \\ - \frac{c}{3}\log\left(\frac{\beta}{\pi\epsilon}\frac{\sin\pi\alpha_\psi}{\alpha_\psi}\right). \end{aligned} \tag{5.43}$$

So

$$\begin{aligned} \pi^2\alpha_\psi^2\epsilon^2\sinh^4\left(\frac{\pi L}{\beta}\right) = \beta^2\sin^2(\pi\alpha_\psi)\cosh\left(\frac{\pi(t^\star_w-y)}{\beta}\right) \\ \cdot\sinh\left(\frac{\pi(t^\star_w-y)}{\beta}\right)\cosh\left(\frac{\pi(t^\star_w-y-L)}{\beta}\right)\sinh\left(\frac{\pi(t^\star_w-y-L)}{\beta}\right), \end{aligned} \tag{5.44}$$

$$\begin{aligned} \left(\frac{\pi\alpha_\psi\epsilon\sinh^2\left(\frac{\pi L}{\beta}\right)}{\beta\sin(\pi\alpha_\psi)}\right)^2 = \frac{1}{4}\sinh^2\frac{2\pi(t^\star_w-y)}{\beta}\cosh\frac{2\pi L}{\beta} - \frac{1}{4}\sinh\frac{2\pi(t^\star_w-y)}{\beta} \\ \cdot\cosh\frac{2\pi(t^\star_w-y)}{\beta}\sinh\frac{2\pi L}{\beta}. \end{aligned} \tag{5.45}$$

This can be rewritten as

$$\left(\frac{2\pi\alpha_\psi\epsilon\sinh^2\left(\frac{\pi L}{\beta}\right)}{\beta\sin(\pi\alpha_\psi)}\right)^2 = \sinh^2\frac{2\pi(t^\star_\omega-y)}{\beta}\cosh\frac{2\pi L}{\beta}\left(1 - \frac{\tanh\frac{2\pi L}{\beta}}{\tanh\frac{2\pi(t^\star_\omega-y)}{\beta}}\right). \tag{5.46}$$

Thus, the vanishing of the mutual information does indeed happen for $t_\omega^\star > y + L$.

Let us denote

$$A = \frac{2\pi\alpha_\psi \epsilon \sinh^2\left(\frac{\pi L}{\beta}\right)}{\beta \sin(\pi\alpha_\psi)}, \tag{5.47}$$

$$T = \sinh^2 \frac{2\pi(t_w^\star - y)}{\beta}. \tag{5.48}$$

Then our equation becomes

$$\left(T\cosh\frac{2\pi L}{\beta} - A^2\right)^2 = T(1+T)\sinh^2\frac{2\pi L}{\beta}, \tag{5.49}$$

or alternatively,

$$T^2 - \left(2A^2\cosh\frac{2\pi L}{\beta} + \sinh^2\frac{2\pi L}{\beta}\right)T + A^4 = 0. \tag{5.50}$$

Vieta's formulae immediately tell us that there are two positive roots.

$$T = A^2\cosh\frac{2\pi L}{\beta} + \frac{1}{2}\sinh^2\frac{2\pi L}{\beta} \pm \sqrt{\left(A^2\cosh\frac{2\pi L}{\beta} + \frac{1}{2}\sinh^2\frac{2\pi L}{\beta}\right)^2 - A^4}, \tag{5.51}$$

$$\frac{T}{\sinh^2\frac{2\pi L}{\beta}} = \frac{1}{2} + \frac{A^2\cosh\frac{2\pi L}{\beta}}{\sinh^2\frac{2\pi L}{\beta}} \pm \sqrt{\frac{1}{4} + \frac{A^2\cosh\frac{2\pi L}{\beta}}{\sinh^2\frac{2\pi L}{\beta}} + \frac{A^4}{\sinh^2\frac{2\pi L}{\beta}}}. \tag{5.52}$$

Roots must satisfy equation (5.45) but only positive root satisfies it while negative is an artifact of squaring. Since $t_\omega^\star > y + L$, the left hand side must be larger than one and it would seem that there is always a unique root in this region. However, we will see later that this is an artifact of expansion in ε. In subsection 5.4.3 we will determine range of parameters when the root is in this region.

5.4.2 Scrambling time when $t_- + t_w^\star \in (y, y + L)$

In this case the condition for vanishing mutual information is

$$\sinh^3\frac{\pi L}{\beta}\sinh\frac{\pi(y + L - t_w^\star)}{\beta} = \cosh\frac{\pi(y - t_w^\star)}{\beta} \tag{5.53}$$

$$\sinh^3\frac{\pi L}{\beta}\left(\sinh\frac{\pi(y - t_w^\star)}{\beta}\cosh\frac{\pi L}{\beta} + \cosh\frac{\pi(y - t_w^\star)}{\beta}\sinh\frac{\pi L}{\beta}\right) = \cosh\frac{\pi(y - t_w^\star)}{\beta} \tag{5.54}$$

$$\tanh\frac{\pi(y - t_w^\star)}{\beta} = \frac{1 - \sinh^4\frac{\pi L}{\beta}}{\sinh^3\frac{\pi L}{\beta}\cosh\frac{\pi L}{\beta}} \tag{5.55}$$

$$t_w^\star = y + \frac{\beta}{\pi}\tanh^{-1}\left(\frac{\sinh^4\frac{\pi L}{\beta} - 1}{\sinh^3\frac{\pi L}{\beta}\cosh\frac{\pi L}{\beta}}\right). \tag{5.56}$$

Curiously, all dependence on α_ψ that carries the information about the perturbation cancels.

Second term in (5.56) is clearly less than L:

$$\frac{\sinh^4\frac{\pi L}{\beta} - 1}{\sinh^3\frac{\pi L}{\beta}\cosh\frac{\pi L}{\beta}} < \tanh\frac{\pi L}{\beta} \tag{5.57}$$

is always valid. Thus, the root, if it exists, belongs to the interval we are studying.

On the other hand, the function $\frac{1-\sinh^4\frac{\pi L}{\beta}}{\sinh^3\frac{\pi L}{\beta}\cosh\frac{\pi L}{\beta}}$ saturates to -1 very quickly. Thus, the root does satisfy being very close to the edge of the interval, i.e. $t_\omega^\star \sim y + L$.

So it would seem that mutual information vanishes at two points, once in $t_- + t_w^\star \in (y, y+L)$ and once in $t_- + t_w^\star > y + L$. However, this is not what we expect from physical considerations.

5.4.3 Scrambling time at higher orders in ϵ

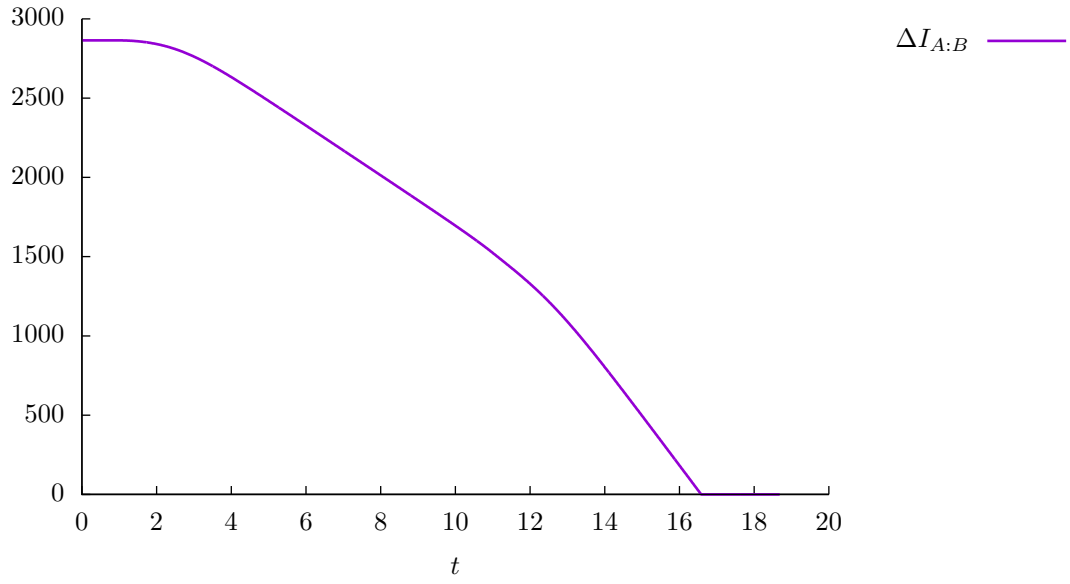

Figure 5.3: Mutual information computed by using exact cross ratios. Parameters are $y = 1, L = 10, \beta = 4, \epsilon = 0.0001, \alpha_\psi = 0.99999$, $c = 600$.

In this section we will argue that one of the roots is in fact an artifact of first order expansion in ϵ. We need to work in higher orders of ϵ to analyse situation more carefully. However, plugging cross-ratios into Fitzpatrick, Kaplan, Walters formula (5.12) would result in overly complicated expressions. To get some intuition about what is happening we can do numerical simulation with exact cross-ratios. Figure 5.3 shows how mutual information behaves. Note that nothing special happens at y or $y+L$, mutual information is smooth and monotonically decreasing until it reaches 0 where we have to switch to S channel and this forces mutual information to be 0.

This differs from what we obtained in first order expansion in ϵ. In fact our approximation breaks down close to $y + L$ and more careful analysis is necessary. Not too close to $y + L$ numerically computed mutual information and the one computed using approximate cross ratios matches nicely. However, close to $y + L$ mutual information computed analytically behave poorly, i.e. one-sided limits are

$$\lim_{t_w \to y+L^-} I_{A:B}(t_w) = -\infty, \tag{5.58}$$

$$\lim_{t_w \to y+L^+} I_{A:B}(t_w) = +\infty. \tag{5.59}$$

Expressions at higher orders in ϵ are extremely complicated, so we need to use other approaches. One possibility is to compare values of mutual information at points $y + L - \epsilon$ and $y + L + \epsilon$.

Let us first consider condition

$$I_{A:B}(y + L - \epsilon) < 0, \tag{5.60}$$

which corresponds to the root being in $(y, y + L)$ and given by equation (5.56)

$$\sinh^3 \frac{\pi L}{\beta} \sinh \frac{\pi \epsilon}{\beta} < \cosh \frac{\pi L}{\beta}. \tag{5.61}$$

We will take ϵ to be small, so

$$\frac{\beta}{\pi\epsilon} > \frac{\sinh^3 \frac{\pi L}{\beta}}{\cosh \frac{\pi L}{\beta}}. \tag{5.62}$$

Now, let us consider

$$I_{A:B}(y + L + \epsilon) > 0, \tag{5.63}$$

$$\sinh^3 \frac{\pi L}{\beta} > \left(\frac{\beta}{\pi\epsilon}\frac{\sin \pi\alpha_\psi}{\alpha_\psi}\right)^2 \cosh \frac{\pi L}{\beta} \sinh \frac{\pi\epsilon}{\beta} \cosh \frac{\pi\epsilon}{\beta}. \tag{5.64}$$

For small ϵ

$$\frac{\beta}{\pi\epsilon}\left(\frac{\sin \pi\alpha_\psi}{\alpha_\psi}\right)^2 < \frac{\sinh^3 \frac{\pi L}{\beta}}{\cosh \frac{\pi L}{\beta}}. \tag{5.65}$$

When neither condition is satisfied then the root must be in $(y + L - \varepsilon, y + L + \varepsilon)$.

Equations (5.62) and (5.65) show that for small perturbations when $\alpha \to 1$ scrambling time $t^\star_\omega$ will satisfy $t_- + t^\star_w > y + L$, and approximations made while deriving equation (5.40) are valid in this regime of parameters.

5.5 Holographic description

As discussed before, in AdS/CFT correspondence, in the semiclassical approximation we can model the effect of local quench by adding a massive particle to bulk spacetime. In general, back-reaction of the particle with mass m on metric is difficult to compute because it requires solving full Einstein's equations. However, in three dimensions Einstein's gravity has no local degrees of freedom, so it is possible to compute back-reaction by mapping [128] metric of eternal BTZ to global AdS_3 coordinates (r, τ, φ)

$$ds^2 = -(r^2 + R^2)d\tau^2 + \frac{R^2}{r^2 + R^2}dr^2 + r^2 d\varphi^2. \tag{5.66}$$

Back-reaction of particle located at the origin of AdS ($r = 0$) is known

$$ds^2 = -(r^2 + R^2 - \mu)d\tau^2 + \frac{R^2}{r^2 + R^2 - \mu}dr^2 + r^2 d\varphi^2. \tag{5.67}$$

where $\mu = 8GR^2m$ is just a rescaled mass of a particle. Depending on the value of μ, this geometry describes conical defect or BTZ black hole.

According to Ryu-Takayanagi proposal, holographic entanglement entropy is proportional to the length of geodesic between two points on the boundary of the BTZ spacetime. We will use the map between Kruskal coordinates and global AdS coordinates. The length between two boundary points in (5.67) is known [121] and gives rise to the following entanglement entropy[2]

$$S_A = \frac{c}{6}\log\left[\frac{2r^{(1)}_\infty \cdot r^{(2)}_\infty}{R^2}\frac{\cos\left(|\Delta\tau_\infty|a\right) - \cos\left(|\Delta\varphi_\infty|a\right)}{a^2}\right], \tag{5.68}$$

where $a \equiv \sqrt{1 - \frac{\mu}{R^2}} = \alpha_\psi$ carries the information about the perturbation, as in the CFT discussion, $\Delta\tau_\infty = \tau^{(2)}_\infty - \tau^{(1)}_\infty$ and $\Delta\varphi_\infty = \varphi^{(2)}_\infty - \varphi^{(1)}_\infty$ satisfies $0 < |\Delta\varphi_\infty| < \pi$.

So our goal in the remainder of the chapter will be to find the positions of boundary points in global AdS. Once we know them, we will see that entanglement entropy agrees with the CFT result, thus mutual information and scrambling time must agree as well.

[2]In order to compare CFT and bulk results easier, we will write holographic entanglement entropy in terms of boundary central charge c which is related to radius of AdS_3 via $\frac{c}{6} = \frac{R}{4G_N}$.

5.5.1 Free falling particle model

The AdS-Schwarzschild patch of the BTZ black hole is

$$ds^2 = \frac{R^2}{z^2}\left[-\left(1-Mz^2\right)dt_-^2 + \frac{dz^2}{1-Mz^2} + d\theta^2\right], \qquad \theta \sim \theta + 2\pi \tag{5.69}$$

where $z = \frac{R}{r}$ is the inverse radial coordinate and M is the mass of black hole which is related to its Hawking temperature as $\beta = \frac{2\pi}{\sqrt{M}}$.

In the CFT we considered fields without spin, so in the bulk we can choose particle to have no angular momentum and to stay at $\theta = 0$ at all times. The action of a free falling particle in this background is

$$S = -mR\int \frac{d\tau}{z(\tau)}\sqrt{1 - Mz(\tau)^2 - \frac{\dot{z}(\tau)^2}{1-Mz(\tau)^2}}\,. \tag{5.70}$$

This action is independent of t, so we can use Noether's theorem. After the change of variables $x^{-2} = 1 - Mz^2$ the Lagrangian becomes

$$\mathcal{L} = \frac{1}{x^2-1}\sqrt{(x^2-1)M - \dot{x}^2}. \tag{5.71}$$

The first integral of Euler-Lagrange equations is

$$\dot{x}\frac{\partial\mathcal{L}}{\partial\dot{x}} - \mathcal{L} \equiv \frac{-\dot{x}^2}{(x^2-1)\sqrt{(x^2-1)M-\dot{x}^2}} - \frac{1}{x^2-1}\sqrt{(x^2-1)M-\dot{x}^2} = -KM, \tag{5.72}$$

for some constant $K \in \mathbb{R}\setminus\{0\}$. This can be rearranged into

$$\dot{x}^2 = Mx^2 - (K^{-2} + M). \tag{5.73}$$

After using initial conditions, the equation above becomes

$$\dot{x}^2 = Mx^2 - \frac{1}{1-M\epsilon^2}. \tag{5.74}$$

Hence, we obtain a trajectory $(t_-(\tilde{\tau}), z(\tilde{\tau}), \theta(\tilde{\tau}))$ of a free falling particle

$$t_- = \tilde{\tau}, \quad \theta = 0, \quad 1 - Mz^2 = (1-M\epsilon^2)\cosh^{-2}\left(\sqrt{M}(\tilde{\tau}+t_\omega)\right), \tag{5.75}$$

satisfying initial condition $z(-t_\omega) = \epsilon$, $\dot{z}(-t_\omega) = 0$. Note that our results hold for any time t_ω. In particular, when the t_ω is large, they reproduce approximate description of the bulk shock-wave propagation along the BTZ horizon [84, 91]. However, unlike back-reaction map approach, bulk shock-wave generalizes to higher dimensions easier.

The energy of the particle is given by

$$E = -\frac{g_{tt}}{\sqrt{-g_{tt}}}\bigg|_{t=0} = \frac{mR}{\epsilon}\sqrt{1-M\epsilon^2}. \tag{5.76}$$

This matches the energy of the CFT perturbation in the small ϵ limit if

$$m = \frac{2h_\psi}{R}. \tag{5.77}$$

5.5.2 Free falling particle in Kruskal coordinates

The BTZ metric in Kruskal coordinates[3] is

$$ds^2 = R^2 \frac{-4dudv + (-1+uv)^2 d\phi^2}{(1+uv)^2}. \tag{5.78}$$

We will again assume $\phi = 0$. Then the action of a free falling particle (5.70) in Kruskal coordinates is

$$S = -2mR \int \frac{\sqrt{v'}}{1+uv} du. \tag{5.79}$$

Its equation of motion

$$v''(uv+1) - 2v'(uv'-v) = 0\,, \tag{5.80}$$

has general solution

$$v(u) = \frac{C_2 + \left(C_1 + C_2^2\right) u}{1 + C_2 u}, \qquad v'(u) = \frac{C_1}{(1+C_2 u)^2}\,. \tag{5.81}$$

This matches trajectory in the Schwarzschild patch (5.75) if constants are chosen to be

$$C_1 = -\frac{v_0(u_0 v_0 + 1)^2}{u_0(u_0 v_0 - 1)^2} = M\epsilon^2 e^{2\sqrt{M}t_\omega}, \qquad C_2 = \frac{2v_0}{1 - u_0 v_0} = -\sqrt{1 - M\epsilon^2}\, e^{\sqrt{M}t_\omega}\,. \tag{5.82}$$

5.5.3 Back-reaction map

Now we will map the free falling particle to the origin of AdS_3 using a map from [128]. However, we need a couple of adjustments. First, in BTZ geometry we put free falling particle at rest at time $-t_\omega$ in the past instead of at $t = 0$. In Kruskal coordinates boosts in time direction are implemented with

$$u \mapsto e^{\lambda_1} u, \qquad v \mapsto e^{-\lambda_1} v. \tag{5.83}$$

Even with this boost the static particle at the origin of AdS in global coordinates does not map to trajectory (5.81). In practice, it is possible to identify the necessary additional boost by looking at AdS_3 embedding coordinates. It turns out that boost in $X_1 - X_3$ plane with an appropriately chosen rapidity λ_2 works. In chapter 6 we will discuss how to identify the necessary boost in more complicated scenarios. Then back-reaction map becomes

$$\begin{aligned}
\sqrt{R^2 + r^2}\sin\tau &= \cosh\lambda_1\, X_0 + \sinh\lambda_1\, X_3 \\
&= R\frac{e^{\lambda_1} u + e^{-\lambda_1} v}{1+uv}, \\
\sqrt{R^2 + r^2}\cos\tau &= \cosh\lambda_2\, X_1 - \sinh\lambda_2\, (\sinh\lambda_1\, X_0 + \cosh\lambda_1\, X_3) \\
&= \frac{R\cosh\lambda_2(1-uv)}{1+uv}\left(\cosh\phi - \tanh\lambda_2 \frac{e^{\lambda_1} u - e^{-\lambda_1} v}{1-uv}\right), \\
r\sin\varphi &= X_2 = R\frac{1-uv}{1+uv}\sinh\phi, \\
r\cos\varphi &= -\sinh\lambda_2\, X_1 + \cosh\lambda_2\, (\sinh\lambda_1\, X_0 + \cosh\lambda_1\, X_3) \\
&= \frac{R\cosh\lambda_2(1-uv)}{1+uv}\left(\frac{e^{\lambda_1} u - e^{-\lambda_1} v}{1-uv} - \tanh\lambda_2\cosh\phi\right).
\end{aligned} \tag{5.84}$$

[3]Notation: note that we will use ϕ for angular coordinate in the context of Kruskal coordinates and θ in the context of BTZ Schwarzschild coordinates. In this chapter $\sqrt{M}\theta = \phi$. On the other hand, φ is completely different angle describing global AdS.

We can determine boost parameters λ_1 and λ_2 form the last two equations by squaring them. Then

$$r = \left|\frac{R(1-uv)\cosh\lambda_2}{1+uv}\right| \sqrt{\frac{\sinh^2\phi}{\cosh^2\lambda_2} + \left(\frac{e^{\lambda_1}u - e^{-\lambda_1}v}{1-uv} - \tanh\lambda_2\cosh\phi\right)^2}. \tag{5.85}$$

Thus $r=0$ gets mapped to geodesic $v(u)$ if

$$\lambda_1 = \sqrt{M}t_\omega\,, \qquad \tanh\lambda_2 = \sqrt{1-M\epsilon^2}\,. \tag{5.86}$$

Hence, the map between a free falling particle and the origin of AdS_3 global coordinates is

$$r = \frac{R}{\sqrt{M}\epsilon}\left|\frac{1-uv}{1+uv}\right| \sqrt{M\epsilon^2\sinh^2\phi + \left(\frac{e^{\sqrt{M}t_\omega}\,u - e^{-\sqrt{M}t_\omega}\,v}{1-uv} - \sqrt{1-M\epsilon^2}\cosh\phi\right)^2}, \tag{5.87}$$

$$\tan\tau = \sqrt{M}\epsilon\frac{\frac{e^{\sqrt{M}t_\omega}u+e^{-\sqrt{M}t_\omega}v}{1-uv}}{\cosh\phi - \sqrt{1-M\epsilon^2}\,\frac{e^{\sqrt{M}t_\omega}\,u-e^{-\sqrt{M}t_\omega}\,v}{1-uv}}\,, \tag{5.88}$$

$$\tan\varphi = \sqrt{M}\epsilon\frac{\sinh\phi}{\frac{e^{\sqrt{M}t_\omega}u-e^{-\sqrt{M}t_\omega}v}{1-uv} - \sqrt{1-M\epsilon^2}\cosh\phi}\,. \tag{5.89}$$

5.5.4 Geodesics on the left boundary

Consider the entanglement region A in BTZ geometry with endpoints (t_-, z_∞, L_1) and (t_-, z_∞, L_2).

In order to apply back-reaction map we first need to convert endpoints in the Schwarzschild coordinates to endpoints in Kruskal coordinates. This map is different for left and right boundary. Here we will provide it for both cases

$$u_\mp = \pm\sqrt{\frac{1-\sqrt{M}z_\infty}{1+\sqrt{M}z_\infty}}e^{\sqrt{M}t_\mp}, \qquad v_\mp = \mp\sqrt{\frac{1-\sqrt{M}z_\infty}{1+\sqrt{M}z_\infty}}e^{-\sqrt{M}t_\mp} \tag{5.90}$$

Thus

$$\frac{e^{\sqrt{M}t_\omega}u_\mp - e^{-\sqrt{M}t_\omega}v_\mp}{1-u_\mp v_\mp} = \pm\sqrt{1-Mz_\infty^2}\cosh\left(\sqrt{M}(t_\mp+t_\omega)\right), \tag{5.91}$$

$$\frac{e^{\sqrt{M}t_\omega}u_\mp + e^{-\sqrt{M}t_\omega}v_\mp}{1-u_\mp v_\mp} = \pm\sqrt{1-Mz_\infty^2}\sinh\left(\sqrt{M}(t_\mp+t_\omega)\right). \tag{5.92}$$

We will now apply formula (5.68) to calculate entanglement entropy S_A. From (5.87) we obtain

$$r^{(1)}r^{(2)} \simeq \left(\frac{R}{M\epsilon z_\infty}\right)^2 D_1 D_2, \tag{5.93}$$

where

$$D_i = |\cosh\sqrt{M}L_i - \cosh\sqrt{M}(t_- + t_\omega)| \quad i=1,2 \tag{5.94}$$

whereas the other coordinates are

$$\tan\tau^{(i)} \simeq \sqrt{M}\epsilon\frac{\sinh\left(\sqrt{M}(t_-+t_\omega)\right)}{\cosh\left(\sqrt{M}L_i\right) - \cosh\left(\sqrt{M}(t_-+t_\omega)\right)} \tag{5.95}$$

$$\tan\varphi^{(i)} \simeq \sqrt{M}\epsilon\frac{\sinh\left(\sqrt{M}L_i\right)}{\cosh\left(\sqrt{M}(t_-+t_\omega)\right) - \cosh\left(\sqrt{M}L_i\right)} \tag{5.96}$$

with $i=1,2$. The exact value of τ and φ depends on the value of $t_- + t_\omega$. There are three

cases.

1. Early time: $t_- + t_\omega < L_1 < L_2$.

2. Intermediate time: $L_1 < t_- + t_\omega < L_2$.

3. Late time: $L_1 < L_2 < t_- + t_\omega$.

Case 1: early time. The boundary points are

$$\tau^{(i)} \simeq \sqrt{M}\epsilon \frac{\sinh\left(\sqrt{M}(t_- + t_\omega)\right)}{D_i}, \qquad \varphi^{(i)} \simeq \pi - \sqrt{M}\epsilon \frac{\sinh\left(\sqrt{M}L_i\right)}{D_i}\,. \tag{5.97}$$

These determine the coordinate intervals to be

$$\begin{aligned} |\Delta\tau| &\simeq \frac{\sqrt{M}\epsilon}{D_1 D_2}|D_2 - D_1| \sinh\sqrt{M}(t_- + t_\omega)\,, \\ |\Delta\varphi| &\simeq \frac{\sqrt{M}\epsilon}{D_1 D_2}\left|D_1 \sinh\sqrt{M}L_2 - D_2 \sinh\sqrt{M}L_1\right|\,. \end{aligned} \tag{5.98}$$

Due to the identity

$$D_1 D_2(|\Delta\varphi|^2 - |\Delta\tau|^2) = 4M\epsilon^2 \sinh^2\frac{\pi\Delta L}{\beta}\,, \tag{5.99}$$

the geodesic length is

$$\begin{aligned} L_\gamma &\simeq \log\left[\frac{2r^{(1)}r^{(2)}}{R^2}\frac{\cos\left(a|\Delta\tau|\right) - \cos\left(a|\Delta\varphi|\right)}{a^2}\right] \simeq \log\left[\frac{r^{(1)}r^{(2)}}{R^2}(|\Delta\varphi|^2 - |\Delta\tau|^2)\right] \\ &\simeq 2\log\left(\frac{\beta}{\pi z_\infty}\sinh\frac{\pi L}{\beta}\right)\,. \end{aligned} \tag{5.100}$$

Thus we obtain that at early time entanglement entropy S_A is purely thermal

$$S_A = \frac{c}{3}\log\left(\frac{\beta}{\pi z_\infty}\sinh\frac{\pi L}{\beta}\right)\,. \tag{5.101}$$

Case 2: intermediate time. The boundary points are

$$\tau^{(1)} \simeq \pi - \sqrt{M}\epsilon\frac{\sinh\sqrt{M}(t_- + t_\omega)}{D_1}\,, \qquad \varphi^{(1)} \simeq \sqrt{M}\epsilon\frac{\sinh\sqrt{M}L_1}{D_1}\,, \tag{5.102}$$

$$\tau^{(2)} \simeq \sqrt{M}\epsilon\frac{\sinh\sqrt{M}(t_- + t_\omega)}{D_2}\,, \qquad \varphi^{(2)} \simeq \pi - \sqrt{M}\epsilon\frac{\sinh\sqrt{M}L_2}{D_2}\,. \tag{5.103}$$

From them we can easily get the absolute values of the intervals

$$\begin{aligned} |\Delta\tau| &\simeq \pi - \frac{\sqrt{M}\epsilon}{D_1 D_2}(D_1 + D_2)\sinh\sqrt{M}(t_- + t_\omega)\,, \\ |\Delta\varphi| &\simeq \pi - \frac{\sqrt{M}\epsilon}{D_1 D_2}\left(D_1 \sinh\sqrt{M}L_2 + D_2 \sinh\sqrt{M}L_1\right)\,. \end{aligned} \tag{5.104}$$

Notice that in the small ϵ limit, $|\Delta\tau|$ and $|\Delta\varphi|$ are close to each other

$$\delta = |\Delta\varphi| - |\Delta\tau| = \frac{\sqrt{M}\epsilon}{D_1 D_2}\left[(D_1 + D_2)\sinh\sqrt{M}(t_- + t_\omega) - D_1 \sinh\sqrt{M}L_2 - D_2 \sinh\sqrt{M}L_1\right]\,. \tag{5.105}$$

This allows us to write the length of the bulk geodesic between these two boundary points as

$$\begin{aligned} L_\gamma &\simeq \log\left[\frac{2r^{(1)}r^{(2)}}{R^2}\frac{\cos\left(a|\Delta\tau|\right)-\cos\left(a|\Delta\varphi|\right)}{a^2}\right] \simeq \log\left[\frac{2r^{(1)}r^{(2)}}{R^2}\frac{\sin\pi a}{a}\delta\right] \\ &\simeq \log\left[\left(\frac{\beta}{\pi z_\infty}\sinh\frac{\pi\Delta L}{\beta}\right)^2\frac{\beta}{\pi\epsilon}\frac{\sin\pi a}{a}\frac{\sinh\frac{\pi(t_\omega+t_--L_1)}{\beta}\sinh\frac{\pi(L_2-t_\omega-t_-)}{\beta}}{\sinh\frac{\pi\Delta L}{\beta}}\right], \end{aligned} \tag{5.106}$$

where $\Delta L = L_2 - L_1$. This also perfectly matches our CFT result (5.17) after employing the Ryu-Takayanagi formula.

Case 3: late time. This case is very similar to case 1. The boundary points

$$\tau^{(i)} \simeq \pi - \sqrt{M}\epsilon\frac{\sinh\left(\sqrt{M}(t_- + t_\omega)\right)}{D_i}, \qquad \varphi^{(i)} \simeq \sqrt{M}\epsilon\frac{\sinh\left(\sqrt{M}L_i\right)}{D_i} \tag{5.107}$$

are different from those in case 1 (5.97), but give rise to the same intervals (5.98). Hence, entanglement entropy is still thermal.

5.5.5 Geodesics on the right boundary

The two endpoints of the entanglement region B in the right boundary are (t_+, z_∞, L_1) and (t_+, z_∞, L_2). On the right boundary we will follow the same strategy as before but some signs in the map between Schwarzschild and Kruskal coordinates are different.

The radial coordinates satisfy

$$r^{(1)}r^{(2)} \simeq \left(\frac{R}{M\epsilon z_\infty}\right)^2 D_1 D_2, \tag{5.108}$$

where

$$D_i = |\cosh\sqrt{M}L_i + \cosh\sqrt{M}(t_+ + t_\omega)| \quad i = 1, 2, \tag{5.109}$$

whereas the other coordinates are

$$\tan\tau^{(i)} \simeq -\sqrt{M}\epsilon\frac{\sinh\left(\sqrt{M}(t_+ + t_\omega)\right)}{D_i}, \quad \tan\varphi^{(i)} \simeq -\sqrt{M}\epsilon\frac{\sinh\left(\sqrt{M}L_i\right)}{D_i}. \tag{5.110}$$

In this case, no matter what the value of t_+ is, the boundary points are identified as

$$\tau^{(i)} \simeq \pi - \sqrt{M}\epsilon\frac{\sinh\left(\sqrt{M}(t_+ + t_\omega)\right)}{D_i}, \quad \varphi^{(i)} \simeq \pi - \sqrt{M}\epsilon\frac{\sinh\left(\sqrt{M}L_i\right)}{D_i}. \tag{5.111}$$

These give rise to the intervals

$$\begin{aligned} |\Delta\tau| &\simeq \frac{\sqrt{M}\epsilon}{D_1 D_2}|D_1 - D_2|\sinh\sqrt{M}(t_+ + t_\omega), \\ |\Delta\varphi| &\simeq \frac{\sqrt{M}\epsilon}{D_1 D_2}\left|D_1\sinh\sqrt{M}L_2 - D_2\sinh\sqrt{M}L_1\right|. \end{aligned} \tag{5.112}$$

Using the identity

$$D_1 D_2(|\Delta\varphi|^2 - |\Delta\tau|^2) = 4M\epsilon^2\sinh^2\frac{\pi\Delta L}{\beta}, \tag{5.113}$$

the geodesic length equals

$$\begin{aligned} L_\gamma &\simeq \log\left[\frac{2r^{(1)}r^{(2)}}{R^2}\frac{\cos\left(a|\Delta\tau|\right)-\cos\left(a|\Delta\varphi|\right)}{a^2}\right] \simeq \log\left[\frac{r^{(1)}r^{(2)}}{R^2}(|\Delta\varphi|^2-|\Delta\tau|^2)\right] \\ &\simeq 2\log\left(\frac{\beta}{\pi z_\infty}\sinh\frac{\pi\Delta L}{\beta}\right). \end{aligned} \tag{5.114}$$

This agrees with our CFT expression for S_B in (5.19) and also agrees with what we obtained in chapter 3 by directly extremising geodesics.

$$S_B \simeq \frac{c}{3}\log\left(\frac{\beta}{\pi z_\infty}\sinh\frac{\pi\Delta L}{\beta}\right) = S_{\text{thermal}}. \tag{5.115}$$

5.5.6 Geodesics across the horizon

The calculation of geodesics across the horizon is again similar as before but there is an important subtlety. Given entanglement region $A\cup B$, the sum of lengths of geodesics connecting the end points of A and the end points of B might be less than the length of geodesics across the horizon connecting the end point of A to the end point of B (see Figure 5.4). This exactly mirrors situation in the CFT when we considered S and T channels. In both cases this ensures non-negativity of mutual information. In fact channel switching happens when $S_{A\cup B} = S_A+S_B$, so this happens precisely at the scrambling time.

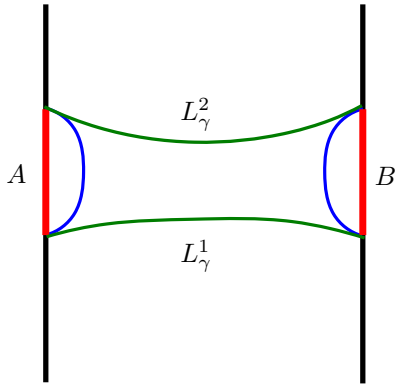

Figure 5.4: Spatial cross-section of BTZ. There is a competition between green geodesics across the horizon and blue geodesics connecting end points on the same boundary.

The endpoints of the entanglement region are $(t_\mp, z_\infty, L_i)$ and $(t_\mp, z_\infty, L_i)$. On the right boundary we will follow the same strategy as before but some signs in the map between Schwarzschild and Kruskal coordinates are different.

The radial coordinates satisfy

$$r^{(1)}r^{(2)} \simeq \left(\frac{R}{M\epsilon z_\infty}\right)^2 D_1 D_2, \tag{5.116}$$

where

$$D_1 = |\cosh\sqrt{M}L_i - \cosh\sqrt{M}(t_- + t_\omega)|, \tag{5.117}$$

$$D_2 = |\cosh\sqrt{M}L_i + \cosh\sqrt{M}(t_+ + t_\omega)|. \tag{5.118}$$

The other coordinates are

$$\tan\tau^{(1)} \simeq \sqrt{M}\epsilon\frac{\sinh\sqrt{M}(t_-+t_\omega)}{\cosh\sqrt{M}L_i-\cosh\sqrt{M}(t_-+t_\omega)} \tag{5.119}$$

$$\tan\varphi^{(1)} \simeq \sqrt{M}\epsilon\frac{\sinh\sqrt{M}L_i}{\cosh\sqrt{M}(t_-+t_\omega)-\cosh\sqrt{M}L_i}\,. \tag{5.120}$$

At early times, $L_i > t_- + t_\omega$, these are given by

$$\tau^{(1)} \simeq \sqrt{M}\epsilon\frac{\sinh\sqrt{M}(t_-+t_\omega)}{\cosh\sqrt{M}L_i-\cosh\sqrt{M}(t_-+t_\omega)}, \tag{5.121}$$

$$\varphi^{(1)} \simeq \pi-\sqrt{M}\epsilon\frac{\sinh\sqrt{M}L_i}{\cosh\sqrt{M}L_i-\cosh\sqrt{M}(t_-+t_\omega)}. \tag{5.122}$$

whereas at late times,

$$\tau^{(1)} \simeq \pi-\sqrt{M}\epsilon\frac{\sinh\sqrt{M}(t_-+t_\omega)}{\cosh\sqrt{M}(t_-+t_\omega)-\cosh\sqrt{M}L_1}, \tag{5.123}$$

$$\varphi^{(1)} \simeq \sqrt{M}\epsilon\frac{\sinh\sqrt{M}L_1}{\cosh\sqrt{M}(t_-+t_\omega)-\cosh\sqrt{M}L_1}. \tag{5.124}$$

The remaining coordinates for the right boundary point are

$$\tan\tau^{(2)} \simeq -\sqrt{M}\epsilon\frac{\sinh\sqrt{M}(t_++t_\omega)}{\cosh\sqrt{M}L_i+\cosh\sqrt{M}(t_++t_\omega)}, \tag{5.125}$$

$$\tan\varphi^{(2)} \simeq -\sqrt{M}\epsilon\frac{\sinh\sqrt{M}L_i}{\cosh\sqrt{M}(t_++t_\omega)+\cosh\sqrt{M}L_i}. \tag{5.126}$$

In this case, they are always given by

$$\tau^{(2)} \simeq -\sqrt{M}\epsilon\frac{\sinh\sqrt{M}(t_++t_\omega)}{D_2}, \tag{5.127}$$

$$\varphi^{(2)} \simeq \pi-\sqrt{M}\epsilon\frac{\sinh\sqrt{M}L_i}{D_2}. \tag{5.128}$$

Case 1. At early times $L_i > t_- + t_\omega$ the interval differences are

$$\begin{aligned}|\Delta\tau| &= |\tau^{(1)}-\tau^{(2)}| \simeq \frac{\sqrt{M}\epsilon}{D_1D_2}\left|D_2\sinh\sqrt{M}(t_-+t_\omega)+D_1\sinh\sqrt{M}\,(t_++t_\omega)\right|,\\ |\Delta\varphi| &= |\varphi^{(1)}-\varphi^{(2)}| \simeq \frac{\sqrt{M}\epsilon}{D_1D_2}\left|D_2\sinh\sqrt{M}L_i-D_1\sinh\sqrt{M}L_i\right|.\end{aligned} \tag{5.129}$$

Plugging this into the geodesic length (5.68), we obtain

$$\begin{aligned}L_\gamma &\simeq \log\left[\frac{2r^{(1)}r^{(2)}}{R^2}\frac{\cos\left(a|\Delta\tau|\right)-\cos\left(a|\Delta\varphi|\right)}{a^2}\right] \simeq \log\left[\frac{r^{(1)}r^{(2)}}{R^2}(|\Delta\varphi|^2-|\Delta\tau|^2)\right]\\ &\simeq 2\log\left[\frac{\beta}{\pi z_\infty}\cosh\frac{\pi\Delta t}{\beta}\right].\end{aligned} \tag{5.130}$$

Case 3. In the late time regime, the interval differences equal

$$|\Delta\tau| \simeq \pi - \frac{\sqrt{M}\epsilon}{D_1 D_2}\left(D_2 \sinh\sqrt{M}(t_- + t_\omega) - D_1 \sinh\sqrt{M}(t_+ + t_\omega)\right) \tag{5.131}$$

$$|\Delta\varphi| \simeq \pi - \frac{\sqrt{M}\epsilon}{D_1 D_2}\left(D_1 \sinh\sqrt{M}L_i + D_2 \sinh\sqrt{M}L_i\right). \tag{5.132}$$

Since they are very close, we have

$$|\Delta\tau| \simeq |\Delta\tau| - \delta, \tag{5.133}$$

where

$$\delta \simeq \frac{\sqrt{M}\epsilon}{D_1 D_2}\left[D_2(\sinh\sqrt{M}(t_- + t_\omega) - \sinh\sqrt{M}L_i) - D_1(\sinh\sqrt{M}(t_+ + t_\omega) + \sinh\sqrt{M}L_i)\right] \tag{5.134}$$

Hence, the length of geodesics is

$$\begin{aligned} L_\gamma &\simeq \log\left[\frac{2r^{(1)}r^{(2)}}{R^2}\frac{\cos(a|\Delta\tau|) - \cos(a|\Delta\varphi|)}{a^2}\right] \simeq \log\left[\frac{2r^{(1)}r^{(2)}}{R^2}\frac{\sin\pi a}{a}\delta\right] \\ &\simeq \log\left[\frac{\beta^2\frac{1}{2}\left(1+\cosh\frac{2\pi\Delta t}{\beta}\right)}{\pi^2 z_\infty^2}\frac{2}{\sqrt{M}\epsilon}\frac{\sin\pi a}{a}\frac{\sinh\frac{\pi(t_-+t_\omega-L_i)}{\beta}\cosh\frac{\pi(L_i-t_+-t_\omega)}{\beta}}{\cosh\frac{\pi\Delta t}{\beta}}\right], \end{aligned} \tag{5.135}$$

where $\Delta t = t_- - t_+$. So the individual lengths of two geodesics are

$$L_\gamma^1 \simeq \log\left[\left(\frac{\beta\cosh\frac{\pi\Delta t}{\beta}}{\pi z_\infty}\right)^2\frac{\beta}{\pi\epsilon}\frac{\sin\pi a}{a}\frac{\sinh\frac{\pi(t_-+t_\omega-L_1)}{\beta}\cosh\frac{\pi(L_1-t_+-t_\omega)}{\beta}}{\cosh\frac{\pi\Delta t}{\beta}}\right], \tag{5.136}$$

$$L_\gamma^2 \simeq \log\left[\left(\frac{\beta\cosh\frac{\pi\Delta t}{\beta}}{\pi z_\infty}\right)^2\frac{\beta}{\pi\epsilon}\frac{\sin\pi a}{a}\frac{\sinh\frac{\pi(t_-+t_\omega-L_2)}{\beta}\cosh\frac{\pi(L_2-t_+-t_\omega)}{\beta}}{\cosh\frac{\pi\Delta t}{\beta}}\right]. \tag{5.137}$$

Finally, the entanglement entropy is given by Ryu-Takayanagi formula

$$S_{A\cup B} \simeq \min\begin{cases}\frac{c}{6}\left(L_\gamma^1 + L_\gamma^2\right), \\ S_A + S_B.\end{cases} \tag{5.138}$$

which matches with the CFT result (5.35).

Case 2. Finally, consider the intermediate time regime when $L_1 < t_- + t_\omega < L_2$. Calculation for the first geodesic ($\theta = L_1$) is exactly the same as in case 3 but calculation for the second geodesic ($\theta = L_2$) proceeds as in case 1. Hence,

$$L_\gamma^1 \simeq \log\left[\left(\frac{\beta\cosh\frac{\pi\Delta t}{\beta}}{\pi z_\infty}\right)^2\frac{\beta}{\pi\epsilon}\frac{\sin\pi a}{a}\frac{\sinh\frac{\pi(t_-+t_\omega-L_1)}{\beta}\cosh\frac{\pi(L_1-t_+-t_\omega)}{\beta}}{\cosh\frac{\pi\Delta t}{\beta}}\right], \tag{5.139}$$

$$L_\gamma^2 \simeq 2\log\left[\frac{\beta}{\pi z_\infty}\cosh\frac{\pi\Delta t}{\beta}\right]. \tag{5.140}$$

Again the entanglement entropy of $A \cup B$ will be given by equation (5.138) which matches the CFT result (5.34).

All entanglement entropies match their CFT equivalents, so bulk mutual information and scrambling time will also match the CFT result.

Chapter 6

Scrambling time from local perturbations of the rotating BTZ black hole

In this chapter we would like to generalize our results from chapter 5 to the case of rotating BTZ black hole and CFT with different temperatures for holomorphic and antiholomorphic modes. A similar problem for shock wave geometries was considered in [90] but in this section we will follow free falling particle model with full back-reaction calculations.

Calculation on the CFT side generalizes fairly easily, so we will quickly go over the differences and in the rest of this chapter we will focus on the calculation in the bulk. Perturbation in the CFT does not carry any spin, so to match that we will consider a free falling particle with zero angular momentum. Note that a priori this is not the same as the particle with no initial velocity in angular coordinate since we are in non-static metric. However, we will show that this is a subleading effect. Nevertheless, the rotation of BTZ black hole would require us to consider an additional boost on top of what we had in section 5.5. This extra boost and the use of co-rotating coordinates defined below are the main technical differences in this chapter.

In chapter 5 calculation is described in the form it was first done in [2]. In this chapter we will try to describe calculation in a more optimal way, for example we will not be using Kruskal coordinates at all and neither we will be integrating equation of motion of a free falling particle.

6.1 CFT results

As in chapter 5 we perturb TFD state with a primary operator ψ in the CFT_L at time $-t_\omega$ in the past. Density matrix is given by the same expression as before

$$\operatorname{tr}\rho_A^n(t)=\frac{\langle\Psi(x_1,\bar{x}_1)\sigma_n(x_2,\bar{x}_2)\tilde{\sigma}_n(x_3,\bar{x}_3)\Psi^\dagger(x_4,\bar{x}_4)\rangle_{C_n}}{\left(\langle\psi(x_1,\bar{x}_1)\psi^\dagger(x_4,\bar{x}_4)\rangle_{C_1}\right)^n}. \tag{6.1}$$

However, calculation of correlators is slightly different. Instead of one exponential map (5.4) we will use

$$w(x)=e^{\frac{2\pi}{\beta_+}x}, \tag{6.2}$$

$$\bar{w}(\bar{x})=e^{\frac{2\pi}{\beta_-}\bar{x}}. \tag{6.3}$$

Then two point function is given by

$$\langle\psi(x_1,\bar{x}_1)\psi(x_4,\bar{x}_4)\rangle_{C_1}=\left|\frac{\beta_+\beta_-}{\pi^2}\sinh\left(\frac{\pi x_{14}}{\beta_+}\right)\sinh\left(\frac{\pi\bar{x}_{14}}{\beta_-}\right)\right|^{-2h_\psi}. \tag{6.4}$$

Similarly, we can compute 4-pt function and then trace of density operator

$$\operatorname{tr}\rho_A^n(t) = \left|\frac{\beta_+\beta_-}{\pi^2\epsilon_{\rm UV}^2}\sinh\left(\frac{\pi x_{23}}{\beta_+}\right)\sinh\left(\frac{\pi \bar{x}_{23}}{\beta_-}\right)\right|^{-2H_\sigma} |1-z|^{4H_\sigma}\, G(z,\bar{z}). \tag{6.5}$$

The Rényi entropies are computed by inserting (6.5) into (1.48)

$$S_A^{(n)} = \frac{c(n+1)}{12}\log\left[\frac{\beta_+\beta_-}{\pi^2\epsilon_{\rm UV}^2}\sinh\left(\frac{\pi L}{\beta_+}\right)\sinh\left(\frac{\pi L}{\beta_-}\right)\right] + \frac{1}{n-1}\log(|1-z|^{4H_\sigma}G(z,\bar{z})). \tag{6.6}$$

In $n\to 1$ limit the first term agrees with the entanglement entropy of rotating BTZ black hole (3.87).

The calculation of $G(z,\bar{z})$ proceeds as before but with different cross ratios z and $\bar{z}$. Cross ratio z now depends on temperature β_+ and $\bar{z}$ depends on β_-. In the small ϵ limit they are given by

$$z \simeq 1 + \frac{2\pi i\epsilon}{\beta_+}\frac{\sinh\frac{\pi L}{\beta_+}}{\sinh\frac{\pi(y+L-t_--t_\omega)}{\beta_+}\sinh\frac{\pi(y-t_--t_\omega)}{\beta_+}} + \mathcal{O}(\epsilon^2), \tag{6.7}$$

$$\bar{z} \simeq 1 - \frac{2\pi i\epsilon}{\beta_-}\frac{\sinh\frac{\pi L}{\beta_-}}{\sinh\frac{\pi(y+L+t_-+t_\omega)}{\beta_-}\sinh\frac{\pi(y+t_-+t_\omega)}{\beta_-}} + \mathcal{O}(\epsilon^2). \tag{6.8}$$

Recall, that in the entanglement entropy calculations we had to use the correct branch of the logarithm. For antiholomorphic coordinates in all cases (S_A, S_B and $S_{A\cup B}$) we had that antiholomorphic cross ratios are close to 1 and do not contribute to the entanglement entropy.

This agrees nicely with out picture of two localized lumps of energy moving in the opposite directions. The lump describing holomorphic mode moves from insertion point at $x=0$ to $x=L$ and passes region A. On the other hand, antiholomorphic mode moves in the opposite direction and never passes through A. So it is expected ΔS_A does not depend on β_-.

Therefore, entanglement entropy is given by

$$\Delta S_A = \begin{cases} 0\,, & t_- + t_\omega < y \text{ or } t_- + t_\omega > y + L, \\ \dfrac{c}{6}\log\left[\dfrac{\beta_+}{\pi\epsilon}\dfrac{\sin\pi\alpha_\psi}{\alpha_\psi}\dfrac{\sinh\left(\dfrac{\pi(y+L-t_--t_\omega)}{\beta_+}\right)\sinh\left(\dfrac{\pi(t_-+t_\omega-y)}{\beta_+}\right)}{\sinh\left(\dfrac{\pi L}{\beta_+}\right)}\right] & \text{otherwise}\,. \end{cases} \tag{6.9}$$

Similarly, $S_B = S_{\rm thermal}$.

$S_{A\cup B}$ again has a "thermal" piece that comes from mapping cylinder to the plane

$$S_{A\cup B} = \frac{c}{6}\log\left[\frac{\beta_+\beta_-}{\pi^2\epsilon_{\rm UV}^2}\cosh\left(\frac{\pi\Delta t}{\beta_+}\right)\cosh\left(\frac{\pi\Delta t}{\beta_-}\right)\right] \qquad \text{when } t_- + t_\omega < y. \tag{6.10}$$

At other times, local quench contributes to $S_{A\cup B}$ as in (5.34) and (5.35) but with $\beta \mapsto \beta_+$. Scrambling time is given by $I_{A:B}(t_\omega^\star) = 0$ at $t_- = t_+ = 0$. Then $\Delta t = 0$ and scrambling time is given by

$$t_\omega^\star = y + \frac{L}{2} - \frac{\beta_+}{2\pi}\log\left(\frac{\beta_+}{\pi\epsilon}\frac{\sin\pi\alpha_\psi}{\alpha_\psi}\right) + \frac{\beta_+}{2\pi}\log\left(4\sinh\frac{\pi L}{\beta_+}\sinh\frac{\pi L}{\beta_-}\right). \tag{6.11}$$

6.2 Free falling particle in the rotating BTZ

6.2.1 Initial conditions

We will model a perturbation in the CFT using a massive particle in the bulk. The perturbation in the boundary CFT did not carry any angular momentum, so we should make sure that the free falling particle has no angular momentum either. Conserved quantities in asymptotically AdS space were considered in [129]. The expression for the angular momentum conserved charge

is

$$L \equiv g_{\mu\nu}(\partial_\varphi)^\mu \dot{z}^\nu(\tau) = \frac{dT}{d\tau}\left[g_{t\varphi} + g_{\varphi\varphi}\frac{d\Phi}{dt}\right], \tag{6.12}$$

where trajectory of the particle is $z^\mu(\tau) = (T(\tau), R(\tau), \Phi(\tau))$ and τ is the proper time. So $L = 0$ corresponds to

$$\frac{d\Phi}{dt} = -\frac{g_{t\varphi}}{g_{\varphi\varphi}} = \frac{r_- r_+}{Rr^2}. \tag{6.13}$$

Similarly, the energy of the particle is

$$E \equiv -g_{\mu\nu}(\partial_t)^\mu \dot{z}^\nu(\tau) = -\frac{dT}{d\tau}\left[g_{tt} + g_{t\varphi}\frac{d\Phi}{dt}\right]. \tag{6.14}$$

Energy for zero angular momentum particle in the rotating BTZ background

$$E = -\frac{g_{tt}}{\sqrt{-\left[g_{tt} + g_{\varphi\varphi}\left(\frac{d\Phi}{dt}\right)^2 + g_{t\varphi}\frac{d\Phi}{dt}\right]}} = \sqrt{-g_{tt}}. \tag{6.15}$$

In the second equality above we used that second and third terms cancel in the denominator because of the equation (6.13).

$$E|_{r=R/\varepsilon} = \frac{mR}{\varepsilon}\sqrt{\left(1 - \frac{r_+^2\varepsilon^2}{R^2}\right)\left(1 - \frac{r_-^2\varepsilon^2}{R^2}\right)}. \tag{6.16}$$

Therefore, energy of the particle to leading order is the same as in non-rotating BTZ and still matches energy of local quench in the CFT if $r = \frac{R}{\varepsilon}$.

6.2.2 Boosts

BTZ metric (1.73) is usually given in terms of dimensionful time t. In order to compare bulk results to CFT we will switch to dimensionless time $t_- = \frac{t}{R}$. Motivated by calculation above and in particular equation (6.13) we choose initial condition for the particle to be

$$r(-t_\omega) = \frac{R}{\varepsilon}, \qquad \phi(-t_\omega) = 0, \tag{6.17}$$

$$\dot{r}(-t_\omega) = 0, \qquad \dot{\phi}(-t_\omega) = \frac{r_- r_+ \varepsilon^2}{R^2}, \qquad \dot{t}_- = 1. \tag{6.18}$$

In order to find how particle back-reacts on the geometry we first map a moving particle in the rotating BTZ to a static particle in AdS_3. In the non-rotating BTZ case we were able to write down the action for a free falling particle and solve the Euler-Lagrange equations explicitly in both Schwarzschild and Kruskal coordinates. The technical reason why it worked was that we could choose $\phi = 0$ at all times. On the other hand, the time evolution of ϕ is more complicated in the rotating BTZ due to frame dragging effect. Therefore, following the same strategy and explicitly finding the geodesic in Kruskal coordinates would not work. Instead we will try to work in the AdS_3 embedding coordinates.

The map between embedding coordinates and BTZ coordinates is

$$\begin{aligned} X_0 &= \pm\sqrt{B(r)}\sinh\tilde{t}, \\ X_1 &= \quad\sqrt{A(r)}\cosh\tilde{\phi}, \\ X_2 &= \quad\sqrt{A(r)}\sinh\tilde{\phi}, \\ X_3 &= \pm\sqrt{B(r)}\cosh\tilde{t}, \end{aligned} \tag{6.19}$$

where $+$ and $-$ signs are for left and right asymptotic regions respectively. Functions A and B

are

$$A(r) = R^2 \frac{r^2 - r_-^2}{r_+^2 - r_-^2},$$
$$B(r) = R^2 \frac{r^2 - r_+^2}{r_+^2 - r_-^2}, \tag{6.20}$$

and co-rotating coordinates are given by

$$\tilde{\phi} = \frac{r_+ \phi}{R} + \frac{r_-(t_\pm + t_\omega)}{R}, \tag{6.21}$$
$$\tilde{t} = \frac{r_+(t_\pm + t_\omega)}{R} + \frac{r_- \phi}{R}. \tag{6.22}$$

Note that we have already shifted time in the co-rotating coordinates by $-t_\omega$. Therefore, we will not have to pre-apply boost in $X_0 - X_3$ plane as we did in section 5.5.

Now we can write initial conditions in the embedding coordinates

$$\begin{aligned} X_0(0) &= 0, & \dot{X}_0(0) &= \sqrt{B(R\varepsilon^{-1})}\,\dot{\tilde{t}}, \\ X_1(0) &= \sqrt{A(R\varepsilon^{-1})}, & \dot{X}_1(0) &= 0, \\ X_2(0) &= 0, & \dot{X}_2(0) &= \sqrt{A(R\varepsilon^{-1})}\,\dot{\tilde{\phi}}, \\ X_3(0) &= \sqrt{B(R\varepsilon^{-1})}, & \dot{X}_3(0) &= 0. \end{aligned} \tag{6.23}$$

Compare it to initial conditions of particle in AdS_3 [1]

$$\begin{aligned} X_0(0) &= 0, & X_0'(0) &= R, \\ X_1(0) &= R, & X_1'(0) &= 0, \\ X_2(0) &= 0, & X_2'(0) &= 0, \\ X_3(0) &= 0, & X_3'(0) &= 0. \end{aligned} \tag{6.24}$$

We can read off the required boosts from equations (6.23)–(6.24). First, we need a boost in $X_1 - X_3$ plane with

$$\cosh\lambda_2 = \sqrt{A(R\varepsilon^{-1})} \simeq \frac{R}{\sqrt{r_+^2 - r_-^2}\,\varepsilon}, \qquad \sinh\lambda_2 = \sqrt{B(R\varepsilon^{-1})} \simeq \frac{R}{\sqrt{r_+^2 - r_-^2}\,\varepsilon}. \tag{6.25}$$

Hence,

$$\tanh\lambda_2 = \sqrt{\frac{R^2 - r_+^2\varepsilon^2}{R^2 - r_-^2\varepsilon^2}} = \sqrt{\frac{1 - \frac{r_+^2\varepsilon^2}{R^2}}{1 - \frac{r_-^2\varepsilon^2}{R^2}}} = \sqrt{1 - \frac{r_+^2 - r_-^2}{R^2}\varepsilon^2} + \mathcal{O}(\varepsilon^2) \approx \sqrt{1 - \kappa r_+ \varepsilon^2}, \tag{6.26}$$

where κ is the surface gravity

$$\kappa = \frac{r_+^2 - r_-^2}{R^2 r_+}. \tag{6.27}$$

We also need a boost in $X_0 - X_2$ plane to account for time derivatives in (6.23).

$$\tanh\lambda_3 = \coth\lambda_2 \frac{r_+\dot{\phi} + r_-\dot{t}_-}{r_+\dot{t}_- + r_-\dot{\phi}} = \frac{r_-}{r_+} + \mathcal{O}(\varepsilon). \tag{6.28}$$

It will also be useful to find

$$\cosh\lambda_3 = \frac{r_+}{\sqrt{r_+^2 - r_-^2}}. \tag{6.29}$$

Note that non-zero but small $\dot{\phi}$ did not affect boost λ_3 at this order. However, perturbation

[1] Note different time coordinate τ in global AdS_3 coordinates, hence different notation for the derivative.

in the CFT with a spin would contribute to λ_3 at leading order.

6.3 Back-reaction map for rotating BTZ

We will again apply equation (5.68) to find the lengths of geodesics. Therefore, we need to map the endpoints of entanglement interval to global AdS coordinates[2] (ρ, τ, φ). For our purposes it is enough to find the leading order terms even though the map that maps moving particle to the origin of AdS_3 can be written explicitly. We will compare Schwarzschild and global coordinates via $\mathbb{R}^{2,2}$ embedding coordinates.

$$\begin{aligned}\sqrt{R^2+\rho^2}\sin\tau &= X_0\cosh\lambda_3 - X_2\sinh\lambda_2,\\ \sqrt{R^2+\rho^2}\cos\tau &= X_1\cosh\lambda_2 - X_3\sinh\lambda_2,\\ \rho\sin\varphi &= X_2\cosh\lambda_3 - X_0\sinh\lambda_3,\\ \rho\cos\varphi &= X_3\cosh\lambda_2 - X_1\sinh\lambda_2.\end{aligned} \tag{6.30}$$

We can substitute embedding coordinates in (6.30) from (6.19). Note that functions from equation (6.20) satisfy $A(r) \simeq B(r)$ at the boundary, so $\cosh\lambda_2 \simeq \sinh\lambda_2$.

$$\tan\varphi = \frac{\sinh\tilde{\phi}\cosh\lambda_3 \mp \sinh\tilde{t}\sinh\lambda_3}{\pm\cosh\tilde{t}\cosh\lambda_2 - \cosh\tilde{\phi}\sinh\lambda_2} \simeq -\frac{\cosh\lambda_3}{\cosh\lambda_2}\frac{\sinh\tilde{\phi}\mp\tanh\lambda_3\sinh\tilde{t}}{\cosh\tilde{\phi}\mp\cosh\tilde{t}}. \tag{6.31}$$

Similarly,

$$\tan\tau \simeq \frac{\cosh\lambda_3}{\cosh\lambda_2}\cdot\frac{\pm\sinh\tilde{t}-\tanh\lambda_3\sinh\tilde{\phi}}{\cosh\tilde{\phi}\mp\cosh\tilde{t}}. \tag{6.32}$$

We can obtain the radial coordinate by squaring last to equations in (6.30)

$$\rho^2 \simeq A^2(r)\left(\left[\cosh\lambda_2(\cosh\tilde{\phi}-\cosh\tilde{t})\right]^2 + \left[\cosh\lambda_3(\sinh\tilde{\phi}-\tanh\lambda_3\sinh\tilde{t})\right]^2\right). \tag{6.33}$$

This sum is dominated[3] by the first term as $\cosh\lambda_2 \gg \cosh\lambda_3$. So

$$\rho \simeq A(r)\cosh\lambda_2\left|\cosh\tilde{\phi}-\cosh\tilde{t}\right|. \tag{6.34}$$

6.4 Geodesic lengths

6.4.1 Geodesic on the left boundary

We can compute the length of the geodesic from the endpoints of the entanglement region A in the back-reacted AdS_3 geometry.

$$S_A = \frac{c}{6}\log\left[\frac{2\rho_\infty^{(1)}\cdot\rho_\infty^{(2)}}{R^2}\frac{\cos\left(|\Delta\tau_\infty|a\right)-\cos\left(|\Delta\varphi_\infty|a\right)}{a^2}\right], \tag{6.35}$$

where $a \equiv \sqrt{1-\frac{\mu}{R^2}} = \alpha_\psi$ carries the information about the perturbation, as in chapter 5. In particular, we need to determine $\rho^{(1)}\rho^{(2)}$, $\Delta\tau$ and $\Delta\varphi$ using the map (6.34), (6.32) and (6.31) given endpoints $(t_-, r_\infty = Rz_\infty^{-1}, L_1)$ and (t_-, r_∞, L_2) in rotating BTZ coordinates. Let us also denote the length of the interval by $L = L_2 - L_1$.

The radial coordinates (6.34) satisfy

$$\rho^{(1)}\rho^{(2)} \simeq R^2\frac{\beta_-\beta_+}{4z_\infty^2}\cosh^2\lambda_2|D_1D_2|, \tag{6.36}$$

[2] We used r in chapter 5 but here we are already using r for BTZ coordinates, so we will change notation to ρ.

[3] This breaks down in the extremal limit. We will not consider this case here. In the extremal case stringy corrections become important [130].

where

$$D_i = \cosh\tilde{\phi}_i - \cosh\tilde{t}_i, \tag{6.37}$$

and co-rotating coordinates are as before

$$\tilde{\phi}_i = \frac{r_+ L_i + r_-(t_- + t_\omega)}{R}, \tag{6.38}$$

$$\tilde{t}_i = \frac{r_+(t_- + t_\omega) + r_- L_i}{R}. \tag{6.39}$$

Similarly, we can write expressions for τ and φ coordinates

$$\tan\tau^{(i)} \simeq \frac{\cosh\lambda_3}{\cosh\lambda_2}\frac{\sinh\tilde{t}_i - \tanh\lambda_3\sinh\tilde{\phi}_i}{D_i}, \tag{6.40}$$

$$\tan\varphi^{(i)} \simeq -\frac{\cosh\lambda_3}{\cosh\lambda_2}\frac{\sinh\tilde{\phi}_i - \tanh\lambda_3\sinh\tilde{t}_i}{D_i}. \tag{6.41}$$

Given $\tan\tau$ and $\tan\varphi$ we can find τ and φ. However, their values depend on whether $\tilde{\phi}_i > \tilde{t}_i$. We have three cases to consider: early time $0 < t+t_\omega < L_1$, intermediate time $L_1 < t+t_\omega < L_2$ and late time $L_2 < t + t_\omega$.

Early time

In this case boundary points are

$$\tau^{(i)} \simeq \frac{\cosh\lambda_3}{\cosh\lambda_2}\frac{\sinh\tilde{t}_i - \tanh\lambda_3\sinh\tilde{\phi}_i}{D_i}, \tag{6.42}$$

$$\varphi^{(i)} \simeq \pi - \frac{\cosh\lambda_3}{\cosh\lambda_2}\frac{\sinh\tilde{\phi}_i - \tanh\lambda_3\sinh\tilde{t}_i}{D_i}. \tag{6.43}$$

$$|\Delta\tau| \simeq \frac{\cosh\lambda_3}{\cosh\lambda_2}\frac{1}{D_1 D_2}\big|D_1(\sinh\tilde{t}_2 - \tanh\lambda_3\sinh\tilde{\phi}_2) - D_2(\sinh\tilde{t}_1 - \tanh\lambda_3\sinh\tilde{\phi}_1)\big|, \tag{6.44}$$

$$|\Delta\varphi| \simeq \frac{\cosh\lambda_3}{\cosh\lambda_2}\frac{1}{D_1 D_2}\big|D_1(\sinh\tilde{\phi}_2 - \tanh\lambda_3\sinh\tilde{t}_2) - D_2(\sinh\tilde{\phi}_1 - \tanh\lambda_3\sinh\tilde{t}_1)\big|. \tag{6.45}$$

We now use the following identity [131]

$$D_1 D_2(|\Delta\varphi|^2 - |\Delta\tau|^2) = 2\frac{\cosh^2\lambda_3}{\cosh^2\lambda_2}(1-\tanh^2\lambda_3)\left[\cosh(\tilde{\phi}_2 - \tilde{\phi}_1) - \cosh(\tilde{t}_2 - \tilde{t}_1)\right] \tag{6.46}$$

$$= 4\frac{\cosh^2\lambda_3}{\cosh^2\lambda_2}(1-\tanh^2\lambda_3)\sinh\frac{\tilde{\phi}_2 - \tilde{\phi}_1 + \tilde{t}_2 - \tilde{t}_1}{2}\sinh\frac{\tilde{\phi}_2 - \tilde{\phi}_1 - \tilde{t}_2 + \tilde{t}_1}{2}, \tag{6.47}$$

or alternatively

$$D_1 D_2(|\Delta\varphi|^2 - |\Delta\tau|^2) = \frac{4}{\cosh^2\lambda_2}\sinh\frac{\pi L}{\beta_-}\sinh\frac{\pi L}{\beta_+}. \tag{6.48}$$

The length of the geodesic connecting boundary points is

$$L_\gamma \simeq \log\left[\frac{2\rho^{(1)}\rho^{(2)}}{R^2}\frac{\cos(a|\Delta\tau|) - \cos(a|\Delta\varphi|)}{a^2}\right] \simeq \log\left[\frac{\rho^{(1)}\rho^{(2)}}{R^2}(|\Delta\varphi|^2 - |\Delta\tau|^2)\right] \tag{6.49}$$

$$\simeq \log\left[\frac{\beta_-\beta_+}{\pi^2 z_\infty^2}\sinh\frac{\pi L}{\beta_-}\sinh\frac{\pi L}{\beta_+}\right]. \tag{6.50}$$

This reproduces thermal entanglement entropy answer

$$S_A = \frac{c}{6}\log\left[\frac{\beta_-\beta_+}{\pi^2 z_\infty^2}\sinh\frac{\pi L}{\beta_-}\sinh\frac{\pi L}{\beta_+}\right]. \tag{6.51}$$

Late time

Just as in non-rotating BTZ, the points in this case are different but differences between the points are the same as in early time case

$$\tau^{(i)} \simeq \pi - \frac{\cosh\lambda_3}{\cosh\lambda_2}\frac{\sinh\tilde{t}_i - \tanh\lambda_3\sinh\tilde{\phi}_i}{|D_i|}, \tag{6.52}$$

$$\varphi^{(i)} \simeq \frac{\cosh\lambda_3}{\cosh\lambda_2}\frac{\sinh\tilde{\phi}_i - \tanh\lambda_3\sinh\tilde{t}_i}{|D_i|}. \tag{6.53}$$

Hence, entanglement entropy is thermal

$$S_A = S_{\text{thermal}} = \frac{c}{6}\log\left[\frac{\beta_-\beta_+}{\pi^2 z_\infty^2}\sinh\frac{\pi L}{\beta_-}\sinh\frac{\pi L}{\beta_+}\right]. \tag{6.54}$$

Intermediate time

In this case, the boundary points are

$$\tau^{(1)} \simeq \pi - \frac{\cosh\lambda_3}{\cosh\lambda_2}\frac{\sinh\tilde{t}_1 - \tanh\lambda_3\sinh\tilde{\phi}_1}{|D_1|}, \tag{6.55}$$

$$\tau^{(2)} \simeq \frac{\cosh\lambda_3}{\cosh\lambda_2}\frac{\sinh\tilde{t}_2 - \tanh\lambda_3\sinh\tilde{\phi}_2}{D_2}, \tag{6.56}$$

$$\varphi^{(1)} \simeq \frac{\cosh\lambda_3}{\cosh\lambda_2}\frac{\sinh\tilde{\phi}_1 - \tanh\lambda_3\sinh\tilde{t}_1}{|D_1|}, \tag{6.57}$$

$$\varphi^{(2)} \simeq \pi - \frac{\cosh\lambda_3}{\cosh\lambda_2}\frac{\sinh\tilde{\phi}_2 - \tanh\lambda_3\sinh\tilde{t}_2}{D_2}. \tag{6.58}$$

So,

$$|\Delta\tau| \simeq \pi - \frac{1}{|D_1|D_2}\big[|D_1|(\sinh\tilde{t}_2 - \tanh\lambda_3\sinh\tilde{\phi}_2) + D_2(\sinh\tilde{t}_1 - \tanh\lambda_3\sinh\tilde{\phi}_1)\big], \tag{6.59}$$

$$|\Delta\varphi| \simeq \pi - \frac{1}{|D_1|D_2}\big[|D_1|(\sinh\tilde{\phi}_2 - \tanh\lambda_3\sinh\tilde{t}_2) + D_2(\sinh\tilde{\phi}_1 - \tanh\lambda_3\sinh\tilde{t}_1)\big]. \tag{6.60}$$

We can use [131] to simplify hyperbolic functions to

$$\begin{aligned}
&|D_1|D_2(|\Delta\varphi| - |\Delta\tau|)\\
&= \frac{\cosh\lambda_3}{\cosh\lambda_2}(1+\tanh\lambda_3)\left[-\sinh(\tilde{t}_2-\tilde{t}_1) + \sinh(\tilde{\phi}_2-\tilde{t}_1) - \sinh(\tilde{\phi}_2-\tilde{\phi}_1) + \sinh(\tilde{t}_2-\tilde{\phi}_1)\right]\\
&= 4\frac{\cosh\lambda_3}{\cosh\lambda_2}(1+\tanh\lambda_3)\sinh\frac{\tilde{t}_1-\tilde{\phi}_1}{2}\sinh\frac{\tilde{t}_2-\tilde{\phi}_2}{2}\sinh\frac{\tilde{t}_1+\tilde{\phi}_1-\tilde{t}_2-\tilde{\phi}_2}{2}.
\end{aligned} \tag{6.61}$$

Let us substitute the values of co-rotating coordinates

$$\begin{aligned}
&|D_1|D_2(|\Delta\varphi| - |\Delta\tau|)\\
&= 4\frac{\cosh\lambda_3}{\cosh\lambda_2}(1+\tanh\lambda_3)\sinh\frac{\pi(t_\omega+t_- - L_1)}{\beta_+}\sinh\frac{\pi(t_\omega+t_- - L_2)}{\beta_+}\sinh\frac{\pi(L_1-L_2)}{\beta_-}\\
&= 4\frac{\cosh\lambda_3}{\cosh\lambda_2}(1+\tanh\lambda_3)\sinh\frac{\pi(t_\omega+t_- - L_1)}{\beta_+}\sinh\frac{\pi(L_2-t_\omega-t_-)}{\beta_+}\sinh\frac{\pi L}{\beta_-}.
\end{aligned} \tag{6.62}$$

We can rewrite this as

$$\begin{aligned}\delta :&= |\Delta\varphi| - |\Delta\tau| \\ &= \frac{4}{|D_1|D_2}\frac{\cosh\lambda_3}{\cosh\lambda_2}(1+\tanh\lambda_3)\sinh\frac{\pi L}{\beta_-}\sinh\frac{\pi L}{\beta_+}\cdot\frac{\sinh\frac{\pi(t_\omega+t_--L_1)}{\beta_+}\sinh\frac{\pi(L_2-t_\omega-t_-)}{\beta_+}}{\sinh\frac{\pi L}{\beta_+}}.\end{aligned} \tag{6.63}$$

Now we can calculate the length of the geodesic connecting the two points

$$L_\gamma \simeq \log\left[\frac{2\rho^{(1)}\rho^{(2)}}{R^2}\frac{\cos(a|\Delta\tau|)-\cos(a|\Delta\varphi|)}{a^2}\right] \tag{6.64}$$

$$\simeq \log\left[\frac{2\rho^{(1)}\rho^{(2)}}{R^2}\frac{\sin\pi a}{a}\delta\right] \tag{6.65}$$

$$\begin{aligned}&\simeq \log\left[\frac{\beta_-\beta_+}{\pi^2 z_\infty^2}\sinh\frac{\pi L}{\beta_-}\sinh\frac{\pi L}{\beta_+}\right] \\ &+\log\left[2\cosh\lambda_2\cosh\lambda_3(1+\tanh\lambda_3)\frac{\sin\pi a}{a}\frac{\sinh\frac{\pi(t_\omega+t_--L_1)}{\beta_+}\sinh\frac{\pi(L_2-t_\omega-t_-)}{\beta_+}}{\sinh\frac{\pi L}{\beta_+}}\right].\end{aligned} \tag{6.66}$$

Note that

$$2\cosh\lambda_2\cosh\lambda_3(1+\tanh\lambda_3) = 2\frac{R}{\epsilon\sqrt{r_+^2-r_-^2}}\frac{r_+}{\sqrt{r_+^2-r_-^2}}\frac{r_++r_-}{r_+} = \frac{\beta_+}{\pi\epsilon}. \tag{6.67}$$

Thus entanglement entropy is

$$S_A = S_{\text{thermal}} + \frac{c}{6}\log\left[\frac{\beta_+}{\pi\epsilon}\frac{\sin\pi a}{a}\frac{\sinh\frac{\pi(t_\omega+t_--L_1)}{\beta_+}\sinh\frac{\pi(L_2-t_\omega-t_-)}{\beta_+}}{\sinh\frac{\pi L}{\beta_+}}\right]. \tag{6.68}$$

So holographic entanglement entropy precisely matches the CFT result (6.9).

6.4.2 Geodesic on the right boundary

The two endpoints of the entanglement region B in the right boundary are (t_+, r_∞, L_1) and (t_+, r_∞, L_2). Their radial coordinates satisfy

$$\rho^{(1)}\rho^{(2)} \simeq R^2\frac{\beta_-\beta_+}{4z_\infty^2}\cosh^2\lambda_2|D_1D_2|, \tag{6.69}$$

where

$$D_i = \cosh\tilde{\phi}_i + \cosh\tilde{t}_i \equiv \cosh\left(\frac{r_+L_i}{R}+\frac{r_-(t_++t_\omega)}{R}\right)+\cosh\left(\frac{r_+(t_++t_\omega)}{R}+\frac{r_-L_i}{R}\right). \tag{6.70}$$

The other coordinates satisfy

$$\tan\tau^{(i)} \simeq -\frac{\cosh\lambda_3}{\cosh\lambda_2}\frac{\sinh\tilde{t}_i+\tanh\lambda_3\sinh\tilde{\phi}_i}{D_i}, \tag{6.71}$$

$$\tan\varphi^{(i)} \simeq -\frac{\cosh\lambda_3}{\cosh\lambda_2}\frac{\sinh\tilde{\phi}_i+\tanh\lambda_3\sinh\tilde{t}_i}{D_i}. \tag{6.72}$$

On the right boundary $D_i > 0$, so we always have

$$\tau^{(i)} \simeq \pi - \frac{\cosh\lambda_3}{\cosh\lambda_2}\frac{\sinh\tilde{t}_i + \tanh\lambda_3 \sinh\tilde{\phi}_i}{D_i}, \tag{6.73}$$

$$\varphi^{(i)} \simeq \pi - \frac{\cosh\lambda_3}{\cosh\lambda_2}\frac{\sinh\tilde{\phi}_i + \tanh\lambda_3 \sinh\tilde{t}_i}{D_i}. \tag{6.74}$$

Calculation proceeds as in early time on the left boundary with $\lambda_3 \mapsto -\lambda_3$. But early time case did not depend on λ_3 anyway.

Geodesic length is

$$L_\gamma \simeq \log\left[\frac{2\rho^{(1)}\rho^{(2)}}{R^2}\frac{\cos(a|\Delta\tau|) - \cos(a|\Delta\varphi|)}{a^2}\right] \simeq \log\left[\frac{\rho^{(1)}\rho^{(2)}}{R^2}(|\Delta\varphi|^2 - |\Delta\tau|^2)\right] \tag{6.75}$$

$$\simeq \log\left[\frac{\beta_-\beta_+}{\pi^2 z_\infty^2}\sinh\frac{\pi L}{\beta_-}\sinh\frac{\pi L}{\beta_+}\right]. \tag{6.76}$$

This again reproduces thermal entanglement entropy answer

$$S_B = \frac{c}{6}\log\left[\frac{\beta_-\beta_+}{\pi^2 z_\infty^2}\sinh\frac{\pi L}{\beta_-}\sinh\frac{\pi L}{\beta_+}\right]. \tag{6.77}$$

6.4.3 Geodesics across the horizon

We will repeat the calculation with points on the different boundaries. In this case geodesic connects points $(t_\mp, r_\infty, L_i)$ (the first point is on the left boundary, the second is on the right). There are two such geodesics for $i = 1, 2$. Just as in section 5.5, geodesics across the horizon compete with geodesics on the same boundary.

The product of radial coordinates satisfies

$$\rho^{(1)}\rho^{(2)} \simeq R^2\frac{\beta_-\beta_+}{4z_\infty^2}\cosh^2\lambda_2|D_1 D_2|, \tag{6.78}$$

as before but now D_1 and D_2 have different expressions. We will add $\pm$ superscripts to keep track of which boundary co-rotating coordinates belong to

$$D_1 = \cosh\tilde{\phi}_i^- - \cosh\tilde{t}_i^-, \tag{6.79}$$

$$D_2 = \cosh\tilde{\phi}_i^+ + \cosh\tilde{t}_i^+. \tag{6.80}$$

Points on the boundary. At early times $L_i > t_- + t_\omega$ points on the left boundary satisfy

$$\tau^{(1)} \simeq \frac{\cosh\lambda_3}{\cosh\lambda_2}\frac{\sinh\tilde{t}_i^- - \tanh\lambda_3\sinh\tilde{\phi}_i^-}{D_1}, \tag{6.81}$$

$$\varphi^{(1)} \simeq \pi - \frac{\cosh\lambda_3}{\cosh\lambda_2}\frac{\sinh\tilde{\phi}_i^- - \tanh\lambda_3\sinh\tilde{t}_i^-}{D_1}. \tag{6.82}$$

whereas at late times

$$\tau^{(1)} \simeq \pi - \frac{\cosh\lambda_3}{\cosh\lambda_2}\frac{\sinh\tilde{t}_i^- - \tanh\lambda_3\sinh\tilde{\phi}_i^-}{D_1}, \tag{6.83}$$

$$\varphi^{(1)} \simeq \frac{\cosh\lambda_3}{\cosh\lambda_2}\frac{\sinh\tilde{\phi}_i^- - \tanh\lambda_3\sinh\tilde{t}_i^-}{D_1}. \tag{6.84}$$

Similarly, coordinates boundary points on the right are always

$$\tau^{(2)} \simeq \quad -\frac{\cosh\lambda_3}{\cosh\lambda_2}\frac{\sinh\tilde{t}_i^+ + \tanh\lambda_3\sinh\tilde{\phi}_i^+}{D_2}, \tag{6.85}$$

$$\varphi^{(2)} \simeq \pi - \frac{\cosh\lambda_3}{\cosh\lambda_2}\frac{\sinh\tilde{\phi}_i^+ + \tanh\lambda_3\sinh\tilde{t}_i^+}{D_2}. \tag{6.86}$$

Early time. At early times $t_- + t_\omega < L_i$ we have

$$\begin{aligned}
|\Delta\tau| = |\tau^{(1)} - \tau^{(2)}| &\simeq \frac{1}{D_1 D_2}\frac{\cosh\lambda_3}{\cosh\lambda_2}\left|D_2(\sinh\tilde{t}_i^- - \tanh\lambda_3\sinh\tilde{\phi}_i^-) + D_1(\sinh\tilde{t}_i^+ + \tanh\lambda_3\sinh\tilde{\phi}_i^+)\right|, \\
|\Delta\varphi| = |\varphi^{(1)} - \varphi^{(2)}| &\simeq \frac{1}{D_1 D_2}\frac{\cosh\lambda_3}{\cosh\lambda_2}\left|D_2(\sinh\tilde{\phi}_i^- - \tanh\lambda_3\sinh\tilde{t}_i^-) - D_1(\sinh\tilde{\phi}_i^+ + \tanh\lambda_3\sinh\tilde{t}_i^+)\right|.
\end{aligned} \tag{6.87}$$

We now use the following identity [131]

$$D_1 D_2(|\Delta\varphi|^2 - |\Delta\tau|^2) = 2\frac{\cosh^2\lambda_3}{\cosh^2\lambda_2}(1-\tanh^2\lambda_3)\left[\cosh(\tilde{\phi}_i^- - \tilde{\phi}_i^+) + \cosh(\tilde{t}_i^- - \tilde{t}_i^+)\right] \tag{6.88}$$

$$= \frac{4}{\cosh^2\lambda_2}\cosh\frac{\tilde{\phi}_i^- - \tilde{\phi}_i^+ + \tilde{t}_i^- - \tilde{t}_i^+}{2}\cosh\frac{\tilde{\phi}_i^- - \tilde{\phi}_i^+ - \tilde{t}_i^- + \tilde{t}_i^+}{2}. \tag{6.89}$$

Let $\Delta t = t_- - t_+$, then

$$D_1 D_2(|\Delta\varphi|^2 - |\Delta\tau|^2) = \frac{4}{\cosh^2\lambda_2}\sinh\frac{\pi\Delta t}{\beta_-}\sinh\frac{\pi\Delta t}{\beta_+}. \tag{6.90}$$

Plugging this into the geodesic length equation (5.68), we obtain that at early times

$$S_{A\cup B} = \frac{c}{6}\log\left[\frac{\beta_-\beta_+}{\pi^2 z_\infty^2}\cosh\frac{\pi\Delta t}{\beta_-}\cosh\frac{\pi\Delta t}{\beta_+}\right]. \tag{6.91}$$

Late time. In the late time regime $t_- + t_\omega > L_i$ we have

$$\begin{aligned}
|\Delta\tau| = |\tau^{(1)} - \tau^{(2)}| &\simeq \pi - \frac{1}{|D_1|D_2}\frac{\cosh\lambda_3}{\cosh\lambda_2}\left|D_2(\sinh\tilde{t}_i^- - \tanh\lambda_3\sinh\tilde{\phi}_i^-) - |D_1|(\sinh\tilde{t}_i^+ + \tanh\lambda_3\sinh\tilde{\phi}_i^+)\right|, \\
|\Delta\varphi| = |\varphi^{(1)} - \varphi^{(2)}| &\simeq \pi - \frac{1}{|D_1|D_2}\frac{\cosh\lambda_3}{\cosh\lambda_2}\left|D_2(\sinh\tilde{\phi}_i^- - \tanh\lambda_3\sinh\tilde{t}_i^-) + |D_1|(\sinh\tilde{\phi}_i^+ + \tanh\lambda_3\sinh\tilde{t}_i^+)\right|.
\end{aligned} \tag{6.92}$$

As in the non-rotating case, $|\Delta\tau|$ and $|\Delta\varphi|$ are close to each other, so we define $\delta = |\Delta\varphi| - |\Delta\tau|$. Then

$$|D_1|D_2(|\Delta\varphi| - |\Delta\tau) = 2\frac{\cosh\lambda_3}{\cosh\lambda_2}(1+\tanh\lambda_3)\left[\sinh(\tilde{t}_i^- - \tilde{t}_i^+) + \sinh(\tilde{t}_i^- - \tilde{\phi}_i^+) - \sinh(\tilde{\phi}_i^- - \tilde{\phi}_i^+) - \sinh(\tilde{\phi}_i^- - \tilde{t}_i^+)\right] \tag{6.93}$$

$$= 4\frac{\cosh\lambda_3}{\cosh\lambda_2}(1+\tanh\lambda_3)\cosh\frac{\tilde{t}_i^- + \tilde{\phi}_i^- - \tilde{t}_i^+ - \tilde{\phi}_i^+}{2}\cosh\frac{\tilde{t}_i^+ - \tilde{\phi}_i^+}{2}\sinh\frac{\tilde{t}_i^- - \tilde{\phi}_i^-}{2}. \tag{6.94}$$

$$|D_1|D_2(|\Delta\varphi| - |\Delta\tau) = 4\frac{\cosh\lambda_3}{\cosh\lambda_2}(1+\tanh\lambda_3)\cosh\frac{\pi\Delta t}{\beta_-}\cosh\frac{\pi(t_+ + t_\omega - L_i)}{\beta_+}\sinh\frac{\pi(t_- + t_\omega - L_i)}{\beta_+}. \tag{6.95}$$

Therefore, the lengths of geodesics are

$$L_\gamma^1 \simeq \log\left[\frac{\beta_-\beta_+\cosh\frac{\pi\Delta t}{\beta_-}\cosh\frac{\pi\Delta t}{\beta_+}}{\pi^2 z_\infty^2}\frac{\beta_+}{\pi\epsilon}\frac{\sin\pi a}{a}\frac{\sinh\frac{\pi(t_-+t_\omega-L_1)}{\beta_+}\cosh\frac{\pi(t_++t_\omega-L_1)}{\beta_+}}{\cosh\frac{\pi\Delta t}{\beta_+}}\right], \tag{6.96}$$

$$L_\gamma^2 \simeq \log\left[\frac{\beta_-\beta_+\cosh\frac{\pi\Delta t}{\beta_-}\cosh\frac{\pi\Delta t}{\beta_+}}{\pi^2 z_\infty^2}\frac{\beta_+}{\pi\epsilon}\frac{\sin\pi a}{a}\frac{\sinh\frac{\pi(t_-+t_\omega-L_2)}{\beta_+}\cosh\frac{\pi(t_++t_\omega-L_2)}{\beta_+}}{\cosh\frac{\pi\Delta t}{\beta_+}}\right]. \tag{6.97}$$

The entanglement entropy is given by Ryu-Takayanagi formula

$$S_{A\cup B} \simeq \min\begin{cases}\frac{c}{6}\left(L_\gamma^1+L_\gamma^2\right),\\ S_A+S_B.\end{cases} \tag{6.98}$$

which matches with the CFT result.

Intermediate time. As in section 5.5 the intermediate time case is a combination of early and late times cases. The lengths of each geodesic are,

$$L_\gamma^1 \simeq \log\left[\frac{\beta_-\beta_+}{\pi^2 z_\infty^2}\cosh\frac{\pi\Delta t}{\beta_-}\cosh\frac{\pi\Delta t}{\beta_+}\frac{\beta_+}{\pi\epsilon}\frac{\sin\pi a}{a}\frac{\sinh\frac{\pi(t_-+t_\omega-L_1)}{\beta_+}\cosh\frac{\pi(t_++t_\omega-L_1)}{\beta_+}}{\cosh\frac{\pi\Delta t}{\beta_+}}\right], \tag{6.99}$$

$$L_\gamma^2 \simeq \log\left[\frac{\beta_-\beta_+}{\pi^2 z_\infty^2}\cosh\frac{\pi\Delta t}{\beta_-}\cosh\frac{\pi\Delta t}{\beta_+}\right]. \tag{6.100}$$

All holographic entanglement entropies in the rotating BTZ case exactly match their CFT equivalents, so bulk mutual information and scrambling time will also match the CFT result.

Chapter 7

Conclusions

In this thesis, we investigated the time evolution of local perturbations on thermal states in 2d CFTs and their holographic gravity duals. On the CFT side, the perturbations were due to the insertion of local primary operators. Universal results were obtained in the large c limit, either using uniformization maps or correlators involving twist operators. These correlators determine quantum information measures, such as the mutual information. Studying the time when this quantity vanishes allowed us to determine the scrambling time, i.e. the time where two local subsystems become uncorrelated. Our results, i.e. $t_\star \propto \beta \log S$, were consistent with the expectations originally drawn from black holes physics and holographic considerations [82]. We also investigated the same quantities in the holographic gravity theory. Describing the local perturbation by a massive free falling particle, we were able to compute its back-reaction on the BTZ black hole, describing the initial thermal state in the gravity theory. Since all these on-shell gravity backgrounds are locally AdS_3, we were able to compute the length of the spacelike geodesic satisfying the relevant RT boundary conditions. Our gravity results match the CFT results with and without the existence of rotation in BTZ.

In chapter 3 we have considered entanglement entropy in the rotating BTZ black hole. We have investigated spacelike geodesics with equal time endpoints as prescribed by HRT proposal. Equal time and length of entanglement interval boundary conditions were integrated. This allowed to express conserved charges in terms of the length of entanglement interval. We have applied HRT proposal and computed holographic entanglement entropy as the length of extremal spacelike geodesic. Perhaps surprisingly, dealing with boundary conditions in general case is a bit easier than in extremal or non-rotating case as we were able to exploit symmetry between r_- and r_+ in the equations. In the end, we have reproduced the result in the literature computed via other means.

In chapter 4 uniformization maps were used to map complicated manifolds arising in replica trick to complex plane. Then conformal block results from the literature were used to calculate the time evolution Rényi entropy and mutual information for free boson and general large c CFT. Calculation was done for two different time evolutions of TFD state, $H_L - H_R$ which is dual to eternal BTZ and $H_L + H_R$ that is dual to two disconnected Schwarzschild-AdS patches. We gave an interpretation of our state as two moving localized energy lumps that are entangled. The presence of quantum thermal fluctuations was reducing entanglement between localized energy lumps.

In chapter 5 we have used twist operators and Fitzpatrick et. al. heavy-light approximation [107] for four point functions to compute entanglement entropy for finite intervals. When calculating entanglement entropy of union of two intervals we considered expansion of 6 point function in terms of 4 point function in S and T channels. We calculated mutual information and scrambling time which agreed with the fast scrambling hypothesis of Susskind et. al. [82]. We investigated both numerically and analytically when our approximations break down.

Later we considered a free falling massive particle in an eternal BTZ black hole. We mapped the trajectory of the particle in BTZ coordinates to origin of AdS space in global coordinates. The map involved a boost as we were mapping moving particle to static particle. This allowed us to compute back-reaction of the particle on the metric of BTZ. It looks like a conical defect. We have used a formula for geodesic lengths in AdS in terms of endpoints of geodesics. We

interpreted contributions to entanglement entropy coming from the different geodesics as corresponding to S and T channel expansion in CFT. At each step of calculation, gravity quantities were equal to their field theory counterparts.

In chapter 6 we generalized calculations of chapter 5 to the case of rotating BTZ black hole. We discovered that only holomorphic part of perturbation contributes to the entanglement entropy and CFT calculation was similar to previous calculation but with inverse temperature β_+. Later we considered a free falling particle in the rotating BTZ black hole. We found more systematic way of identifying the boosts required to map particle to the origin of AdS. A new extra boost and co-rotating coordinates were the main differences from the non-rotating case. We calculated the back-reaction of the particle and used the same method as in chapter 5 to find entanglement entropies, mutual information and scrambling time.

One of the possible related projects is to consider perturbation with a spin. Fitzpatrick, et. al. formula can be used in that case, so similar method should work in that case too. On the gravity side we will have to consider a free falling particle with non-zero angular momentum. The method described in chapter 6 can be used to determine the required boost. This setup can be considered for for rotating BTZ as we have already included the boost in that plane. Another possibility is to investigate what can be said about perturbations by non-primary operators.

Entanglement entropy is important in reconstructing bulk spacetime from the boundary data. There are attempts to understand this process better by using tensor networks to model quantum states on the lattice. The entanglement entropy is then closely related to the number of links between nodes in tensor network. On the other hand, we already saw that spacelike geodesics anchored at the boundary do not probe all volume of the bulk in some asymptotically AdS spacetimes such as BTZ black hole, part of the spacetime is in the entanglement shadow [132, 133]. It would be interesting to understand what other quantum information concepts might help to reconstruct bulk geometry.

Entanglement entropy, just like thermal entropy satisfies 1st law of thermodynamics, we can relate differences in entanglement entropy to differences in energy of the states. It is interesting how Einstein equations could arise from the behaviour of entanglement entropy [51]. The first law and entanglement entropy can also be studied in more complicated geometries such as LLM [134]. However, many entanglement entropy problems in LLM space involve higher dimensional surfaces and require solving PDEs, so are hard to tackle analytically.

Bibliography

[1] P. Caputa, J. Simón, A. Štikonas, and T. Takayanagi, "Quantum Entanglement of Localized Excited States at Finite Temperature," *JHEP* **01** (2015) 102, arXiv:1410.2287 [hep-th].

[2] P. Caputa, J. Simón, A. Štikonas, T. Takayanagi, and K. Watanabe, "Scrambling time from local perturbations of the eternal BTZ black hole," *JHEP* **08** (2015) 011, arXiv:1503.08161 [hep-th].

[3] C. Montonen and D. I. Olive, "Magnetic Monopoles as Gauge Particles?," *Phys. Lett.* **72B** (1977) 117–120.

[4] L. Alvarez-Gaume and S. F. Hassan, "Introduction to S-Duality in N=2 Supersymmetric Gauge Theory. (A pedagogical review of the work of Seiberg and Witten)," *Fortsch.Phys.* **45** (Jan., 1997) 159–236, arXiv:hep-th/9701069v1 [hep-th].

[5] S. V. Ketov, "Solitons, monopoles and duality: from sine-Gordon to Seiberg-Witten,". http://cds.cern.ch/record/315614.

[6] R. C. Tolman, "Static solutions of Einstein's field equations for spheres of fluid," *Phys. Rev.* **55** (1939) 364–373.

[7] J. R. Oppenheimer and G. M. Volkoff, "On Massive neutron cores," *Phys. Rev.* **55** (1939) 374–381.

[8] K. Schwarzschild, "On the gravitational field of a mass point according to Einstein's theory," *Sitzungsber. Preuss. Akad. Wiss. Berlin (Math. Phys.)* **1916** (1916) 189–196, arXiv:physics/9905030 [physics].

[9] S. W. Hawking and G. F. R. Ellis, *The large-scale structure of space-time*. Cambridge University Press, 1973.

[10] J. F. Donoghue, M. M. Ivanov, and A. Shkerin, "EPFL Lectures on General Relativity as a Quantum Field Theory," Feb., 2017.

[11] M. B. Green, J. H. Schwarz, and E. Witten, *SUPERSTRING THEORY. VOL. 1: INTRODUCTION*. Cambridge Monographs on Mathematical Physics. Cambridge University Press, 1988.

[12] J. Polchinski, *String theory. Vol. 2: Superstring theory and beyond*. Cambridge University Press, 2007.

[13] M. Rigol, V. Dunjko, and M. Olshanii, "Thermalization and its mechanism for generic isolated quantum systems," *Nature* (June, 2008) 854–858, arXiv:0708.1324v2 [cond-mat.stat-mech].

[14] P. Reimann, "Canonical thermalization," *New J. Phys.* **12** (May, 2010) 055027, arXiv:1005.5625v1 [cond-mat.stat-mech].

[15] S. Goldstein, J. L. Lebowitz, R. Tumulka, and N. Zanghi, "Long-Time Behavior of Macroscopic Quantum Systems: Commentary Accompanying the English Translation of John von Neumann's 1929 Article on the Quantum Ergodic Theorem," *European Phys. J. H* **35** (Sept., 2010) 173–200, arXiv:1003.2129v2 [quant-ph].

[16] L. F. Santos and M. Rigol, "Localization and the effects of symmetries in the thermalization properties of one-dimensional quantum systems," *Phys. Rev. E* **82** (Feb., 2010) 031130, arXiv:1006.0729v3 [cond-mat.stat-mech].

[17] J. von Neumann, "Thermodynamik quantenmechanischer Gesamtheiten," *Nachrichten von der Gesellschaft der Wissenschaften zu Göttingen* **1** (1927) 273–291.

[18] C. E. Shannon, "A mathematical theory of communication," *Bell Syst. Tech. J.* **27** (1948) 379–423. [Bell Syst. Tech. J.27,623(1948)].

[19] N. Arkani-Hamed, S. Dubovsky, A. Nicolis, E. Trincherini, and G. Villadoro, "A Measure of de Sitter entropy and eternal inflation," *JHEP* **05** (2007) 055, arXiv:0704.1814 [hep-th].

[20] S. B. Giddings, D. Marolf, and J. B. Hartle, "Observables in effective gravity," *Phys. Rev.* **D74** (2006) 064018, arXiv:hep-th/0512200 [hep-th].

[21] R. Wald, *General Relativity*. University of Chicago Press, 1984.

[22] G. 't Hooft, "Dimensional reduction in quantum gravity," in *Salamfest 1993:0284-296*, pp. 0284–296. 1993. arXiv:gr-qc/9310026 [gr-qc].

[23] L. Susskind, "Strings, Black Holes and Lorentz Contraction," *Phys.Rev.D* **49** (Aug., 1994) 6606–6611, arXiv:hep-th/9308139v1 [hep-th].

[24] L. Susskind, "The World as a Hologram," *J.Math.Phys.* **36** (Sept., 1995) 6377–6396, arXiv:hep-th/9409089v2 [hep-th].

[25] N. Laflorencie, "Quantum entanglement in condensed matter systems," arXiv:1512.03388v3 [cond-mat.str-el].

[26] A. Einstein, "Die Grundlage der allgemeinen Relativitätstheorie," *Annalen der Physik* **354** no. 7, (1916) 769–862.

[27] J. Wheeler and K. Ford, *Geons, Black Holes, and Quantum Foam: A Life in Physics*. W. W. Norton, 2010.

[28] J. D. Bekenstein, "Black holes and the second law," *Lett. Nuovo Cim.* **4** (1972) 737–740.

[29] Ya. B. Zeldovich and A. A. Starobinsky, "Particle production and vacuum polarization in an anisotropic gravitational field," *Sov. Phys. JETP* **34** (1972) 1159–1166. [Zh. Eksp. Teor. Fiz.61,2161(1971)].

[30] S. W. Hawking, "Black hole explosions?," *Nature* **248** no. 5443, (Mar., 1974) 30–31. http://dx.doi.org/10.1038/248030a0.

[31] J. M. Bardeen, B. Carter, and S. W. Hawking, "The Four laws of black hole mechanics," *Commun. Math. Phys.* **31** (1973) 161–170.

[32] A. Strominger and C. Vafa, "Microscopic origin of the Bekenstein-Hawking entropy," *Phys. Lett.* **B379** (1996) 99–104, arXiv:hep-th/9601029 [hep-th].

[33] J. M. Maldacena, "The Large N limit of superconformal field theories and supergravity," *Int. J. Theor. Phys.* **38** (1999) 1113–1133, arXiv:hep-th/9711200 [hep-th]. [Adv. Theor. Math. Phys.2,231(1998)].

[34] O. Aharony, S. S. Gubser, J. Maldacena, H. Ooguri, and Y. Oz, "Large N Field Theories, String Theory and Gravity," arXiv:hep-th/9905111 [hep-th].

[35] B. Zwiebach, *A First Course in String Theory*. Cambridge University Press, 2009.

[36] K. Becker, M. Becker, and J. Schwarz, *String Theory and M-Theory: A Modern Introduction*. Cambridge University Press, 2006.

[37] J. Polchinski, "Dirichlet Branes and Ramond-Ramond charges," *Phys. Rev. Lett.* **75** (1995) 4724–4727, arXiv:hep-th/9510017 [hep-th].

[38] E. Witten, "Bound states of strings and p-branes," *Nucl. Phys.* **B460** (1996) 335–350, arXiv:hep-th/9510135 [hep-th].

[39] H. Nastase, "Introduction to AdS-CFT," arXiv:0712.0689 [hep-th].

[40] E. Witten, "Anti-de Sitter space and holography," *Adv. Theor. Math. Phys.* **2** (1998) 253–291, arXiv:hep-th/9802150 [hep-th].

[41] E. Witten, "Anti-de Sitter Space, Thermal Phase Transition, And Confinement in Gauge Theories," *Adv. Theor. Math. Phys.* **2** no. hep-th/9803131, (1998) 505–532. http://cds.cern.ch/record/349131.

[42] A. A. Belavin, A. M. Polyakov, and A. B. Zamolodchikov, "Infinite Conformal Symmetry in Two-Dimensional Quantum Field Theory," *Nucl. Phys.* **B241** (1984) 333–380.

[43] S. Deser and R. Jackiw, "Three-dimensional cosmological gravity: Dynamics of constant curvature," *Annals of Physics* **153** no. 2, (1984) 405–416.

[44] K. Skenderis, "Lecture Notes on Holographic Renormalization," *Class.Quant.Grav.* **19** (Oct., 2002) 5849–5876, arXiv:hep-th/0209067v2 [hep-th].

[45] A. Hamilton, D. N. Kabat, G. Lifschytz, and D. A. Lowe, "Holographic representation of local bulk operators," *Phys. Rev.* **D74** (2006) 066009, arXiv:hep-th/0606141 [hep-th].

[46] M. Van Raamsdonk, "Building up spacetime with quantum entanglement," *General Relativity and Gravitation* **42** no. 10, (2010) 2323–2329.

[47] M. Van Raamsdonk, "Lectures on Gravity and Entanglement," in *Proceedings, Theoretical Advanced Study Institute in Elementary Particle Physics: New Frontiers in Fields and Strings (TASI 2015): Boulder, CO, USA, June 1-26, 2015*, pp. 297–351. 2017. arXiv:1609.00026 [hep-th].

[48] T. Faulkner, F. M. Haehl, E. Hijano, O. Parrikar, C. Rabideau, and M. Van Raamsdonk, "Nonlinear Gravity from Entanglement in Conformal Field Theories," arXiv:1705.03026 [hep-th].

[49] N. Lashkari, M. B. McDermott, and M. V. Raamsdonk, "Gravitational Dynamics From Entanglement "Thermodynamics"," *JHEP* **1404** (Aug., 2014) 195, arXiv:1308.3716v2 [hep-th].

[50] M. Nozaki, T. Numasawa, A. Prudenziati, and T. Takayanagi, "Dynamics of Entanglement Entropy from Einstein Equation," May, 2013.

[51] T. Jacobson, "Entanglement Equilibrium and the Einstein Equation," *Phys. Rev. Lett.* **116** (June, 2016) 201101, arXiv:1505.04753v4 [gr-qc].

[52] T. Jacobson, "Thermodynamics of Spacetime: The Einstein Equation of State," *Phys.Rev.Lett.* **75** (June, 1995) 1260–1263, arXiv:gr-qc/9504004v2 [gr-qc].

[53] M. A. Nielsen and I. L. Chuang, *Quantum Computation and Quantum Information: 10th Anniversary Edition*. Cambridge University Press, 2010.

[54] D. K. Faddeev, "On the concept of entropy of a finite probabilistic scheme," *Uspehi Mat. Nauk (N.S.)* **11** no. 1(67), (1956) 227–231.

[55] T. Cover and J. Thomas, *Elements of Information Theory*. John Wiley and Sons, 2006.

[56] K. Zyczkowski, P. Horodecki, A. Sanpera, and M. Lewenstein, "On the volume of the set of mixed entangled states," *Phys.Rev. A* **58** (Apr., 1998) 883, arXiv:quant-ph/9804024v1 [quant-ph].

[57] P. Calabrese and J. L. Cardy, "Entanglement entropy and quantum field theory," *J. Stat. Mech.* **0406** (2004) P06002, arXiv:hep-th/0405152 [hep-th].

[58] S. Ryu and T. Takayanagi, "Aspects of Holographic Entanglement Entropy," *JHEP* **0608** (2006) 045, arXiv:hep-th/0605073 [hep-th].

[59] M. Rangamani and T. Takayanagi, "Holographic Entanglement Entropy," arXiv:1609.01287 [hep-th].

[60] M. Srednicki, *Quantum Field Theory*. Cambridge Univ. Press, Cambridge, 2007.

[61] F. Carlson, *Sur une classe de séries de Taylor*. PhD thesis, Uppsala, 1914.

[62] G. H. Hardy, "On two theorems of F. Carlson and S. Wigert," *Acta Mathematica* **42** no. 1, (1920) 327. http://dx.doi.org/10.1007/BF02404414.

[63] S. Ryu and T. Takayanagi, "Holographic derivation of entanglement entropy from AdS/CFT," *Phys.Rev.Lett.* **96** (2006) 181602, arXiv:hep-th/0603001 [hep-th].

[64] V. E. Hubeny, M. Rangamani, and T. Takayanagi, "A Covariant holographic entanglement entropy proposal," *JHEP* **0707** (2007) 062, arXiv:0705.0016 [hep-th].

[65] H. Casini, M. Huerta, and R. C. Myers, "Towards a derivation of holographic entanglement entropy," *JHEP* **1105** (Feb., 2011) 036, arXiv:1102.0440v2 [hep-th].

[66] A. Lewkowycz and J. Maldacena, "Generalized gravitational entropy," *JHEP* **08** (2013) 090, arXiv:1304.4926 [hep-th].

[67] F. M. Haehl, R. Loganayagam, and M. Rangamani, "Schwinger-Keldysh formalism. Part I: BRST symmetries and superspace," *Journal of High Energy Physics* **6** (June, 2017) 69, arXiv:1610.01940 [hep-th].

[68] X. Dong, A. Lewkowycz, and M. Rangamani, "Deriving covariant holographic entanglement," *JHEP* **11** (2016) 028, arXiv:1607.07506 [hep-th].

[69] E. H. Lieb and M. B. Ruskai, *Proof of the strong subadditivity of quantum-mechanical entropy*, pp. 63–66. Springer Berlin Heidelberg, Berlin, Heidelberg, 2002.

[70] M. Headrick and T. Takayanagi, "A Holographic proof of the strong subadditivity of entanglement entropy," *Phys. Rev.* **D76** (2007) 106013, arXiv:0704.3719 [hep-th].

[71] M. Bañados, C. Teitelboim, and J. Zanelli, "Black hole in three-dimensional spacetime," *Phys. Rev. Lett.* **69** (Sep, 1992) 1849–1851.

[72] M. Banados, M. Henneaux, C. Teitelboim, and J. Zanelli, "Geometry of the (2+1) black hole," *Phys. Rev.* **D48** (1993) 1506–1525, arXiv:gr-qc/9302012 [gr-qc]. [Erratum: Phys. Rev.D88,069902(2013)].

[73] C. W. Misner, K. S. Thorne, and J. A. Wheeler, *Gravitation*. W. H. Freeman, San Francisco, 1973.

[74] D. Birmingham, I. Sachs, and S. Sen, "Exact Results for the BTZ Black Hole," *Int.J.Mod.Phys. D* **10** (Mar., 2001) 833–858, arXiv:hep-th/0102155v2 [hep-th].

[75] D. C. Robinson, "Uniqueness of the Kerr black hole," *Phys. Rev. Lett.* **34** (1975) 905–906.

[76] D. Harlow, "Jerusalem Lectures on Black Holes and Quantum Information," *Rev. Mod. Phys.* **88** (2016) 15002, arXiv:1409.1231 [hep-th]. [Rev. Mod. Phys.88,15002(2016)].

[77] J. M. Maldacena, "Eternal black holes in anti-de Sitter," *JHEP* **0304** (2003) 021, arXiv:hep-th/0106112 [hep-th].

[78] T. Hartman, "Lectures on Quantum Gravity and Black Holes.".

[79] J. B. Hartle and S. W. Hawking, "Path-integral derivation of black-hole radiance," *Phys. Rev. D* **13** (Apr, 1976) 2188–2203.

[80] W. Israel, "Thermo field dynamics of black holes," *Phys. Lett.* **A57** (1976) 107–110.

[81] J. Maldacena and L. Susskind, "Cool horizons for entangled black holes," *Fortsch. Phys.* **61** (2013) 781–811, arXiv:1306.0533 [hep-th].

[82] Y. Sekino and L. Susskind, "Fast Scramblers," *JHEP* **0810** (Aug., 2008) 065, arXiv:0808.2096v1 [hep-th].

[83] V. Cardoso and J. P. S. Lemos, "Scalar, electromagnetic and Weyl perturbations of BTZ black holes: quasi normal modes," *Phys.Rev. D* **63** (Apr., 2001) 124015, arXiv:gr-qc/0101052v2 [gr-qc].

[84] S. H. Shenker and D. Stanford, "Black holes and the butterfly effect," *JHEP* **03** (2014) 067, arXiv:1306.0622 [hep-th].

[85] L. D'Alessio, Y. Kafri, A. Polkovnikov, and M. Rigol, "From Quantum Chaos and Eigenstate Thermalization to Statistical Mechanics and Thermodynamics," *Adv. Phys.* **65** (Aug., 2016) 239, arXiv:1509.06411v3 [cond-mat.stat-mech].

[86] S. Leichenauer, "Disrupting Entanglement of Black Holes," *Phys. Rev.* **D90** no. 4, (2014) 046009, arXiv:1405.7365 [hep-th].

[87] J. Maldacena, S. H. Shenker, and D. Stanford, "A bound on chaos," *Journal of High Energy Physics* **2016** no. 8, (2016) 1–17, arXiv:1503.01409 [hep-th].

[88] E. Perlmutter, "Bounding the space of holographic CFTs with chaos," *Journal of High Energy Physics* **2016** no. 10, (2016) 1–60, arXiv:1602.08272 [hep-th].

[89] S. H. Shenker and D. Stanford, "Multiple Shocks," *JHEP* **12** (2014) 046, arXiv:1312.3296 [hep-th].

[90] A. P. Reynolds and S. F. Ross, "Butterflies with rotation and charge," *Classical and Quantum Gravity* **33** no. 21, (Apr., 2016) 215008, 1604.04099v1 [hep-th].

[91] D. A. Roberts, D. Stanford, and L. Susskind, "Localized shocks," *JHEP* **03** (2015) 051, arXiv:1409.8180 [hep-th].

[92] P. Ginsparg, "Applied Conformal Field Theory," arXiv:hep-th/9108028v1 [hep-th].

[93] J. D. Qualls, "Lectures on Conformal Field Theory," arXiv:1511.04074v2 [hep-th].

[94] J. Polchinski, *String theory. Vol. 1: An introduction to the bosonic string*. Cambridge University Press, 2007.

[95] P. D. Francesco, P. Mathieu, and D. Senechal, *Conformal Field Theory*. Graduate Texts in Contemporary Physics. Springer, 1997.

[96] J. Conway, *Functions of One Complex Variable I*. Functions of one complex variable / John B. Conway. Springer, 1978.

[97] A. B. Zamolodchikov, "Infinite additional symmetries in two-dimensional conformal quantum field theory," *Teor. Mat. Fiz.* **65** no. 3, (1985) 347–359.

[98] K. G. Wilson and W. Zimmermann, "Operator product expansions and composite field operators in the general framework of quantum field theory," *Comm. Math. Phys.* **24** no. 2, (1972) 87–106.

[99] R. Blumenhagen, D. Lüst, and S. Theisen, *Introduction to Conformal Field Theory*. Springer, 2013.

[100] D. Tong, "Lectures on String Theory," arXiv:0908.0333v3 [hep-th].

[101] M. Nozaki, T. Numasawa, and T. Takayanagi, "Quantum Entanglement of Local Operators in Conformal Field Theories," *Phys. Rev. Lett.* **112** (2014) 111602, arXiv:1401.0539 [hep-th].

[102] S. He, T. Numasawa, T. Takayanagi, and K. Watanabe, "Quantum dimension as entanglement entropy in two dimensional conformal field theories," *Phys. Rev.* **D90** no. 4, (2014) 041701, arXiv:1403.0702 [hep-th].

[103] P. Calabrese and J. L. Cardy, "Evolution of entanglement entropy in one-dimensional systems," *J. Stat. Mech.* **0504** (2005) P04010, arXiv:cond-mat/0503393 [cond-mat].

[104] A. Einstein, B. Podolsky, and N. Rosen, "Can Quantum-Mechanical Description of Physical Reality Be Considered Complete?," *Phys. Rev.* **47** (May, 1935) 777–780.

[105] J. L. Cardy, O. A. Castro-Alvaredo, and B. Doyon, "Form factors of branch-point twist fields in quantum integrable models and entanglement entropy," *J. Statist. Phys.* **130** (2008) 129–168, arXiv:0706.3384 [hep-th].

[106] F. M. Haehl and M. Rangamani, "Permutation orbifolds and holography," *Journal of High Energy Physics* **2015** no. 3, (2015) 1–45.

[107] A. L. Fitzpatrick, J. Kaplan, and M. T. Walters, "Universality of Long-Distance AdS Physics from the CFT Bootstrap," *JHEP* **08** (2014) 145, arXiv:1403.6829 [hep-th].

[108] A. L. Fitzpatrick, J. Kaplan, and M. T. Walters, "Virasoro Conformal Blocks and Thermality from Classical Background Fields," *Journal of High Energy Physics* no. 11, (2015) 1–32, arXiv:1501.05315 [hep-th].

[109] A. B. Zamolodchikov, "Conformal symmetry in two-dimensional space: Recursion representation of conformal block," *Theoretical and Mathematical Physics* **73** (Oct., 1987) 1088–1093.

[110] C. T. Asplund, A. Bernamonti, F. Galli, and T. Hartman, "Holographic Entanglement Entropy from 2d CFT: Heavy States and Local Quenches," *JHEP* **02** (2015) 171, arXiv:1410.1392 [hep-th].

[111] T. Hartman and J. Maldacena, "Time Evolution of Entanglement Entropy from Black Hole Interiors," *JHEP* **1305** (2013) 014, arXiv:1303.1080 [hep-th].

[112] C. P. Herzog and D. T. Son, "Schwinger-Keldysh Propagators from AdS/CFT Correspondence," *JHEP* **0303** (Apr., 2003) 046, arXiv:hep-th/0212072v4 [hep-th].

[113] S. Carlip and C. Teitelboim, "Aspects of Black Hole Quantum Mechanics and Thermodynamics in 2+1 Dimensions," *Phys.Rev. D* **51** (May, 1995) 622–631, arXiv:gr-qc/9405070v1 [gr-qc].

[114] J. D. Brown and M. Henneaux, "Central charges in the canonical realization of asymptotic symmetries: An example from three dimensional gravity," *Communications in Mathematical Physics* **104** (June, 1986) 207–226.

[115] V. Balasubramanian, B. D. Chowdhury, B. Czech, and J. Boer, "Entwinement and the emergence of spacetime," *Journal of High Energy Physics* **2015** no. 1, (2015) 1–22.

[116] P. Calabrese and J. Cardy, "Quantum Quenches in Extended Systems," *J. Stat. Mech.* **0706** (2007) P06008, arXiv:0704.1880 [cond-mat.stat-mech].

[117] S. Sotiriadis and G. Martelloni, "Equilibration and GGE in interacting-to-free Quantum Quenches in dimensions $d > 1$," *Math. Theor.* **49** no. arXiv:1505.08150, (May, 2015) 095002. 21 p. Comments: 21 pages.

[118] C. T. Asplund, A. Bernamonti, F. Galli, and T. Hartman, "Entanglement Scrambling in 2d Conformal Field Theory," *JHEP* **09** (2015) 110, arXiv:1506.03772 [hep-th].

[119] J. S. Cotler, M. P. Hertzberg, M. Mezei, and M. T. Mueller, "Entanglement Growth after a Global Quench in Free Scalar Field Theory," *JHEP* **11** (Dec., 2016) 166, arXiv:1609.00872v2 [hep-th].

[120] P. Calabrese and J. Cardy, "Entanglement and correlation functions following a local quench: a conformal field theory approach," *J. Stat. Mech.* **0710** no. 10, (2007) P10004, arXiv:0708.3750 [quant-ph].

[121] M. Nozaki, T. Numasawa, and T. Takayanagi, "Holographic Local Quenches and Entanglement Density," *JHEP* **05** (2013) 080, arXiv:1302.5703 [hep-th].

[122] P. Caputa and A. Veliz-Osorio, "Entanglement constant for conformal families," *Phys. Rev. D* **92** (Sept., 2015) 065010, arXiv:1507.00582v2 [hep-th].

[123] T. Hartman, "Entanglement Entropy at Large Central Charge," arXiv:1303.6955 [hep-th].

[124] P. Caputa, M. Nozaki, and T. Takayanagi, "Entanglement of local operators in large-N conformal field theories," *PTEP* **2014** (2014) 093B06, arXiv:1405.5946 [hep-th].

[125] V. Fateev and S. Ribault, "The Large central charge limit of conformal blocks," *JHEP* **02** (2012) 001, arXiv:1109.6764 [hep-th].

[126] I. A. Morrison and M. M. Roberts, "Mutual information between thermo-field doubles and disconnected holographic boundaries," *JHEP* (June, 2013) 081, arXiv:1211.2887v2 [hep-th].

[127] V. Coffman, J. Kundu, and W. K. Wootters, "Distributed entanglement," *Phys. Rev.* **A61** (2000) 052306, arXiv:quant-ph/9907047 [quant-ph].

[128] G. T. Horowitz and N. Itzhaki, "Black Holes, Shock Waves, and Causality in the AdS/CFT Correspondence," *JHEP* **9902** (Jan., 1999) 010, arXiv:hep-th/9901012v2 [hep-th].

[129] J. V. Rocha and V. Cardoso, "Gravitational perturbation of the BTZ black hole induced by test particles and weak cosmic censorship in AdS spacetime," *Phys.Rev.D* **83** (May, 2011) 104037, arXiv:1102.4352v2 [gr-qc].

[130] J. Maldacena and D. Stanford, "Remarks on the Sachdev-Ye-Kitaev model," *Phys. Rev.* **D94** no. 10, (2016) 106002, arXiv:1604.07818 [hep-th].

[131] Maxima, "Maxima, a Computer Algebra System. Version 5.38.1," 2016. http://maxima.sourceforge.net/.

[132] S. A. Gentle and M. Rangamani, "Holographic entanglement and causal information in coherent states," *JHEP* **1401** (Aug., 2014) 120, arXiv:1311.0015v3 [hep-th].

[133] F. Nogueira, "Extremal Surfaces in Asymptotically AdS Charged Boson Stars Backgrounds,". http://cds.cern.ch/record/1507482. Comments: 22 pages, 11 figures.

[134] H. Lin, O. Lunin, and J. M. Maldacena, "Bubbling AdS space and 1/2 BPS geometries," *JHEP* **10** (2004) 025, arXiv:hep-th/0409174 [hep-th].